Spectroscopic and Theoretical Studies of Transition Metal Oxides and Dioxygen Complexes

Yu Gong and Mingfei Zhou*

Department of Chemistry, Shanghai Key Laboratory of Molecular Catalysts and Innovative Materials, Advanced Materials Laboratory, Fudan University, Shanghai 200433, China

Lester Andrews[†]

Department of Chemistry, University of Virginia, Charlottesville, Virginia 22901

Received May 9, 2009

Contents

1. Introduction

Dioxygen binding and activation at metal centers are of major importance in a wide range of catalytic and biological processes. Metal oxides and dioxygen complexes are potential intermediates or products during oxidation of metal atoms or clusters. Consequently, great effort has been devoted to the preparation and characterization of various metal oxides and dioxygen complexes. The structures, physicochemical properties, and reactivity of these species have been the subject of intensive experimental and theoretical studies, which have been described in numerous reviews.[1−5] As the initially formed species in most metal oxidation processes, metal dioxygen complexes are of particular interest in light of their postulated involvement in oxygen carrier systems in biology. Dioxygen reacts with biological molecules at isolated metallic active sites in forming metal−dioxygen adducts. Due to the intrinsic chemical interest in understanding metal−dioxygen interactions, a host of transition metal−dioxygen complexes that are structural and functional analogues of biological dioxygen carriers have been synthesized and are spectroscopically and structurally characterized. Progress on the characterization of such transition metal−dioxygen complexes stabilized by bulky ligands has been the subject of a series of recent reviews,[2−5] which is beyond the scope of this review.

Transition metal oxide materials are widely used as catalyst systems. As has been pointed out in a recent review,[6] gas-phase studies of neutral and ionic metal oxide clusters aid in the identification of the reactive sites in heterogeneous catalysis.[7] Many investigations including oxide cluster reactions in the gas phase have shown a direct similarity between reaction mechanisms involving clusters and similar ones effected by industrial catalysts.[8] The reactivity on size-

* To whom correspondence should be addressed. E-mail: mfzhou@fudan.edu.cn.
[†] E-mail: lsa@virginia.edu.

10.1021/cr900185x
Published on Web 09/17/2009

Yu Gong was born in Shanghai, People's Republic of China, in 1982. He received his B.S. degree in chemistry at Fudan University in 2005. He is now a Ph.D. student in the group of Mingfei Zhou at Fudan University. His research interest mainly focuses on the reactions between transition metals and small molecules in solid matrix.

Mingfei Zhou was born in Zhejiang province of China in 1968. He received his B.S. and Ph.D degrees in chemistry from Fudan University in 1990 and 1995, respectively. After a postdoctoral stay at the University of Virgina with Professor Lester Andrews, he joined the chemistry faculty at Fudan University in 1999. His research interests include experimental and theoretical studies of reactive intermediates and free radicals.

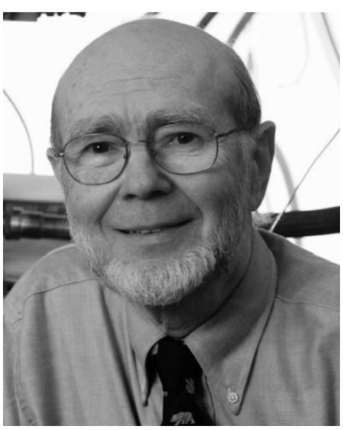

Lester Andrews was born in Lincolnton, NC, on January 31, 1942. He earned a B.S. degree in Chemical Engineering from Mississippi State University in 1963 and a Ph.D. degree in Physical Chemistry from the University of California, Berkeley, in 1966. Dr. Andrews joined the faculty of the University of Virginia in 1966 where he has been active in matrix-isolation spectroscopy, publishing over 750 research papers on novel chemical species. He is now Professor Emeritus. In addition, he enjoys playing the E-flat soprano clarinet.

selected transition metal oxide molecules and clusters has been widely studied in the gas phase in order to gain insight into the relationship between geometric structure and observed reactivity patterns. Investigations on such a topic have been intensively discussed[9−12] and will not be included in this review.

Here we will review spectroscopic and theoretical studies on the geometric and electronic structures of transition metal−oxygen molecules and small clusters. We mainly focus on binary transition metal−oxygen molecular species with several metal and oxygen atoms, which may exist in several structural forms and involve different chemical bonding. Molecular oxygen can bond either side-on or end-on to a metal center in forming dioxygen complexes, which are intermediate states for the complete cleavage of the O−O bond to form metal oxides. These species can be considered as the simplest model for oxygen binding to metal centers. Such model systems can be studied under well-defined conditions at the molecular level that are free of effects from ligands, solvents, surface active sites, and the crystal lattice.

Much of our knowledge about the geometric and electronic structures of transition metal oxides and dioxygen complexes comes from molecular spectroscopic studies. Although mass spectrometry excels at determining the composition and reactivity of molecular ions, these gas-phase mass spectrometric studies are blind to neutral species and thus are unable to provide detailed structural information. Laser-based spectroscopic techniques including laser-induced fluorescence spectroscopy (LIF), resonantly enhanced multiphoton ionization spectroscopy (REMPI), zero kinetic energy spectroscopy (ZEKE), and infrared photon dissociation spectroscopy (IR-PD) offer precise and detailed measurements of vibrational or rotational transitions of some simple transition metal oxide molecules as well as oxide clusters. Detailed analysis of rotational structures in the gas-phase spectrum may even yield a quantitative determination of the molecular structure. Negative ion photoelectron spectroscopic studies in the gas phase are able to provide valuable information on the vibrational and electronic structure of mass-selected transition metal oxides and dioxygen complexes. This technique can provide spectroscopic information on both neutral and anionic species. Different from the other LIF, ZEKE, and rotational gas-phase spectroscopic methods, which mainly focused on metal monoxides and dioxides, photoelectron spectroscopy can handle large species including metal oxide clusters and oxygen-rich molecules. Besides photoelectron and electronic spectroscopy, infrared absorption spectroscopy is another commonly used technique for probing the molecular properties of metal oxides and dioxygen complexes. All metal oxide molecules and metal−dioxygen complexes have infrared absorptions. Analysis of the vibrational transitions in characteristic spectral regions permits the identification of different structural isomers and provides detailed information about specific types of bonding. Due to its low sensitivity, conventional infrared absorption spectroscopy is mainly used in conjunction with the matrix isolation technique. It is very difficult to carry out a straightforward infrared absorption study in the gas phase. However, with advances in free electron lasers and tunable IR lasers, vibrational spectroscopic investigations in the gas phase have become possible. Recently developed infrared photon dissociation experiments with tunable IR lasers have allowed for detailed gas-phase vibrational spectroscopic studies of a number of transition metal oxide ions.

Spectroscopic studies of binary metal−oxygen species face strong challenges, because most of them are highly chemically reactive and are transient species at normal experimental conditions. Spectroscopic detection of such species formed in the gas phase requires sensitive and time-resolved techniques. Laser-based molecular spectroscopy, which is not only highly sensitive but also time specific in a wide range of time scales, is well-suited for such studies. Matrix isolation has proven to be a powerful technique in trapping transient reactive intermediates for spectroscopic studies.[13−20] Noble gases, such as Ne and Ar, are commonly used as matrices, which are sufficiently rigid to effectively isolate the reactive species at low temperatures (4−10 K). The chemically inert noble gas matrix that confines the reactive species is generally electronically innocent, that is, the species trapped in the solid matrix are normally regarded as isolated "gas-phase" molecules. The molecular properties measured in solid noble gas matrices are slightly different from those measured in the gas phase in most cases, as has been addressed by Jacox in a series of reviews.[21]

Matrix isolation is suited for trapping not only neutral molecules but also charged species including cations as well as anions.[15,22] Since noble gas matrices are transparent in the infrared spectral range, the structure-specific infrared absorption spectroscopy is most commonly employed to study the target species trapped in solid matrices. Unlike spectra recorded in solution or the solid state, it is straightforward to obtain well-resolved infrared spectra of species trapped in solid matrices, and most of the time, a diagnostic identification and vibrational assignment can be made. Such conditions are very suitable for the study of isotopic shifts and splittings, which are extremely important for product identification and structure determination. In addition to the spectroscopic assignment, isotopic substitution also provides information for the interpretation of reaction mechanisms.

Besides experimental investigations, a number of theoretical studies have been devoted to transition metal oxides and dioxygen complexes. Due to the existence of d electrons, transition metal systems require more sophisticated computational approaches. Various quantum chemical methods including ab initio as well as density functional theory (DFT) are now feasible that allow quantitative computations of vibrational frequencies and thermochemical properties with high accuracy. Theoretical studies have successfully reproduced experimental results, and disagreement between experiment and theory often initiates more accurate experimental as well as theoretical studies. In addition, theoretical calculations are especially valuable in predicting properties such as bonding, charge, and spin distribution, which often cannot be directly obtained from experiment.

In this review, we will describe advances in the spectroscopic and theoretical studies of binary transition metal−oxygen molecular and small cluster species. Both neutral and singly charged species will be included. We will emphasize spectroscopic and theoretical investigations of vibrational frequencies and structures of mononuclear transition metal oxides and dioxygen complexes. Besides the well-studied monoxide and dioxide species that have previously been reviewed,[23−29] we will also include oxygen-rich (MO_x, $x \geq 3$) species, which reveal diverse structural and bonding properties. The periodic trends on reaction mechanisms of transition metal atoms and dioxygen will be discussed. Numerous matrix isolation as well as gas-phase spectroscopic results will be included. Studies on large metal oxide clusters and bulk metal oxide materials go beyond the scope of this review and will not be included. However, some small metal oxide clusters with their spectral and structural information being clearly determined will be discussed, in particular, dinuclear oxide species. These small clusters are fundamental building blocks for the formation of large metal oxide clusters. There are a large number of gas-phase studies on metal oxide cations using various mass spectrometric methods, which have provided valuable thermodynamic properties of metal oxide cations. These methods do not give detailed spectroscopic and structural information and will not be discussed in detail in this review.

2. Spectroscopic and Theoretical Methods

2.1. Spectroscopic Methods

2.1.1. Matrix Isolation Infrared Absorption Spectroscopy

Infrared absorption spectroscopy is commonly employed in conjunction with the matrix isolation technique to characterize transition metal−oxygen species. Vibrational spectroscopy is bond specific and can identify new species particularly when isotopic substitution is employed. Matrix isolated transition metal oxides and dioxygen complexes are mainly prepared via reactions of metal atoms with dioxygen in solid matrices. Thermal evaporation has been successfully employed in the preparation of matrix samples for spectroscopic studies.[17,30] The ground-state metal atoms are generated either from a continuously heated tantalum or boron nitride Knudsen cell or from a heated tungsten filament wetted with target metals. Thermally evaporated metal atoms react with co-deposited dioxygen to form transition metal oxides or dioxygen complexes on sample annealing or on irradiation. Metal oxide molecules can also be produced via direct evaporation of bulk metal oxide target materials.

Laser ablation is another convenient technique that is used in our laboratories to prepare matrix-isolated transition metal oxides and dioxygen complexes. This method has been widely used to produce novel species for spectroscopic studies.[15,16,26,31] In contrast to conventional thermal evaporation techniques, with laser ablation only a small amount of the material is directly heated, thus minimizing the heat load and the introduction of impurities into the sample, particularly for transition metals, which have a very high melting point temperature. Simple transition metal oxide molecules, such as monoxides and dioxides, can also be prepared via laser evaporation of bulk metal oxide targets under controlled experimental conditions. With relatively low evaporation laser energy, matrix reactions are dominated by mononuclear species. However, multinuclear products may also be formed when relatively high evaporation laser energy is employed. The experimental apparatus for pulsed laser-evaporation matrix isolation infrared spectroscopy has been described in detail previously.[15,16] In general, the matrix sample is maintained at 6−10 K for argon matrix studies or at 4 K for neon matrix investigations. Because of the very low temperature of the deposit, the laser-evaporated species are quenched to their ground state in solid matrices. The as-deposited samples are annealed to higher temperatures to allow trapped reactants to diffuse and to react. The reaction can be very effectively quenched after the primary reaction, and the energy-rich intermediates, which fragment readily in the gas phase can be stabilized in solid matrices. Different wavelength range photolysis experiments are frequently performed to initiate further photoinduced isomerization or dissociation reactions.

As a structure-specific spectroscopic technique, infrared absorption spectroscopy is sensitive in detecting transition metal oxides and dioxygen complexes in solid matrices. Under low-temperature matrix isolation conditions, the fine structures derived from rotational transitions are suppressed. Well-resolved infrared absorptions with typical half width of less than 1 cm^{-1} are obtained. Transition metal dioxygen complexes often exhibit strong O−O stretching absorptions, which are quite structurally sensitive. Metal dioxygen complexes are generally defined as superoxides and peroxides depending on the extent of charge transfer from metal center to dioxygen. It is often quite difficult to determine the amount of charge transferred experimentally; hence, the classification is regularly based on the experimentally observed or theoretically predicted O−O stretching vibrational frequencies. Complexes with O−O stretching frequencies in the range of 1050−1200 cm^{-1} are assigned as superoxides, whereas those with O−O stretching frequencies in the range of 800−930 cm^{-1} are designated as peroxides.[32−36] Metal oxide molecules also exhibit strong absorptions in the terminal M=O and bridged M−O−M stretching vibrational regions. The terminal M=O stretching vibrations are commonly located in the 1050−800 cm^{-1} range, whereas the bridged oxide species absorb at a much lower frequency region.

Isotopic substitution experiments are extremely important for product identifications and structural determination. Isotopically labeled $^{18}O_2$ samples are always used in the transition metal and dioxygen reaction experiments. The experimentally observed oxygen isotopic shifts give information on the extent of oxygen atom(s) participation in the observed vibrational modes. The use of isotopic $^{16}O_2 + {}^{18}O_2$ and $^{16}O_2 + {}^{16}O^{18}O + {}^{18}O_2$ mixtures results in multiple absorptions for different isotopomers, which is a major factor for determining the number of oxygen atoms involved in the observed vibrational modes.

Transition metal-containing species such as simple transition metal oxides and dioxygen complexes are polar species. The metal center in these species is positively charged and electrophilic and, hence, is able to interact with noble gas atoms in many cases. Some transition metal-containing species trapped in solid noble gas matrices are chemically coordinated by one or multiple noble gas atoms and cannot be regarded as completely isolated species.[37,38] Noble gas coordination may change the spectra and geometric and electronic structure, as well as reactivity, of the species trapped in solid matrices.[39] In order to determine whether the transition metal oxides and dioxygen complexes trapped in solid noble gas matrices are coordinated by noble gas atoms and to determine the number of coordinated noble gas atoms experimentally, one can use mixtures of a lighter noble gas host doped with heavier noble gas atoms as matrix. If the trapped species are coordinated by noble gas atoms, the coordinated lighter noble gas atoms can be successively substituted by heavier noble gas atoms when the solid matrix sample is annealed, which will induce vibrational frequency shifts on the infrared spectrum. The coordination number can be determined by the number of new absorption bands formed.

2.1.2. Photoelectron Spectroscopy (PES)

Photoelectron spectroscopy is one of the most important techniques in spectroscopic investigation of mass-selected transition metal oxide species in the gas phase. Since the pioneering work by Lineberger's group on the photodetachment PES study of transition metal species including several transition metal oxides,[40,41] systematic investigations on transition metal oxide species using anion photoelectron spectroscopy have been conducted by Wang's group, which have been summarized in a recent review.[26] The difficulty in studying transition metal oxide species in the gas phase is how to generate them with sufficient number density. Pulsed laser evaporation coupled with supersonic expansion is the most frequently used source in producing transition metal oxide anions for PES study. The details of PES experiment have been described in detail in previous publications.[26,42] Briefly, a focused pulsed laser beam is used to vaporize metal species. A short and intense helium carrier gas beam doped with a small amount of O_2 mixes with the laser-evaporated metal species and undergoes a supersonic expansion to form a cluster beam. Negatively charged species are extracted from the beam and are subjected to a time-of-flight mass analysis. The anions of interest are mass selected and are interacted with a pulsed detachment laser beam. Pulsed lasers including the harmonics of Nd:YAG laser (532, 355, and 266 nm) and excimer lasers (248, 193, and 157 nm) are used for detachment. Low photon energies allow optimum spectral resolution, while high photon energies can reveal more highly excited states. The kinetic energy of detached electrons is detected by a magnetic-bottle time-of-flight photoelectron analyzer.

PES studies on transition metal oxide species can provide direct information on their electron affinities, low-lying electronic states, and vibrational frequencies. Although the vibrational assignment is less accurate due to limited resolution compared with other spectroscopic methods, PES is a versatile and convenient method in gas-phase studies, which complements the extensively used matrix isolation infrared spectroscopic investigations. Since the selection rules for vibrational transitions are determined by the Franck−Condon factors, it is often possible to observe vibrational states that are forbidden or weak in infrared spectroscopy. For example, the symmetric stretching vibration for a linear transition metal dioxide molecule is IR inactive and cannot be observed with infrared absorption spectroscopy. However, the vibrational frequency of this mode can be determined from the resolved vibrational structures of PES of metal dioxide anion.

2.1.3. Electron Spin Resonance Spectroscopy (ESR)

Electron spin resonance spectroscopy is of great importance in understanding the neutral and charged radicals with unpaired electrons.[43,44] **A**- and **g**-tensors are the most useful parameters obtained from ESR experiments, from which direct information on singly occupied orbitals can be derived. No ESR signals can be obtained if target molecules possess a closed-shell singlet ground state with all the electrons involved being paired. In addition, molecules with degenerate ground states (Π, Δ, etc.) are not suitable for ESR investigations due to the broadening of the absorption lines caused from anisotropy of **g**-tensor. ESR spectroscopy in conjunction with the matrix isolation technique has been extensively employed in the electronic characterization of some transition metal oxide species.[44]

2.1.4. Infrared Photon Dissociation Spectroscopy (IR-PD)

With the development of tunable infrared lasers, infrared photon dissociation spectroscopy has become a very powerful method for studying mass-selected molecular and cluster ions in the gas phase, as has been reviewed.[45,46] The vibrations of transition metal oxides and dioxygen complexes are roughly located in the range of 1600−400 cm^{-1}. Free electron laser can generate intense and continuously tunable IR irradiation in this wavelength range. More recently, intense and tunable middle IR laboratory lasers have become available. Gas-phase ions are produced via the laser evaporation−supersonic expansion technique as used in anion PES studies. The ion beam from the source is mass-selected. The selected ions are interacted with a pulsed IR dissociation laser beam. Infrared photodissociation spectra are obtained by monitoring the fragment ion signal. For weakly bound complexes, one absorbed IR photon can be sufficient to bring the complex above the dissociation barrier such that it can undergo vibrational predissociation. For strongly bound clusters, many IR photons need to be absorbed in order to induce fragmentation. The IR spectrum from multiple photon processes may not be the same as a regular linear absorption spectrum. A useful method to avoid multiple photon excitation and measure IR photodissociation spectra in the linear regime is the messenger atom technique. Generally, noble gas atoms are chosen as messenger atoms. By formation of ion−noble gas atom complexes, the dissociation threshold of the system is lowered. If the binding energy of the cluster ion−noble gas complex is below the photon energy, absorption of a single photon will be followed by vibrational predissociation. In general, the perturbation of the geometric and electronic structures of cluster ions by the messenger atom is negligible; hence, the IR spectrum of the cluster ion−noble gas atom complex reflects the IR spectrum of the free cluster ion.

2.1.5. Laser-Induced Fluorescence (LIF)

With widespread application of lasers especially tunable lasers, laser-induced fluorescence has become a valuable spectroscopic method in studying metal atoms, clusters, radicals, and molecular ions both in the gas phase and in the condensed phases.[13,31] The LIF studies benefit from the rather high sensitivity over other spectroscopic techniques. Pulsed laser vaporization or discharge is commonly combined with the supersonic jet technique for producing target species in the gas phase for LIF studies. High-resolution gas-phase studies can provide well-resolved vibrational and rotational structures of target species. Both the ground state and excited states accessible by allowed transition from ground state can be studied. LIF study of matrix-isolated species was first introduced by Bondybey and co-workers.[31] In solid matrices, the selection rules are often relaxed, and hence, some rigorously forbiddened transitions in the gas phase can be studied in the matrices. However, the rotational structure that is important in determining the geometric parameters is lost in solid matrices. LIF studies on transition metal−oxygen species are mainly focused on monoxides and some dioxide molecules due to the complex transitions involved in polyatomic systems.

2.1.6. Other Spectroscopic Methods

Besides the above-mentioned spectroscopic methods, other techniques, such as rotational spectroscopy,[47] infrared emission spectroscopy,[48] resonance-enhanced multiple photon ionization/dissociation spectroscopy (REMPI/D),[49] and pulsed-field ionization zero kinetic energy (PFI-ZEKE) photoelectron spectroscopy,[50] have also been used for spectroscopic studies. These techniques are helpful in understanding the electronic and geometric structures of simple transition metal−oxygen species.

2.2. Theoretical Methods

Dramatically increased computational power allows the application of various quantum chemical methods to predict molecular properties including equilibrium geometries, energies, and vibrational frequencies of transition metal-containing species. In order to give accurate predictions, electron correlation must be included. Single-reference post-Hartree−Fock ab initio methods such as Møller−Plesset perturbation theory[51] and coupled-cluster approaches[52] have been used to calculate equilibrium geometries, relative stabilities, and vibrational frequencies for some simple metal−oxygen species. However, high-level ab initio calculations such as CCSD(T) with reasonably large basis sets are very computationally demanding and are not practical methods for larger systems such as multinuclear transition metal oxides and mononuclear oxygen-rich species. Density functional theory (DFT), which also incorporates electron correlation effects, is more commonly used in the calculation of transition metal−oxygen species. DFT has the advantage of predicting equilibrium geometries and vibrational frequencies that are comparable in quality to those obtained with more highly correlated methods. Several well-calibrated DFT methods such as BLYP, BPW91, B3LYP, BH and HLYP, and BP86, which have proven to give good results for transition metal-containing compounds, are frequently employed.[53] In addition, some new methods have also been developed for transition metal systems in recent years.[54] For some species that show strong multireference character, calculations using single-reference based methods may give unreliable results. In such cases, multireference methods such as CASSCF[55] and internally contracted MRCI[56] methods should be used to give a reliable prediction. Taking FeO_2^- anion as an example, the FeO_2^- anion is experimentally determined to be linear. However, single-reference based methods including MP2−4, CCSD(T), and various DFT methods all gave unreliable predictions due to the strong multireference character of the FeO_2^- anion and the symmetry-breaking problems in the single-reference wave functions. Only the state-averaged multireference MRCI methods, which incorporate both dynamical and nondynamical correlation effects, predict that the anion has a linear doublet ground state, consistent with the experimental observations.[57]

Relativistic effects should be taken into consideration when calculating transition metal oxides and dioxygen complexes, particularly for heavy transition metals.[58,59] Upon geometric optimization and vibrational frequency calculations, the scalar relativistic effects can be included by use of suitably parametrized relativistic pseudopotentials. Spin−orbital coupling effect should also be taken into consideration, particularly for open-shell species. Although spin−orbital effects are found not to be important in many cases, they may be important for f-element metal-containing species in order to obtain reliable energy predictions.

3. Neutral Mononuclear Transition Metal Oxides and Dioxygen Complexes

Neutral MO_x series spectroscopically characterized both in the gas phase and in solid matrices will be summarized

Table 1. Ground Spin States and Vibrational Frequencies (cm^{-1}) for Transition Metal Monoxides in the Gas Phase and in Solid Neon and Argon Matrices[a]

molecule	ground state	vibrational frequency: gas phase	Ne	Ar	refs
ScO	$^2\Sigma^+$	965.0	962.1[b]	954.8	24, 105
TiO	$^3\Delta$	1000.0	997.7[b]	987.8	24, 27, 132
VO	$^4\Sigma^-$	1001.8	998.3[b]	983.6	24, 27, 182
CrO	$^5\Pi$	885.0	880.2	846.3	24, 201, 202
MnO	$^6\Sigma^+$	832.4	830.9[b]	833.1	24, 246
FeO	$^5\Delta$	871.2	869.8[b]	872.8	24, 270
CoO	$^4\Delta$	851.7	851.2	846.2	24, 27, 318, 320
NiO	$^3\Sigma^-$	828.3	831.4[b]	825.7	24, 27, 347
CuO	$^2\Pi$	631.3[c]		627.7	24, 383
ZnO	$^1\Sigma^+$	738[d]		769.2	456, 464, 465
YO	$^2\Sigma^+$	855.2	852.2[b]	843.1	25, 109
ZrO	$^1\Sigma^+$	969.8	966.9[b]	958.6	25, 70, 95, 132
NbO	$^4\Sigma^-$	981.4	978.5[b]	970.6	25, 183
MoO	$^5\Pi$			893.5	70, 71, 157, 208
TcO	$^6\Sigma^+$				70, 71, 207
RuO	$^5\Delta$	863.5	849.7	834.2	261, 314
RhO	$^4\Sigma^-$	805	799.8	799.0	332, 334, 337
PdO	$^3\Sigma^-(^3\Pi)$[e]				356
AgO	$^2\Pi$	485		499.2	71, 430, 434
CdO	$^1\Sigma^+$			645.1	464, 466, 468
LaO	$^2\Sigma^+$	808.3	808.5[b]	796.7	25, 109
HfO	$^1\Sigma^+$	974.1	965.8[b]	958.3	73, 129, 132
TaO	$^2\Delta$	1028.9	1020.0[b]	1014.2	73, 175, 183
WO	$^3\Sigma^-(^5\Pi)$[e]	1053.7	1056.1	1051.3	25, 201, 210
ReO	$^4\Phi(^2\Delta,^6\Sigma^+)$[e]	979.1			73, 259−261
OsO	$^5\Sigma^+(^3\Phi)$[e]				73, 261
IrO	$^4\Sigma^-$		827.2	822.1	340, 341
PtO	$^3\Sigma^-$	841.1	837.7[b]	828.0	357, 366, 367
AuO	$^2\Pi$	624.6		619.2	430, 443
HgO	$^3\Pi$			676	475, 477
CeO	$^3\Phi$	824.3	819.9[b]	808.3	74, 480, 504
PrO			828.0	816.9	504
NdO			825.1	814.2	504
PmO	$^6\Sigma^+$				74
SmO			819	807.4	503, 504
EuO	$^8\Sigma^-$			667.8	74, 504
GdO	$^9\Sigma^-$	790 ± 40	824	812.7	74, 489, 503, 504
TbO			833.5[b]	823.9	505
DyO			839.0	829.0	505
HoO		841.4	838.1	828.1	497, 505
ErO				828.5	505
TmO				832.0	505
YbO	$^1\Sigma^+$	683.1		660.0	74, 501, 505
LuO	$^2\Sigma^+$		811	829.3	74, 503, 505
ThO	$^1\Sigma^+$	895.8[d]	887.1	876.4	521, 533, 534, 538, 580
UO	quintet	882.4	889.5	819.8	532, 546, 549
PuO	$^7\Pi$			822.3	563, 564

[a] Only the values for the most abundant metal isotope and major site are listed. [b] Unpublished results. [c] 631.3 cm^{-1} for $^2\Pi_{3/2}$ and 627.5 cm^{-1} for $^2\Pi_{1/2}$. [d] Harmonic frequency. [e] Ground state undetermined.

in this section. We will focus on the structures and vibrational frequencies of the MO_x species in their electronic ground states. Since various experimental studies have been performed using different methods for producing and characterization transition metal−oxygen species, controversy assignments on measured vibrational fundamentals have been reported in many cases. Assignments from earlier reports now known to be incorrect will not be mentioned here, but these are discussed in the recent literature where the new assignments are given.

For the simplest member in this series, transition metal monoxides are among the most studied species. The spectra, electronic structures, and bonding of transition metal monoxides have been systematically reported.[24−29,60−75] The ground spin states and vibrational frequencies of all transition metal monoxides in the gas phase and in solid argon and neon matrices are summarized in Table 1. In general, the matrix frequencies are usually slightly red-shifted from the gas-phase values with the argon matrix shift being larger than that of neon.

Table 2. Ground Spin States, Symmetry Point Groups, and Vibrational Frequencies (cm^{-1}) for $M(O_2)$ Species in Solid Argon[a]

molecule	ground state	point group	vibrational frequency	ref
$Rh(\eta^2\text{-}O_2)$	$^2A_2$	C_{2v}	959.5	336
$Ni(\eta^2\text{-}O_2)$	$^1A_1(^3B_1)$[b]	C_{2v}	967.1, 538.3, 511.7	76, 239, 347, 371, 372, 375−379
$Pd(\eta^2\text{-}O_2)$	$^1A_1$	C_{2v}	1023.0	357, 380
$Pt(\eta^2\text{-}O_2)$	$^1A_1$	C_{2v}	928.1, 512.3, 551.2	372
$Cu(\eta^1\text{-}O_2)$	$^2A''$	C_s	1089.0	383
$Ag(\eta^1\text{-}O_2)$	$^2A''$	C_s	1075.7	430
$Au(\eta^1\text{-}O_2)$	$^2A''$	C_s	1093.8	430

[a] Only the values for the most abundant metal isotope are listed. [b] These two states are close in energy, and the vibrational frequencies for the $^1A_1$ state are in better agreement with the experimental values.

There are three structural isomers for triatomic MO_2 species, namely, the side-on and end-on bonded metal dioxygen complexes and the inserted metal dioxide molecule. The electronic structure and bonding of first and second row transition metal dioxygen complexes and dioxide species have been systematically investigated theoretically.[76−78] Experimentally, the dioxide form has been observed for all transition metals except technetium, silver, and mercury, while the dioxygen complex isomers are only reported for some late transition metals. The geometric structures and vibrational frequencies of transition metal dioxygen complexes are summarized in Table 2. Both the side-on and end-on bonded metal−dioxygen complexes usually show strong O−O stretching vibrations. The coordination fashion (side-on versus end-on) can be sorted out from the spectrum with mixed isotopic samples. In the experiment with a 1:2:1 molar mixture of $^{16}O_2/^{16}O^{18}O/^{18}O_2$, the O−O stretching mode of side-on bonded $M(O_2)$ complex will split into a triplet with approximately 1:2:1 relative intensities; but the O−O stretching mode of the end-on bonded complex will consist of a quartet with two closely spaced mixed isotopic absorptions for the $M^{16}O^{18}O$ and $M^{18}O^{16}O$ isotopic molecules. The geometric structures and vibrational frequencies of all transition metal dioxides in gas phase and in solid noble gas matrices are organized in Table 3. The inserted dioxide structure may be either bent or linear. The symmetric stretching mode (ν_1) of linear OMO is IR inactive. However, the ν_1 fundamental of $^{16}OM^{18}O$ is IR activated because of the reduced symmetry. Along with the observation of the $\nu_1 + \nu_3$ combination, the crossed anharmonic term, X_{13} can be obtained. Hence, the band position of the ν_1 fundamental can be predicted. Both the symmetric (ν_1) and antisymmetric (ν_3) stretching modes of bent insertion molecules are IR active. The observed isotopic frequency ratio of the antisymmetric stretching mode provides a route to estimate the bond angle of a bent metal dioxide molecule.[79] The upper limit of bond angle can be determined from the oxygen isotopic frequency ratio, while the lower limit can be deduced from the metal isotopic frequency ratio if the metal isotopic shift can be resolved. The average of upper and lower limits is very close to the true bond angle, as has been demonstrated earlier for SO_2 and more recently for S_3.[80,81]

Three structures have been observed for species with MO_3 stoichiometry: metal trioxide with planar D_{3h} or nonplanar C_{3v} symmetry, metal ozonide complex, and metal monox-

Table 3. Ground Spin States, Experimental Bond Angles (Degree) and Vibrational Frequencies (cm^{-1}) for Transition Metal Dioxides in the Gas Phase and in Solid Neon and Argon Matrices[a]

				Ne		Ar		
molecule	ground state	bond angle[b]	gas phase frequency	ν_1	ν_3	ν_1	ν_3	ref
ScO_2	$^2B_2$	bent	740 ± 80 (ν_1)					89, 108, 109
TiO_2	$^1A_1$	113 ± 5	960 ± 40 (ν_1)	962.7[c]	936.5[c]	946.9	917.1	115, 132, 139
VO_2	$^2A_1$	118 ± 3	970 ± 40 (ν_1)	958.0[c]	947.4[c]	946.3	935.9	77, 165, 182
CrO_2	$^3B_1$	128 ± 4	895 ± 20 (ν_1)	920.8	974.9	914.4	965.4	201, 202, 217
			220 ± 20 (ν_2)					
MnO_2	$^4B_1$	135 ± 5	800 ± 40 (ν_1)	834.0[c]	962.8[c]	816.4	948.0	240, 246
FeO_2	$^3B_1$	150 ± 10		811.1[c]	957.7[c]	797.1	945.8	270, 286
CoO_2	$^2\Sigma_g^+$	180		796.2[d]	954.7	783.7[d]	945.4	320, 326
NiO_2	$^1\Sigma_g^+$	180	750 ± 30 (ν_1)		967.7		954.9	344, 347, 371, 372
CuO_2	$^2\Pi_g$	180			836.7[c]		823.0	382, 383
ZnO_2	$^3\Sigma_g^-$	180			762.9		748.2	464, 612
YO_2	$^2B_2$	bent	640 ± 80 (ν_1)			708.2		89, 109
ZrO_2	$^1A_1$	113 ± 5	887 ± 40 (ν_1)	903.4[c]	838.7[c]	884.3	818.0	132, 137, 146
NbO_2	$^2A_1$	108 ± 5		957.2[c]	907.8[c]	933.5	875.9	183
MoO_2	$^3B_1$	118 ± 4		950.7	901.3	939.3	885.5	201, 210
TcO_2	$^4B_1(^4B_2)$[e]	bent						78, 258
RuO_2	$^1A_1$	151 ± 5			911.9		902.1	261
RhO_2	$^2\Sigma_g^+$[f]	180			908.6	845[d]	899.9	325, 334, 337
PdO_2	*e*		680 ± 30 (ν_1)					342
AgO_2	$^4\Sigma_g^+$	180						355
CdO_2	$^3\Sigma_g^-$	180			638.8		625.4	464, 612
LaO_2	$^2B_2$	bent				569.8		109
HfO_2	$^1A_1$	113 ± 5	887 ± 40 (ν_1)	901.9[c]	831.9[c]	883.4	814.0	132, 137, 146
TaO_2	$^2A_1$	106 ± 5	968	979.2[c]	920.9[c]	965.3	912.2	174, 183
WO_2	$^1A_1$	108 ± 5	325 ± 15 (ν_2)	1030.3	983.9	978.3	938.0	201, 210, 225
ReO_2	$^4B_1$	127 ± 4		989.1	941.0	981.9	931.7	261
OsO_2	$^3B_1$	135 ± 5			957.3		949.9	261
IrO_2	$^2\Sigma_g^+$	180			938.2	960[d]	929.0	340, 341
PtO_2	$^1\Sigma_g^+$	180	895 ± 30 (ν_1)		958.7		961.8	342, 355, 357, 372
AuO_2	$^2\Pi_g$	180	740 ± 60 (ν_1)		824.2		817.9	355, 357, 440
CeO_2	$^1A_1$	139		780.3[c]	755.6[c]	757.3	736.7	504, 510
PrO_2		180			752.5		730.1	504
NdO_2		180			737.6		716.9	504
SmO_2		180					643.2	504
EuO_2		90					622.8	504
GdO_2		97					635.5	504
TbO_2		125		769.5[c]	730.4[c]	758.6	718.6	505
DyO_2		180			599.2		580.5	505
HoO_2		125		668.2		649.2	549	505
TmO_2		128				706.6	615.7	505
YbO_2		180					627.7	505
ThO_2	$^1A_1$	122 ± 2		808.4	756.8	787.1	735.1	521, 533, 538
UO_2	$^3\Phi_u$	180			914.8		775.7	546, 549
PuO_2	$^5\Sigma_g^+$	180					794.2	563−565

[a] Only the values for the most abundant metal isotope and major site are listed. [b] Angles are estimated from oxygen 16/18 isotopic ratio and metal isotopic ratio (if available) for the ν_3 mode. For HoO_2, the angle is estimated from oxygen 16/18 isotopic ratio for the ν_1 mode. [c] Unpublished results. [d] Calculated by $(\nu_1 + \nu_3)_{exp} - (\nu_3)_{exp}$ with the anharmonic term corrected. [e] Ground state undetermined. [f] A linear geometry is proposed from matrix ESR experiments (ref 325) but a slightly bent geometry is obtained from theoretical caluclations (ref 334 and 336).

ide−dioxygen complex. For early transition metals (Sc group and Ti group), only the metal monoxide−dioxygen complex structure has been observed due to limited valence electrons available for bonding, while both the trioxide and monoxide−dioxygen complex structures have been reported for some late transition metals. The metal ozonide structure is rare, only very few ozonide complexes have been experimentally reported. The experimentally characterized structures of MO_3 species are listed in Table 4.

For oxygen-rich MO_x species with $x \geq 4$, the number of possible structures is much larger than that of the simple MO_2 and MO_3 species. However, only some of them have been experimentally characterized, which will be discussed in detail in this section. The geometric structures and vibrational frequencies of oxygen-rich MO_x species with $x \geq 4$ are organized in Tables 5 and 6. In the matrix isolation studies, each structural isomer exhibits characteristic infrared absorptions in different spectral regions. The isotopic shifts and splitting in mixed isotopic spectra provide detailed information about the number of dioxygen units or oxygen atoms involved in a transition metal−oxygen species. Theoretical calculations at various levels have been intensively performed to predict the ground-state structure and vibrational frequencies of transition metal−oxygen species for comparison with the experimental values to support the experimental identification of new species. Due to problems such as near-degeneracy effects and s−d energy separation, the unambiguous assignment of the ground state of transition metal oxides and dioxygen complexes based solely on theoretical predictions is often quite complicated, particularly for late transition metal systems. Contradictory results are frequently obtained using different theoretical methods. Nevertheless, the experimentally determined spectroscopic properties pro-

Table 4. Ground Spin States, Symmetry Point Groups, and Vibrational Frequencies (cm^{-1}) for the MO_3 Species in Solid Argon[a]

molecule	ground state	point group	vibrational frequency[b]	ref
$(\eta^2\text{-}O_2)ScO$	$^2A'$	C_s	1109.5, 922.0, 466.3	85, 105
$(\eta^2\text{-}O_2)YO$	$^2A''$	C_s	1111.1, 798.7	109
$(\eta^2\text{-}O_2)LaO$	$^2A''$	C_s	1123.4, 757.8	109
$(\eta^2\text{-}O_2)TiO$	$^1A'$	C_s	863.3, 971.9, 624.8, 611.1	147
$(\eta^2\text{-}O_2)ZrO$	$^1A'$	C_s	808.8, 885.7, 590.8, 580.2	148
$(\eta^2\text{-}O_2)HfO$	$^1A'$	C_s	782.8, 879.4, 614.9, 557.3	148
$(\eta^2\text{-}O_2)FeO$	$^5B_2$	C_{2v}	1002.3	295
$(\eta^2\text{-}O_2)NiO$	triplet	C_{2v}	1095.5	347
$(\eta^2\text{-}O_2)PtO$	$^3B_2$	C_{2v}	1174.2	357
$(\eta^1\text{-}O_2)NiO$	singlet	C_s	1393.7	347
$(\eta^1\text{-}O_2)PtO$	$^5A'$	C_s	1402.1	357
$Cu(\eta^2\text{-}O_3)$	$^2B_1$	C_{2v}	802.7	383, 391
$Ag(\eta^2\text{-}O_3)$	$^2B_1$	C_{2v}	791.8	430, 431
CrO_3	$^1A_1$	C_{3v}	968.4	201, 202
MoO_3	$^1A_1$	C_{3v}	915.8	201, 210
WO_3	$^1A_1$	C_{3v}	922.5	201, 210
ReO_3	$^2A_1$	C_{3v}	953.4	261
FeO_3	$^1A_1'$	D_{3h}	948.6	295
RuO_3	$^1A_1'$	D_{3h}	893.3	261
OsO_3	$^1A_1'$	D_{3h}	959.1	261
UO_3	$^1A_1$	C_{2v}	852.5, 843.5, 745.5, 211.6, 186.2, 151.5	367, 368, 549

[a] Only the values for the most abundant metal isotope are listed. [b] The mode assigments are discussed in the cited literature.

Table 5. Ground Spin States, Symmetry Point Groups, and Vibrational Frequencies (cm^{-1}) for the MO_4 Species in Solid Argon[a]

molecule	ground state	point group	vibrational frequency[b]	ref
$(\eta^2\text{-}O_2)LaO_2$	$^2A_2$	C_{2v}	1111.1, 602.9	109, 112
$(\eta^2\text{-}O_2)VO_2$	$^2A_2$	C_{2v}	1121.9, 974.1, 975.3, 506.9, 555.6	183
$(\eta^2\text{-}O_2)NbO_2$	$^2A_2$	C_{2v}	1109.3, 903.6, 945.9, 511.3	183
$(\eta^2\text{-}O_2)TaO_2$	$^2A_2$	C_{2v}	1095.7, 894.5, 950.5, 524.2	183
$(\eta^2\text{-}O_2)MnO_2$	$^2A_1$	C_{2v}	974.8, 951.3	247
$(\eta^2\text{-}O_2)ReO_2$	$^2A_1$	C_{2v}	992.4, 964.6, 882.4	261
$(\eta^2\text{-}O_2)FeO_2$	$^1A_1$	C_{2v}	968.8, 955.8, 558.1, 548.3	288
$(\eta^2\text{-}O_2)RuO_2$	$^1A_1$	C_{2v}	921.8, 920.7, 940.2, 579.8, 558.4	261
$(\eta^2\text{-}O_2)OsO_2$	$^1A_1$	C_{2v}	898.1, 970.0, 1004.8	261
$(\eta^2\text{-}O_2)CoO_2$	$^2A_2$	C_{2v}	950.6, 898.2, 842.8, 405.7, 419.6	327
$(\eta^2\text{-}O_2)RhO_2$	$^2A_2$	C_{2v}	928.6, 831.1, 865.0, 473.5	334, 337
$(\eta^2\text{-}O_2)IrO_2$	$^2A_2$	C_{2v}	894.8, 874.9, 937.7, 547.9, 517.8	340
$(\eta^2\text{-}O_2)NiO_2$	triplet	C_{2v}	1135.8, 851.0	347
$(\eta^1\text{-}O_2)FeO_2$	$^3A''$	C_s	1204.5, 975.3, 871.6	288
$(\eta^1\text{-}O_2)CoO_2$	$^4A'$	C_s	1286.2, 953.1, 805.8	327
$(\eta^1\text{-}O_2)RhO_2$	$^2A'$	C_s	1116.5, 890.6, 837.7	334, 337
$(\eta^1\text{-}O_2)IrO_2$	$^2A''$	C_s	1022.6, 947.4, 946.6	340
$Sc(\eta^2\text{-}O_2)_2$	$^2A_2$	C_{2v}	1102.4, 836.0, 631.7, 612.7	111
$Y(\eta^2\text{-}O_2)_2$	$^2A_2$	C_{2v}	1104.5, 773.6, 565.8	112
$Rh(\eta^2\text{-}O_2)_2$	$^4B_{1u}$	D_{2h}	1048.4	336
$Ni(\eta^2\text{-}O_2)_2$	triplet	D_{2h}	1063.9	347
$Pd(\eta^2\text{-}O_2)_2$	^1A_g	D_{2h}	1110.1	380
$Pt(\eta^2\text{-}O_2)_2$	^1A_g	D_{2h}	1051.3	357
$Cu(\eta^2\text{-}O_2)_2$	$^4B_{2u}$	D_{2h}	1110.1	424, 425
$Ag(\eta^1\text{-}O_2)_2$	$^4B_1$	C_{2v}	1299.2, 1053.9[c]	355
$OSc(\eta^2\text{-}O_3)$	$^2A'$	C_s	921.7, 801.8	111
$OY(\eta^2\text{-}O_3)$	$^2A'$	C_s	805.6, 795.7	112
$OLa(\eta^2\text{-}O_3)$	$^2A'$	C_s	763.9, 792.0	112
RuO_4	$^1A_1$	T_d	916.6	261
OsO_4	$^1A_1$	T_d	956.2	261
IrO_4	$^2A_1$	D_{2d}	870.5, 859.5	340

[a] Only the values for the most abundant metal isotope are listed. [b] The mode assigments are discussed in the cited literature. [c] Neon matrix values, unpublished results.

vide a criterion to compare with the calculated values, which aids in determining the true ground state.

3.1. Sc Group

As the starting point for transition metals, scandium possesses the simplest electronic structure with only three valence electrons. The ground state of ScO is found to be $^2\Sigma$ from matrix isolation ESR as well as gas-phase experiments,[24,82,83] which is further confirmed by a series of theoretical calculations at different levels.[27−29,61−69,76,84−88] The Sc $4s_\sigma$ and $3d_\pi$ orbtials can interact with O 2p orbitals in forming σ and π bonds, respectively. The lone pair electrons on oxygen can be donated to the vacant 3d orbital of Sc with the formation of a dative bond. Hence ScO can be formally described as a diatomic molecule with a Sc≡O triple bond. The remaining electron of Sc is located on an σ orbital, which is mainly metal-based 4s orbital in character. Both experiments and theoretical calculations reveal that yttrium and lanthanum monoxide molecules possess the same $^2\Sigma$ ground state as ScO, and the spectroscopic properties of these two diatomic molecules have been well studied.[71,72,74,75,82,83,89−102]

Scandium dioxide is the only molecule that has not been identified in solid matrices among the first row transition metal dioxides. Mass spectrometric study on the reaction of scandium dioxide cation and nitrogen dioxide provides evidence for the existence of scandium dioxide molecule in the gas phase.[103] The symmetric stretching mode (ν_1) for ScO_2 is determined to be 740 ± 80 cm^{-1} by photoelectron spectroscopy.[89] An infrared absorption at 722.5 cm^{-1} has been assigned to the antisymmetric stretching mode (ν_3) of scandium dioxide in solid argon,[104] but late study reassigns this absorption to the $OScO^-$ anion instead of the neutral dioxide molecule.[105] According to the DFT and high-level ab initio calculations, both the C_{2v} and symmetry-broken C_s structures are stable minima. However, the relative stability depends strongly on the theoretical levels used.[76,77,84,85,105−107] A recent benchmark study by Kim and Crawford[108] using high-level coupled cluster methods up to full CCSD(T) indicates that the scandium dioxide molecule lies in a flat symmetry-breaking potential with indefinite sign and the zero-point vibrational energy lies above the barrier for the interconversion between the C_s and C_{2v} isomers. Although the symmetry-broken C_s structure is predicted to be lower in energy than the C_{2v} isomer, it is unlikely for the C_s structure to be experimentally detected due to an overall dynamical C_{2v} symmetry for this unusual molecule. Although the scandium dioxide molecule is not observed in solid matrices, the yttrium and lanthanum dioxide molecules have been formed via the reactions of metal atoms with dioxygen in solid argon, which are characterized to have a bent C_{2v} structure[109,110] A recent CASPT2 calculation predicts a $^2B_1$ ground state for LaO_2.[100] The 708.2 cm^{-1} symmetric stretching frequency (ν_1) observed in solid argon is in good agreement with the gas-phase value derived from the photoelectron spectroscopic study of YO_2.[89]

The experimentally observed structure for the MO_3 (M = Sc, Y, and La) species in solid matrices is the metal monoxide−dioxygen complex structure, which is characterized to have a doublet ground state with nonplanar C_s symmetry.[104,105,109] All three complexes are due to superoxide species with the metal centers in their formal +3 oxidation state. The previously assigned ozonide complexes in solid argon[104,105,109] are due to oxygen-rich species.[111,112] The $(O_2)ScO$ and $(O_2)LaO$ complexes are proposed to be the photodetachment products of the ScO_3^- and LaO_3^- anions

Table 6. Ground Spin States, Symmetry Point Groups, and Vibrational Frequencies (cm^{-1}) for the Oxygen-Rich MO_x ($x \geq 5$) Species in Solid Argon

molecule	ground state	point group	vibrational frequency[a]	ref
$(\eta^2\text{-}O_2)_2TiO$	$^3A''$	C_s	1124.1, 1116.6, 996.8, 596.4	147
$(\eta^2\text{-}O_2)_2CrO_2$	$^3B_2$	C_{2v}	1153.9, 1134.2, 971.5, 939.6, 632.0	238
$(\eta^2\text{-}O_2)_2MoO_2$		C_{2v}	1119.3, 1111.2, 944.2, 966.4, 522.8	201
$(\eta^2\text{-}O_2)_2WO_2$		C_{2v}	1105.5, 1098.1, 951.2, 990.3, 497.7	201
$OTi(\eta^2\text{-}O_2)(\eta^2\text{-}O_3)$	^3A	C_1	1131.8, 1022.4, 999.8, 806.3, 686.8, 561.4	152
$OZr(\eta^2\text{-}O_2)(\eta^2\text{-}O_3)$	^3A	C_1	1117.8, 1015.2, 912.9, 796.4, 668.3, 472.2	148
$OHf(\eta^2\text{-}O_2)(\eta^2\text{-}O_3)$	^3A	C_1	1105.6, 1014.3, 902.3, 801.3, 680.2, 451.0	153
$OTi(\eta^2\text{-}O_2)(\eta^1\text{-}O_3)$	$^3A'$	C_s	1341.2, 1117.6, 993.4, 679.8, 554.2, 516.7	152
$(\eta^2\text{-}O_2)MnO_4$	$^2A_2$	C_{2v}	1511.7, 959.2, 929.8	247
$Cu(\eta^2\text{-}O_2)(\eta^2\text{-}O_3)$	$^4A_1$	C_{2v}	1109.6, 796.4, 733.4	425
$Cu(\eta^2\text{-}O_2)(\eta^1\text{-}O_2)_2$	$^4B_1$	C_{2v}	1299.8, 1135.2, 1060.7	428
$Rh(\eta^2\text{-}O_2)_2(\eta^1\text{-}O_2)$	$^2A'$	C_s	1280.1, 1127.6, 1076.7	336
$Sc(\eta^2\text{-}O_2)_3$	$^4A_1''$	D_{3h}	1106.7, 551.7	111
$Hf(\eta^2\text{-}O_2)_3$	^3B	C_2	1092.1, 1090.2, 804.4, 563.2, 438.5	153
$(\eta^2\text{-}O_2)Sc(\eta^2\text{-}O_3)_2$	^4B	C_2	818.7, 681.2, 678.7, 544.6	111
$(\eta^2\text{-}O_2)Y(\eta^2\text{-}O_3)_2$	^4B	C_2	1107.9, 1014.9, 811.6, 656.9, 447.0	112
$Hf(\eta^2\text{-}O_2)_4$	$^5B_2$	D_{2d}	1102.4, 476.6, 423.3	153

[a] The mode assigments are discussed in the cited literature.

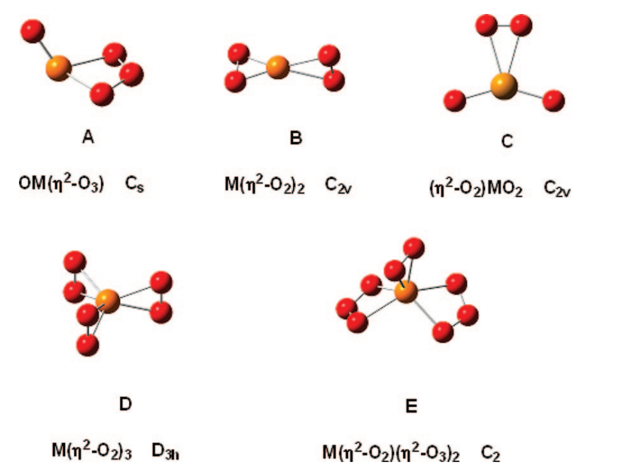

Figure 1. Optimized structures for oxygen-rich group III metal−oxygen species.

in the photoelectron spectroscopic studies,[89,93] while an ozonide complex is identified in the PES study of YO_3.[89]

Although scandium dioxide molecule is not produced in solid matrices, our recent experiments on the Sc + O_2 reaction have shown that the ground-state scandium atoms react spontaneously with two dioxygen molecules to form $OSc(\eta^2\text{-}O_3)$, which is predicted to have a $^2A'$ ground state with nonplanar C_s symmetry (Figure 1A).[111] The $OSc(\eta^2\text{-}O_3)$ complex can be regarded as $[(ScO)^+(O_3)^-]$, a scandium monoxide cation coordinated by a side-on bonded O_3^- anion. The $OSc(\eta^2\text{-}O_3)$ complex isomerizes to the $Sc(\eta^2\text{-}O_2)_2$ complex upon visible light ($400 < \lambda < 580$ nm) irradiation, which is characterized to be a superoxo scandium peroxide complex, that is, a scandium trication coordinated by an O_2^- anion and an O_2^{2-} anion. The $Sc(\eta^2\text{-}O_2)_2$ complex has a doublet ground state ($^2A_2$) with C_{2v} symmetry, in which the superoxo ScO_2 plane is perpendicular to the peroxo ScO_2 plane (Figure 1 B).[111] The $OY(\eta^2\text{-}O_3)$ and $Y(\eta^2\text{-}O_2)_2$ complexes are formed in the Y + O_2 reaction, which exhibit similar spectral, structural, and bonding properties to the scandium analogs.[112] In the lanthanum and dioxygen reaction, a $(\eta^2\text{-}O_2)LaO_2$ complex is also observed, which is the precursor for the formation of the $OLa(\eta^2\text{-}O_3)$ complex under near-infrared excitation. The $(\eta^2\text{-}O_2)LaO_2$ complex possesses a planar C_{2v} symmetry with a strong O−O stretching vibration in the superoxide region (Figure 1C).[112]

The MO_5 species (M = Y, La) have been reported only in gas-phase photoelectron spectroscopic studies. The PES spectra are quite broad and featureless.[89,93] The floppy $(O_2)_2YO$ complex is tentatively assigned as the major isomer from the PES spectrum of YO_5^-. The geometry of the neutral may be significantly changed upon detachment of the electron from the anion.[89] No structural information can be derived from the PES spectrum of LaO_5^-.[93]

The $Sc(\eta^2\text{-}O_2)_3$ complex, which possesses a strong Sc−O_2 vibration and a weak doubly degenerate O−O vibration, is the only example experimentally known with MO_6 stoichiometry in this group.[111] It is characterized to have a $^4A_1''$ ground state with D_{3h} symmetry having three side-on bonded O_2 ligands around the scandium atom, which thus presents a 6-fold coordination (Figure 1D). This complex can be described as $[Sc^{3+}(O_2^-)_3]$, a side-on bonded homoleptic scandium trisuperoxide complex. Population analysis indicates that the three unpaired electrons are mainly distributed on the three equivalent O_2^- fragments. The $Sc(\eta^2\text{-}O_2)_3$ complex is quite similar to the recently characterized 6-fold coordinated trisuperoxo $Al(\eta^2\text{-}O_2)_3$ complex.[113] Scandium is isovalent with aluminum, and both metals have three valence electrons with the highest oxidation state of +3.

The highest MO_x species reported in this group is MO_8 (M = Sc, Y), which is determined to be a 6-fold coordinated superoxo scandium (yttrium) bisozonide complex.[111,112] The complex is predicted to have a ^4B ground state with C_2 symmetry, in which the O_2 and O_3 ligands are side-on bonded to the metal center (Figure 1E). The observation of the MO_8 complex provides not only a rare example that up to eight oxygen atoms can be bound to the same metal center but also a new model complex bearing two molecular ozonide ligands in one molecule. Similar ozonide complexes of early transition metals have been theoretically proposed.[114]

3.2. Ti Group

The spectroscopic properties of ground-state TiO have been the subject of a number of experimental investigations due to its importance in catalysis and astrophysics.[24−26,115−121] Theoretical calculations confirm that the diatomic TiO molecule possesses a $^3\Delta$ ground state, in which the two unpaired electrons occupy the 1δ and 9σ orbitals that are largely derived from the Ti 3d orbitals.[27−29,61−69,122−124] For the next two members in this group, the ground state of

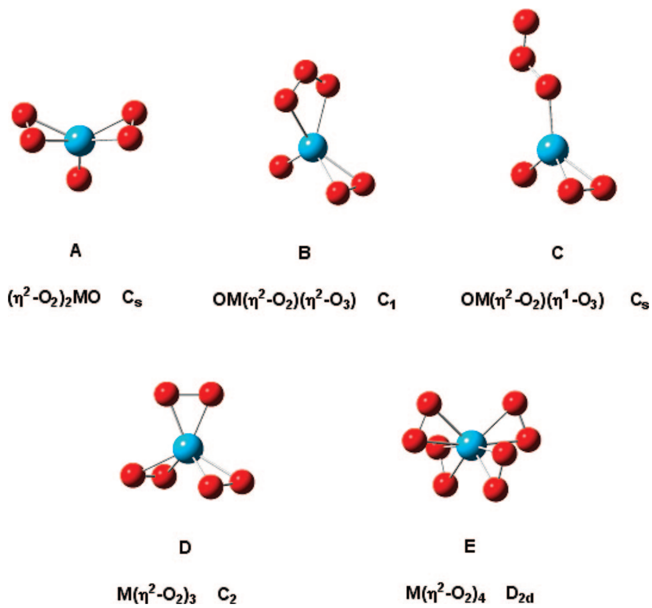

Figure 2. Optimized structures for oxygen-rich group IV metal−oxygen species.

both ZrO and HfO molecules is a closed-shell singlet ($^1\Sigma^+$),[70,73,95,116,125−129] but the energy separation between the $^3\Delta$ and $^1\Sigma^+$ states of ZrO is rather small (1099 cm^{-1}).[130] Due to lanthanide contraction, the vibrational fundamentals of ZrO and HfO, which lie lower than that of TiO, are quite close to each other.[131,132] The geometric and electronic structures of group IV metal dioxide molecules have been well established.[26,76−78,107,115,122,132−146] All of the three molecules possess a $^1A_1$ ground state with bent structure. The valence angle for TiO_2 is determined to be 113° ± 5°.[132] The HfO_2 stretching frequencies are about the same as those of ZrO_2 due to a combination of lanthanide contraction and relativistic effects for hafnium.[132]

The only experimentally observed MO_3 species in this group is the $(\eta^2\text{-}O_2)$MO complex structure.[115,147,148] All three MO_3 complexes possess a closed-shell singlet ground state and nonplanar C_s geometry with the O_2 ligand side-on bonded to the metal center.[122,147−150] These complexes are predicted to have rather long O−O bond lengths around 1.5 Å, which fall into the peroxide category. DFT/B3LYP calculations reveal that the O−O bond length increases from titanium (1.471 Å) to zirconium (1.493 Å) and hafnium (1.523 Å), which implies that the metal center tends to donate more electrons to the dioxygen ligand going down the series. As a result, the HfO_3 molecule has the longest O−O bond length and lowest O−O stretching vibrational frequency (782.8 cm^{-1}).[148] A similar periodic trend has been observed in group IV metal monocarbonyls.[151] The $(\eta^2\text{-}O_2)$TiO complex can further coordinate another dioxygen to form the TiO_5 molecule, which is characterized to be a disuperoxo titanium monoxide complex, $(\eta^2\text{-}O_2)_2$TiO. The complex is predicted to have a $^3A''$ ground state with nonplanar C_s geometry, in which the two superoxo ligands are equivalent and are side-on bonded (Figure 2A).[147]

No stable species with MO_4 stoichiometry in this group are experimentally known, due to the high stability of the closed-shell metal dioxide molecules. However, our recent studies show that the metal dioxide molecules are able to react with two dioxygen molecules to form the $OM(\eta^2\text{-}O_2)(\eta^2\text{-}O_3)$ complexes (M = Ti, Zr, Hf) in solid argon, featuring characteristic O−O stretching, antisymmetric O_3 stretching, and M═O stretching vibrations in the infrared spectra.[152,153] The geometric and electronic structures of these complexes are very similar. Taking the $OTi(\eta^2\text{-}O_2)(\eta^2\text{-}O_3)$ complex as an example, the complex is predicted to be slightly distorted from the C_s symmetry in which the O_3 subunit and the central Ti atom lie in the same plane that is perpendicular to the molecular plane, as shown in Figure 2B.[152] The side-on-bonded O_2 fragment is due to a superoxide ligand based on the observed O−O stretching frequency.[32−36] The O_3 fragment also bound in an η^2 side-on fashion with two nearly equivalent Ti−O bonds. The experimentally observed antisymmetric O−O stretching vibration of the O_3 subunit (806.3 cm^{-1}) is very close to that of the O_3^- anion isolated in solid argon.[154] While the O_2 and O_3 subunits coordinate with the Ti atom by forming weak Ti−O bonds with bond order of 0.5, the terminal Ti−O bond is strongly covalent bonded with a bond order close to 3. Therefore, the complex can be regarded as a side-on-bonded oxo−superoxo titanium ozonide complex, $[(TiO)^{2+}(O_2^-)(O_3^-)]$, that is, a TiO^{2+} dication coordinated by one O_2^- anion and one O_3^- anion.[152]

The $OTi(\eta^2\text{-}O_2)(\eta^2\text{-}O_3)$ complex rearranges to a less stable $OTi(\eta^2\text{-}O_2)(\eta^1\text{-}O_3)$ isomer under 532 nm laser irradiation, in which the O_3 unit is end-on bonded to Ti.[152] The $OTi(\eta^2\text{-}O_2)(\eta^1\text{-}O_3)$ complex is predicted to have a $^3A'$ ground state with C_s symmetry (Figure 2C). The geometric features of the $OTi(\eta^2\text{-}O_2)$ structural unit in $OTi(\eta^2\text{-}O_2)(\eta^1\text{-}O_3)$ are about the same as those in the $OTi(\eta^2\text{-}O_2)(\eta^2\text{-}O_3)$ isomer. The O_3 fragment lies in the molecular plane and binds in an η^1 end-on fashion with two different O−O bonds. The complex can also be described as $[(TiO)^{2+}(O_2^-)(O_3^-)]$, an end-on bonded oxo−superoxo titanium ozonide complex. It is found that these two structural isomers are interconvertible, that is, formation of the end-on-bonded isomer is accompanied by demise of the side-on-bonded complex under 532 nm laser irradiation and vice versa upon sample annealing. Theoretical calculations predict that the side-on bonded complex is 7.3 kcal/mol more stable than the end-on bonded isomer at the B3LYP/6-311+G(d) level of theory. The reaction from side-on to end-on is endothermic and is computed to have a barrier height of 10.5 kcal/mol at the triplet potential energy surface. Figure 3 clearly shows the formation and interconversion of the two TiO_6 isomers.

The photoinduced isomerization reaction feature of $OHf(\eta^2\text{-}O_2)(\eta^2\text{-}O_3)$ is different from that of $OTi(\eta^2\text{-}O_2)(\eta^2\text{-}O_3)$. The $OHf(\eta^2\text{-}O_2)(\eta^2\text{-}O_3)$ complex rearranges to a $Hf(\eta^2\text{-}O_2)_3$ isomer under visible light irradiation and the rearrangement is reversed upon UV irradiation (266 nm).[153] Unlike the trisuperoxo complexes of scandium and aluminum, which have D_{3h} and D_3 symmetry with three equivalent superoxo ligands,[111,113] the $Hf(\eta^2\text{-}O_2)_3$ complex is characterized to have a ^3B ground state with C_2 symmetry (Figure 2D).[153] According to DFT calculations, the $Hf(\eta^2\text{-}O_2)_3$ complex is 6.1 kcal/mol more stable than the $OHf(\eta^2\text{-}O_2)(\eta^2\text{-}O_3)$ isomer. At the optimized geometry of $Hf(\eta^2\text{-}O_2)_3$, two O_2 subunits are side-on bonded and are equivalent with an O−O bond length of 1.338 Å, which falls into the range of superoxide. The third O_2 subunit is also side-on bonded with a much longer O−O bond length than that of the other two O_2 subunits. The predicted O−O bond length of 1.512 Å is appropriate for a peroxide complex. Accordingly, the $Hf(\eta^2\text{-}O_2)_3$ molecule can be considered as $[Hf^{4+}(O_2^-)_2(O_2^{2-})]$, a side-on bonded disuperoxo hafnium peroxide complex.

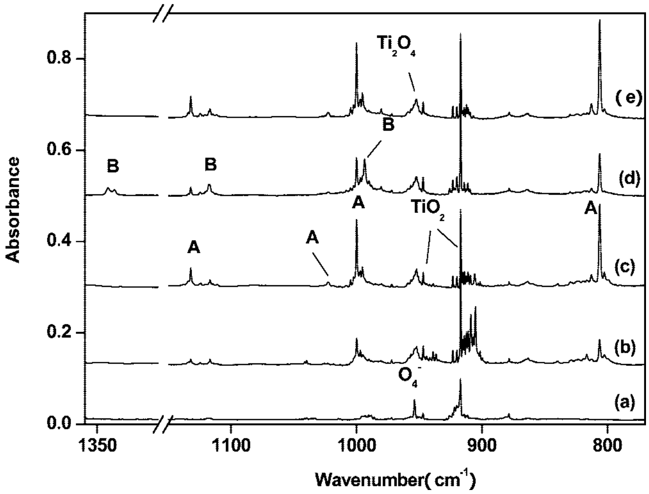

Figure 3. Infrared spectra in the 1360−1300 and 1150−770 cm^{-1} regions from co-deposition of laser-evaporated titanium atoms with 0.5% O_2 in argon: (a) 1 h of sample deposition at 6 K; (b) after 35 K annealing; (c) after 40 K annealing; (d) after 15 min 532 nm irradiation; (e) after 35 K annealing (A and B denote absorptions of $OTi(\eta^2\text{-}O_2)(\eta^2\text{-}O_3)$ and $OTi(\eta^2\text{-}O_2)(\eta^1\text{-}O_3)$). Reproduced from ref 152. Copyright 2007 American Chemical Society.

According to our recent studies on the reaction of hafnium atoms and O_2, the hafnium center can be coordinated by up to four O_2 molecules in forming a homoleptic tetrasuperoxo hafnium complex, $Hf(\eta^2\text{-}O_2)_4$.[153] DFT/B3LYP calculations predict a $^5B_2$ ground state with D_{2d} symmetry, in which the four O_2 ligands are side-on bonded with the two oxygen atoms in each O_2 subunit being slightly inequivalent (Figure 2E). Similar structure has been observed previously in group V and VI tetraperoxometallate anions.[4g,155] The $^5B_2$ ground state of $Hf(\eta^2\text{-}O_2)_4$ has an electronic configuration of (core) $(a_2)^1(b_1)^1(e)^2$ with two unpaired electrons occupying the nonbonding a_2 and b_1 molecular orbitals, which are the combinations of four O_2^- π^* orbitals. The remaining two unpaired electrons occupy the doubly degenerate e molecular orbitals, which are also combinations of four O_2^- π^* orbitals but comprise significant O_2^- π^* to Hf^{4+} bonding. The $Hf(\eta^2\text{-}O_2)_4$ complex is the only example of a binary neutral transition metal complex with four side-on bonded superoxide ligands.

3.3. V Group

Both the VO and NbO diatomic molecules are determined to have a $^4\Sigma^-$ ground state.[24−29,61−72,88,156−171] In contrast, the ground state of TaO is a $^2\Delta$ state.[73,168,172−178] The metal dioxides of this group are bent molecules.[26,76−78,160−165,172,174,179−181] Both the symmetric (ν_1) and antisymmetric (ν_3) stretching modes have been observed in solid matrices.[182−187] Recent experiments indicate that the dioxide molecules trapped in solid argon are coordinated by two argon atoms and should be regarded as the $MO_2(Ar)_2$ complexes.[188,189] However, argon atom coordination only slightly changes the spectral and structural properties of the dioxide molecules. Based on the observed isotopic frequency ratios of the ν_3 mode, the valence bond angle is estimated to be 118° ± 3° for VO_2, 108° ± 5° for NbO_2, and 106° ± 5° for TaO_2.[182,183] Due to the anharmonicity in the ν_3 mode, the true angles of these dioxide molecules will be on the order of 4° lower than the estimated upper limits. While the stretching frequencies for VO_2 and TiO_2 are similar,[132,182] the stretching frequencies for NbO_2 and TaO_2 are some 50−100 cm^{-1} higher than their neighboring ZrO_2 and HfO_2 molecules, which are estimated to have similar valence angle upper limits around 115° ± 5°.[132] The frequencies for TaO_2 are some 30 cm^{-1} higher than those for the lighter NbO_2 molecule.[183] This suggests greater lanthanide contraction and relativistic effect for Ta relative to Nb than that for Hf relative to Zr. All three dioxide molecules are predicted to have a $^2A_1$ ground state.[76−78,160−164,172,179,183]

The infrared spectrum of the neutral VO_3 molecule has not been reported in solid matrices. DFT/B3LYP and BP86 calculations suggest a pyramidal structure with C_s symmetry to be the most stable structure for VO_3.[160,161] However, a nonplanar trigonal geometry with C_{3v} symmetry is predicted to be the ground state at the BPW91 level of theory,[162] which is consistent with the result given by diffusion quantum Monte Carlo calculations using BP86 and B3LYP methods.[163] In a matrix ESR spectroscopic investigation on the VO_x (x = 1−3) system, an anisotropic octet absorption (g = 2.022) with a relatively small ^{51}V $A_\perp$ value of ±62 MHz is tentatively assigned to the VO_3 radical.[164] Although the CASSCF calculations suggest that the minimum energy structure is pyramidal with C_s symmetry, a planar isomer with C_{2v} symmetry is calculated to be about 31 kcal/mol lower in energy than the C_s structure using MR-SDCI method. This planar C_{2v} structure is proposed to be the origin of the observed matrix ESR signal. A gas-phase PES study indicates that the VO_3 molecule has a large adiabatic electron affinity of 4.36(5) eV due to the closed-shell nature of the VO_3^- anion.[165] The first detachment feature of the VO_3^- anion in the PES spectrum is associated with the bending mode involving two oxygen atoms, and no VO stretching vibrational progression has been observed. No detailed structural information on the neutral TaO_3 molecule can be derived from the photoelectron spectrum of TaO_3^- except for a broad featureless band beginning at around 2 eV.[161] Both the NbO_3 and TaO_3 molecules are theoretically predicted to have three-dimensional pyramidal structures.[172,180]

The metal dioxide−dioxygen complex structure is the only structure experimentally characterized with MO_4 stoichiometry (M = V, Nb, Ta).[182,183] In an early report on photoinduced oxidation of $V(CO)_6$ in the presence of O_2 in solid argon, a group of absorptions are attributed to an end-on bonded $OOVO_2$ complex.[190] In the following study on the reaction of laser-ablated vanadium atoms with O_2, similar absorptions are assigned to the end-on coordinated $OOVO_2$ complex.[182] The assignment of the end-on bonded structure is based on the observation of 1.8 cm^{-1} split for the intermediate absorption of the O−O stretching vibration in the spectrum using a $^{16}O_2$ + $^{16}O^{18}O$ + $^{18}O_2$ sample. However, the side-on bonded $(\eta^2\text{-}O_2)VO_2$ isomer is theoretically predicted to be more stable than the end-on bonded isomer.[160−163,183] Recent matrix isolation infrared spectroscopic work in this laboratory shows that the experimentally observed absorptions should be reassigned to the side-on bonded complex, which is coordinated by one argon atom to form the $VO_4(Ar)$ complex in a solid argon matrix.[188] The $VO_4(Ar)$ complex has a $^2A''$ ground state with C_s symmetry (Figure 4). The Ar atom and the coordinated O_2 subunits are in the same plane, which is perpendicular to the VO_2 plane. The two oxygen atoms in the coordinated O_2 subunit are slightly inequivalent due to argon atom coordination. As a result, the intermediate absorption of the O−O stretching vibration should split into two closely spaced absorptions in the spectrum with the $^{16}O_2$ + $^{16}O^{18}O$ + $^{18}O_2$ sample. The NbO_4 and TaO_4 complexes have the same structure as the

$(\eta^2\text{-}O_2)VO_2$ C_{2v} $(\eta^2\text{-}O_2)VO_2(Ar)$ C_s

Figure 4. Optimized structures for VO_4 and $VO_4(Ar)$.

vanadium analog.[189] The metal−Ar binding energies for these noble gas atom complexes are predicted to be within several kcalories per mole, which are comparable with those of previously reported transition metal−noble gas complexes.[191]

The $(O_2)_2VO$ complex is the only example in this group with MO_5 stoichiometry that has been theoretically reported. The geometry of this complex is similar to that of the $(O_2)_2TiO$ complex, which is determined to have nonplanar C_s symmetry. The $(O_2)_2VO$ complex has a $^2A''$ ground state with quite long O−O bonds (1.45 Å predicted at the BPW91/LANL2DZ level of theory).[162] It is found that the $(\eta^2\text{-}O_2)MO_2$ complexes are able to coordinate another dioxygen molecule to form the very weakly bonded $(\eta^2\text{-}O_2)MO_2{-}O_2$ complexes.[188,189] No other structures have been reported.

3.4. Cr Group

Chromium monoxide possesses a $^5\Pi$ ground state with a $(\text{core})(9\sigma)^1(1\delta)^2(4\pi)^1$ electronic configuration, in which the last electron occupies the 4π antibonding orbital derived from the Cr $3d_\pi$ and O $2p_\pi$ orbitals due to the large 3d−3d exchanged energy.[24−29,61−69,192−200] The population in the antibonding orbital suggests the decrease in the Cr−O bond order. The Cr−O fundamental observed at 885 cm^{-1} in the gas phase is about 100 cm^{-1} red-shifted from that of its neighboring vanadium monoxide.[24] The CrO fundamental in neon (880.2 cm^{-1}) is slightly red-shifted from the gas-phase value,[201] but a large shift about 35 cm^{-1} is observed for the corresponding argon matrix value (846.3 cm^{-1}).[202] Recent study shows that the CrO molecule trapped in solid argon is coordinated by an argon atom. The absorption at 846.3 cm^{-1} in solid argon should be assigned to ArCrO instead of the isolated diatomic molecule.[38]

Similar to the chromium congener, molybdenum monoxide also has a $^5\Pi$ ground state,[70,71,116,157,192,196,203−207] whose infrared absorption is observed at 893.5 cm^{-1} in solid argon.[208] The ground electronic state of the diatomic WO molecule remains unclear. A $^3\Sigma^-$ spin state has been considered as the ground state in most experimental and theoretical studies.[192,203,209−212] However, a $^5\Pi$ state was predicted to be the lowest state from the SCF and CASSCF calculations,[213] on the basis of which several low-lying electronic states in the near-infrared region are identified.[214] In a more recent theoretical investigation, a closed-shell singlet state was calculated to be lowest in energy using a series of DFT methods.[73] The vibrational fundamentals of WO were experimentally determined to be around 1050 cm^{-1} both in the gas phase and in different noble gas matrices.[25,201,210]

The chromium dioxide molecule has been produced either via the reaction of chromium atom with O_2 or from photo-oxidation of $Cr(CO)_6$ in O_2-doped matrices.[215,216] According to the most recent matrix investigations, the symmetric and antisymmetric stretching vibrations are observed at 914.4 and 965.4 cm^{-1} in argon and 920.8 and 971.9 cm^{-1} in neon.[201,202] The symmetric stretching and bending vibrations are determined to be 895 ± 20 and 220 ± 20 cm^{-1} from photoelectron spectroscopy in the gas phase.[217] Theoretical calculations at different levels reveal that CrO_2 has a $^3B_1$ ground state with bent geometry.[76,77,197,201,202,218−221] The bond angle is determined to be 128° ± 4° based on the observed chromium and oxygen isotopic shifts of the ν_3 mode.[202] Besides the dioxide structure, the chromium dioxygen complex isomer has also been reported from photoelectron spectroscopic study of the CrO_2^- anion in the gas phase. A weak signal observed around 1.5 eV is assigned to the photodetachment band of the $Cr(O_2)^-$ anion, which results in the formation of the chromium peroxide complex, $Cr(O_2)$.[197]

The molybdenum dioxide molecule has also been characterized to have a triplet ground state with bent geometry.[71,201,216,219,222−224] The bond angle is estimated to be around 118° ± 4° from the observed Mo and O isotopic frequencies in solid argon and neon.[201,202] The last member in this group, the tungsten dioxide molecule, has a singlet ground state.[201,219] The singlet−triplet separation was experimentally determined to be 0.327(6) eV from photoelectron spectroscopy.[225] The vibrational frequencies of ground state WO_2 are measured at 1030 cm^{-1} (ν_1) and 983 cm^{-1} (ν_3) in solid neon,[201,214] about 50 cm^{-1} higher than those observed in solid argon and krypton.[201,210,226] The large neon-to-argon shifts suggest the existence of strong interactions between tungsten dioxide and matrix noble gas atoms.

The trioxide molecules of group VI metals are the only experimentally observed isomers with MO_3 stoichiometry.[197,201,202,210,212,216,224,226−231] Gas-phase PES studies reveal that all three trioxide molecules in this group possess large HOMO−LUMO gaps, suggesting that these oxides are highly stable species and can serve as building blocks for large clusters and bulk materials.[197,227−229] All three trioxide molecules have been identified in matrix infrared studies from their characteristic doubly degenerate M=O stretching vibrations.[201,202,210,212,224,226] Calculations at various levels predict that these trioxide molecules all have a closed-shell $^1A_1$ ground state with pyramidal C_{3v} symmetry.[78,197,201,210,223,227,228,232−235] All the metal valence electrons are involved in bonding with oxygen, and the metal centers are in their highest +6 oxidation state.

The information on group VI MO_4 species is mainly obtained from gas-phase PES investigations, as well as theoretical calculations. The vibrational assignments of MO_4 species remain unclear in solid matrices although some assignments have been proposed.[202,210,216] A PES study on the CrO_n ($n = 1{-}5$) system suggests that CrO_4 is a chromium dioxide−dioxygen complex, $(O_2)CrO_2$, which is predicted to have a closed-shell singlet ground state with C_2 symmetry (DFT/BPW91).[197] The vertical electron detachment energy for the ground state of $(O_2)CrO_2^-$ anion is predicted to be 4.95 eV, in good agreement with the experimental value of 5.07 eV. Recent density functional calculations at B3LYP level on the WO_4 isomers reveal that the spectroscopic character of an end-on bonded tungsten dioxide−dioxygen complex structure is identical to the results from a vibrationally resolved PES study despite its metastable character.[236,237] However, a more recent PES investigation indicates that tungsten prefers tetrahedral coordination with oxygen without an O−O bond.[228] WO_4, as well as MoO_4, possesses extremely high electron affinities; thus, they belong to the category of strong oxidizers called superhalogens. The calculation of the ground state of neutral WO_4 is particularly difficult due to symmetry-breaking issues. At the CCSD(T)/aug-cc-pVDZ level of theory, the ground state of WO_4 is predicted to be

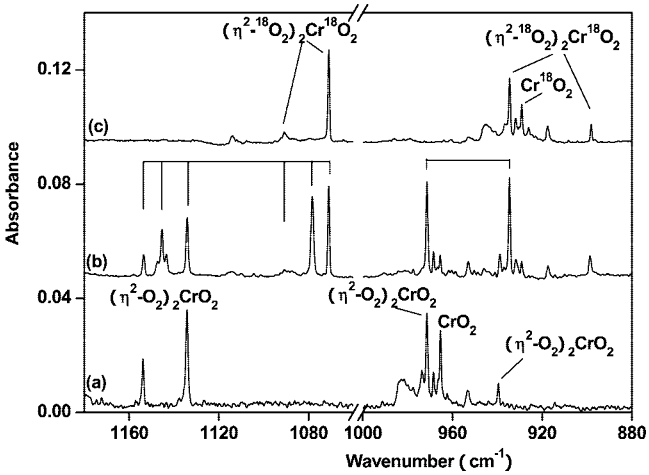

Figure 5. Infrared spectra in the 1180−1060 and 1000−880 cm^{-1} regions from co-deposition of laser-ablated chromium atoms with isotopically substituted O_2 in excess argon at 12 K. Spectra are taken after 1 h of sample deposition followed by 45 K annealing: (a) 2.0% $^{16}O_2$; (b) 1.5% $^{16}O_2$ + 1.5% $^{18}O_2$; and (c) 2.0% $^{18}O_2$. Reproduced from ref 238. Copyright 2008 American Chemical Society.

a triplet $^3A_2$ state with D_{2d} symmetry with a W−O distance of 1.828 Å and a ∠OWO bond angle of 102.2°, significantly distorted from the ideal T_d geometry. The W−O bond distance is not that of an oxo O but is more like that of an oxyl (−O•).[228] The metal dioxide−dioxygen complex isomer, which is proposed to exist in solid noble gas matrices, is predicted to be higher in energy than the D_{2d} structure.

Structural information on the ground-state MO_5 species has been obtained only from photoelectron spectroscopy, as well as theoretical predictions.[197,228] The most stable structure for all three MO_5 species is found to be a dioxygen complex of metal trioxide, $(O_2)MO_3$. On the basis of experimental electron detachment energies and theoretical calculations, the $(O_2)CrO_3$ complex is determined to have a $^3A''$ ground state with an end-on bonded O_2 moiety. The O−O bond distance is predicted to be 1.22 Å at the BPW91 level of theory, only slightly longer than that of free O_2, suggesting a weak interaction between O_2 and CrO_3.[197] The O_2 ligand is much more activated upon coordination to tungsten trioxide.[228] The O−O bond length of the $(O_2)WO_3$ complex is predicted to be 1.312 Å at the B3LYP level; thus, WO_5 can be described as an O_2^- interacting with WO_3^+. In the ground state of WO_5, one unpaired electron is localized on the O_2 fragment as in the case of the anion, and the other unpaired electron is localized on one of the O atoms of WO_3, giving rise to the unusual charge-transfer complex, $(O_2^-)WO_3^+$. The energy for addition of O_2 to WO_3 to form WO_5 is estimated to be exothermic by only 13.7 kcal/mol at the CCSD(T)/aug-cc-pVTZ level. This exothermicity is 3 eV less than that of WO_2 plus O_2 and shows that only a weak complex of O_2 with WO_3 is formed because the three oxo bonds in WO_3 have consumed all the available valency of W.[228]

The metal dioxide−bisdioxygen complex structure is the only structural isomer experimentally characterized with MO_6 stoichiometry. A group of absorptions at 1153.9, 1134.2, 971.5, 939.6, and 532.0 cm^{-1} from the reaction of chromium atom with dioxygen in solid argon have been assigned to CrO_6 based upon the observed mixed isotopic spectral features (Figure 5).[201,238] The assignment of the 1153.9, 1134.2, and 971.5 cm^{-1} absorptions to CrOO, OOCrOO, and $OOCrO_2$ species in early matrix isolation studies is incorrect.[202] The $(\eta^2\text{-}O_2)_2CrO_2$ complex is predicted to have a $^3B_2$ ground state with a tetrahedral skeleton of C_{2v} symmetry, in which the two O_2 fragments lie in the same plane, which is perpendicular to the OCrO plane.[238] The two η^2-O_2 fragments are equivalent and bound in an asymmetric, side-on fashion, with two slightly inequivalent Cr−O bonds (Figure 6). The $(\eta^2\text{-}O_2)_2CrO_2$ complex can be regarded as a side-on bonded disuperoxo chromium dioxide complex, $[(O_2^-)_2(CrO_2)^{2+}]$, where two O_2^- anions are bound to a CrO_2^{2+} dication.[238] The MoO_6 and WO_6 complexes are characterized to have similar structures as CrO_6.[201]

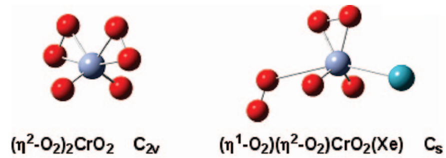

Figure 6. Optimized structures for CrO_6 and CrO_6(Xe).

Our recent matrix experiments reveal that the $(\eta^2\text{-}O_2)_2CrO_2$ complex can undergo a xenon-atom-induced disproportionation reaction to give a xenon atom coordinated $(\eta^1\text{-}OO)(\eta^2\text{-}O_2)CrO_2(Xe)$ complex.[238] The $(\eta^1\text{-}OO)(\eta^2\text{-}O_2)CrO_2(Xe)$ complex is predicted to have a C_s symmetry and $^3A''$ ground state with the two O_2 fragments and xenon atom in the same plane, which is perpendicular to the OCrO plane (Figure 6). The end-on bonded η^1-OO fragment is predicted to have an O−O bond length of 1.206 Å, which is about the same as that of free O_2, while the Cr−OO distance is calculated to be rather long (3.903 Å) at the B3LYP level. Therefore, the complex is regarded as a triplet O_2 molecule adsorbed on a closed-shell $(\eta^2\text{-}O_2)CrO_2(Xe)$ complex. The conversion from the disuperoxo chromium dioxide complex to the peroxo−chromium dioxide−xenon complex reaction provides a model system in demonstrating O_2 activation through electron transfer from metal oxides to form the superoxo complex and further convert to dioxygen and peroxide complex.

3.5. Mn Group

Due to the occupation of another doubly degenerate antibonding 4π orbital, the diatomic MnO molecule has a $^6\Sigma^+$ ground state with a (core)$(9\sigma)^1(1\delta)^2(4\pi)^2$ electronic configuration. The ground-state MnO molecule has the highest magnetic moment among the first row transition metal monoxide molecules.[27−29,61−69,239−243] The MnO bond is even weaker than that of its neighboring CrO. Therefore, the vibrational fundamental of MnO observed in the gas phase and in solid matrices is slightly lower than that of CrO.[24,244−246] An early ESR investigation suggested that the inserted manganese dioxide molecule is linear in the noble gas matrix.[243] However, subsequent matrix isolation infrared absorption spectroscopic investigation provided solid evidence that manganese dioxide is bent. Both the symmetric and antisymmetric stretching vibrations are observed in solid matrices.[246] The upper limit of valence angle is estimated to be 140° ± 5° from the ν_3 isotopic frequency ratio. The symmetric stretching mode is determined to be 800 ± 40 cm^{-1} from PES study in the gas phase,[240] which is in good agreement with the 816.4 cm^{-1} value in solid argon.[246] Theoretical calculations at different levels reveal that the inserted MnO_2 molecule has a $^4B_1$ ground state with a bent structure.[76,77,239,240,246] The end-on bonded superoxide complex MnOO and the side-on bonded peroxide complex $Mn(O_2)$ were suggested to exist in solid matrices from early matrix isolation studies.[246] However, recent investigation in our laboratory indicates that the absorptions previously assigned to the $Mn(O_2)$ complexes are due to larger clusters.[247] Theoretical calculations indicate that both the side-on and end-on bonded $Mn(O_2)$ complexes are much higher in energy than the inserted dioxide isomer.[76,77,239] Gas-phase studies suggest that the ground-state manganese atoms are unreactive toward O_2.[248] It is very unlikely that these high-energy manganese dioxygen complexes can be formed and trapped in noble gas matrices.

Two structural isomers have been reported for MnO_3. A matrix-isolation ESR study indicated that MnO_3 exhibits very large manganese hyperfine coupling, which suggests that the unpaired spin is best described as occupying an sd_{z^2} hybrid orbital, resulting in a molecule of planar D_{3h} symmetry and $^2A_1$ ground state.[243] Theoretical calculations predict that the ground state of MnO_3 is $^2A_1$, which possesses a pyramidal C_{3v} geometry.[240] The photoelectron spectrum of MnO_3^- at 266 nm reveals a single vibrationally resolved band with an 840 cm^{-1} vibrational spacing and an adiabatic binding energy of 3.335 eV. The observed features are assigned to detachment transitions from the ground state of MnO_3^- to that of MnO_3. The observed vibrational progression is attributed to the symmetric Mn=O stretching vibration.[240] Matrix-isolation infrared absorption spectroscopic investigation of the reactions of laser-ablated manganese atoms with dioxygen failed to produce the manganese trioxide molecule. In contrast, a $(\eta^2\text{-}O_2)MnO$ complex was tentatively identified with the Mn=O stretching vibration observed at 886.9 cm^{-1} in solid argon.[246]

Two structural isomers have been reported experimentally for MnO_4. In a photoelectron spectroscopic study of MnO_4^- in gas phase, the observed spectral features were attributed to transitions from the ground state of the tetrahedral MnO_4^- anion to the ground and excited states of the MnO_4 neutral, which is proposed to be a distorted tetrahedron with all four oxygen atoms bonded to the Mn center dissociatively.[249] This MnO_4 structure was determined to have an electron affinity of 5 eV, which is significantly larger than that of atomic chlorine, the most electronegative element in the periodic table. In our recent matrix isolation study, a manganese dioxide−dioxygen complex, $(\eta^2\text{-}O_2)MnO_2$, is formed via the reaction of MnO_2 and O_2 in solid argon. The complex is characterized to be a side-on bonded peroxo manganese dioxide complex.[247] Theoretical calculations on MnO_4 present contradictory results. The side-on bonded $(\eta^2\text{-}O_2)MnO_2$ complex structure and the distorted tetrahedral isomer without O−O bonding are predicted to be close in energy with the complex structure being slightly (0.18 eV) less stable than the distorted tetrahedral isomer according to the BPW91 calculations.[249,250] In contrast, the complex structure is predicted to be about 4.4 kcal/mol more stable than the distorted tetrahedral isomer from our newly performed B3LYP calculations.[247] Single point energy calculations at the CCSD(T) level with the B3LYP optimized geometries give an even larger energy separation of 12.5 kcal/mol.[247]

The only experimentally characterized species with MnO_6 stoichiometry is $(\eta^2\text{-}O_2)MnO_4$, a dioxygen complex of manganese tetroxide, which is produced from the reaction of O_2 and the $(\eta^2\text{-}O_2)MnO_2$ complex in solid argon.[247] This complex features an unusually intense O−O stretching vibration at 1511.7 cm^{-1}. Theoretical calculations predict that the $(\eta^2\text{-}O_2)MnO_4$ complex has a $^2A_2$ ground state with C_{2v} symmetry, in which the O_2 fragment is coordinated to two oxygen atoms of the MnO_4 fragment, as shown in Figure 7.

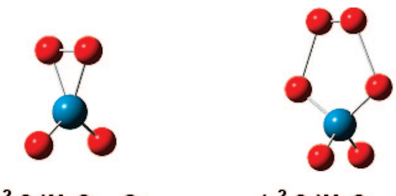

Figure 7. Optimized structures for MnO_4 and MnO_6.

The O−O bond length of the O_2 fragment in the $^2A_2$ ground state $(\eta^2\text{-}O_2)MnO_4$ complex is predicted to be 1.184 Å at the B3LYP/6-311+G(d) level, slightly shorter than the value of free molecular oxygen, whereas the O−O distance between the O_2 and MnO_4 fragments is computed to be 2.226 Å,[247] significantly longer than that of typical O−O single bond and even longer than that of the H_2OOO^+ cation, which is characterized to be a 3c−1e bond.[251] Unlike a number of transition metal dioxygen complexes, in which the O_2 fragment is negatively charged, natural charge population analysis shows that the O_2 ligand in $(\eta^2\text{-}O_2)MnO_4$ is positively charged by about +0.21 e. However, the $(\eta^2\text{-}O_2)MnO_4$ complex cannot be regarded as a pure ionic $[O_2^+][MnO_4^-]$ charge-transfer complex. Generally, the O−O stretching vibrational modes of dioxygenyl fluorometallate salts, which are regarded as pure ionic compounds, lie around 1850 cm^{-1}.[252] The O−O stretching frequency of $(\eta^2\text{-}O_2)MnO_4$ is very close to that of the $XeOO^+$ cation (1507.9 cm^{-1}) in solid argon, which is characterized to involve a $(p-\pi^*)$ σ bonding between Xe and O_2.[253] The interaction between O_2 and MnO_4 in $(\eta^2\text{-}O_2)MnO_4$ is similar to that in the dioxygen complex of FSO_3 radical.[254] The experimental electron affinity of MnO_4 is determined to be 4.80 ± 0.10 eV,[249] about the same as that of the FSO_3 radical,[255] but is much smaller than that of PtF_6 (7.00 ± 0.35 eV).[256] PtF_6 is well-known to be able to oxidize the O_2 molecule to form the $[O_2^+][PtF_6^-]$ charge-transfer complex.[257]

Experimental reports on simple oxide and dioxygen complexes of Tc are rare due to the radioactive character of Tc. Much of the information on Tc system comes from theoretical calculations. Technetium monoxide is predicted to have a $^6\Sigma^+$ ground state using both density functional and modified coupled pair functional (MCPF) methods.[70,71,207] These calculations yield an equilibrium bond length around 1.76 Å and a vibrational fundamental in the range of 840−910 cm^{-1}. All three structural isomers with TcO_2 stoichiometry have been calculated.[78] For the inserted technetium dioxide molecule with bent C_{2v} symmetry, a $^4B_2$ state is predicted to be the ground state using the MCPF method.[78] However, calculations at the DFT/B3LYP level find a $^4B_1$ state to be the ground state, which is about 12 kcal/mol lower in energy than the $^4B_2$ state.[258] Both the end-on superoxo ($^8A''$) and side-on peroxo ($^4B_2$) complexes are predicted to be about 90 kcal/mol less stable than the inserted dioxide isomer at the MCPF level of theory.[78] The technetium trioxide molecule is computed to have a $^2A_1'$ ground state with planar D_{3h} symmetry.[78]

The ground state of rhenium monoxide remains unclear. The vibrational frequency of ReO is determined to be 979.1 cm^{-1} from the emission spectrum in the gas phase.[259] In a recent intermodulated fluorescence spectroscopic study, a $^2\Delta$ state with (core)$1\sigma^2 2\sigma^2 1\pi^4 1\delta^3 3\sigma^2$ electronic configuration is found to be consistent with the experimentally observed magnetic hyperfine constant.[260] However, a $^4\Phi$ state is predicted to be the ground state by BP86 and B3LYP calculations with the $^2\Delta$ and $^6\Sigma^+$ states lying slightly higher in energy;[261] the $^6\Sigma^+$ state is suggested to be the ground state in a recent theoretical study using various DFT methods.[73]

Both rhenium dioxide and trioxide molecules have been reported in solid matrix-isolation infrared spectroscopic and gas-phase PES studies.[261,262] The inserted ReO_2 molecule is determined to have a $^4B_1$ ground state with bent C_{2v} symmetry.[258,261] The rhenium trioxide molecule is found to have a $^2A_1$ state with pyramidal C_{3v} geometry.[261] The electron affinities of ReO_2 and ReO_3 are measured to be 2.5 ± 0.1 and 3.6 ± 0.1 eV, respectively.[262] For the oxygen-rich ReO_4 species, a peroxo rhenium dioxide complex, $(\eta^2\text{-}O_2)ReO_2$, has been identified in solid matrices. Theoretical calculations at the BP86 and B3LYP levels reveal that the $(\eta^2\text{-}O_2)ReO_2$ complex has a closed-shell singlet ground state with non-planar C_{2v} symmetry.[261]

3.6. Fe Group

The diatomic FeO molecule is one of the most studied metal oxide species. Its molecular constants have been obtained by matrix infrared, photoelectron, photoluminescent, microwave, and electronic spectroscopy.[24−26,40,263−275] It has also been the subject of a number of theoretical studies.[27−29,61−69,123,239,276−282] It is well established that FeO has a $^5\Delta$ ground state with five closely spaced spin orbital components (about 200 cm^{-1}). The vibrational fundamental is experimentally determined to be around 870 cm^{-1} in the gas phase as well as in solid noble gas matrices.[24,266,270,272,274]

The FeO_2 species have been the subject of a number of gas-phase and matrix experimental studies. Anion photoelectron spectroscopic investigation on FeO_2^- indicates that only the inserted FeO_2 neutral structure is observed in the gas phase.[268,269] The photoelectron spectra of FeO_x^- (x = 1−4) are shown in Figure 8. However, spectral assignments on the FeO_2 species in solid matrices are not straightforward, and many disagreements are found in the literature. In an early matrix-isolation infrared spectroscopic study on the reaction of thermally evaporated iron atoms with dioxygen, absorptions at 945.9 and 517.1 cm^{-1} are assigned to vibrations of the cyclic $Fe(O_2)$ molecule in solid argon.[283] In the next work, three FeO_2 isomers were proposed to be formed from the reactions of hollow-cathode sputtered iron atoms with dioxygen in argon. A band at 956 cm^{-1} was assigned to the O−O stretching mode of the cyclic $Fe(O_2)$ structure, while the bands at 969 and 946 cm^{-1} were attributed to the linear and bent OFeO isomers.[284] In the photooxidation of matrix-isolated iron pentacarbonyl in the presence of oxygen, a 956 cm^{-1} absorption was also assigned to the cyclic $Fe(O_2)$ molecule, but a 945 cm^{-1} absorption was attributed to FeO_3 instead of OFeO.[285] More recent investigations employed the reactions of laser-ablated iron atoms with dioxygen; the absorption at 956.0 cm^{-1} was retained for cyclic $Fe(O_2)$, but the absorptions at 945.8 and 797.1 cm^{-1} were assigned to the antisymmetric and symmetric stretching modes of the inserted FeO_2 molecule, while an absorption at 1204.5 cm^{-1} was characterized as the O−O stretching mode of a FeOO isomer.[270,286] The assignment of the bent inserted FeO_2 molecule was further supported by a matrix-isolation Mössbauer spectroscopic study.[287] The bond angle was determined to be 150° ± 10° based upon the observed oxygen and iron isotopic ν_3 frequencies.[270,286] Recently, we reinvestigated the reaction of iron atoms and dioxygen using matrix-isolation infrared absorption spectroscopy.[288] We found that the inserted iron dioxide molecule was the only isomer with FeO_2 stoichiometry formed in solid argon. The absorptions previously assigned to FeOO (1204.5 cm^{-1}) and cyclic $Fe(O_2)$ (956.0 cm^{-1}) are due to the end-on and side-on bonded dioxygen−iron dioxide complexes formed by the reactions of inserted FeO_2 molecule with dioxygen in the matrix.[288] It was not possible to determine the ground state of iron dioxide from the theoretical point of view since the relative stability of different spin states depends strongly on the theoretical levels employed.[76,77,239,270,286,289−294] The ground state of iron dioxide was determined to be $^3B_1$ based on comparison between the calculated and experimentally observed vibrational frequencies and isotopic frequency ratios.[270,286] Both the side-on bonded $Fe(O_2)$ and end-on bonded FeOO complexes were predicted to lie much higher in energy than the inserted FeO_2 isomer according to most theoretical predictions.[76,77,270,286]

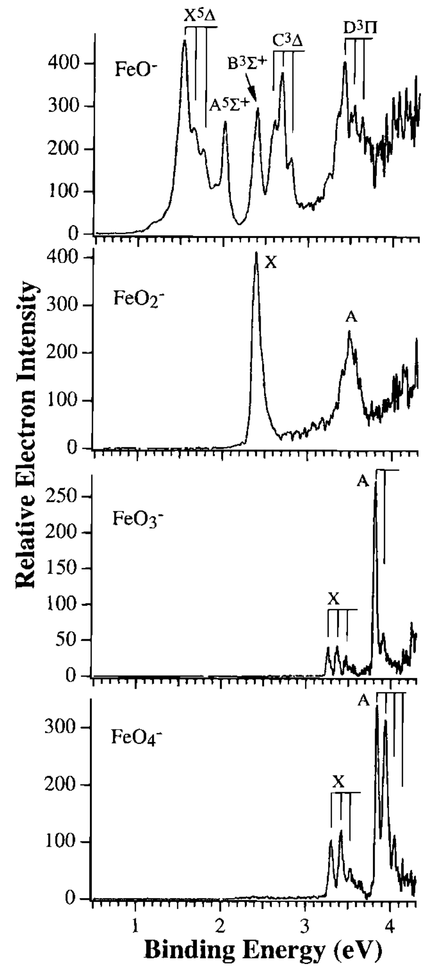

Figure 8. Photoelectron spectra of FeO_x^- (x = 1−4) at 266 nm. The vertical lines indicate the resolved vibrational structures. X represents the ground state of the neutrals, and the other letters represent the excited states. Reproduced from ref 268a. Copyright 1996 American Chemical Society.

Two structural isomers with FeO_3 stoichiometry have been reported. A vibrationally resolved photoelectron spectroscopic study indicates that the observed FeO_3 species is due to the D_{3h} iron trioxide molecule with three Fe═O bonds. The symmetric Fe═O stretching vibrational frequency was determined to be 850 ± 50 cm^{-1}.[268] Both the trioxide structure and an iron monoxide−dioxygen complex structure, $(O_2)FeO$, were suggested to be formed in previous matrix-isolation studies.[270] However, the spectral assignments were proven to be incorrect. Recently, both the $(O_2)FeO$ complex

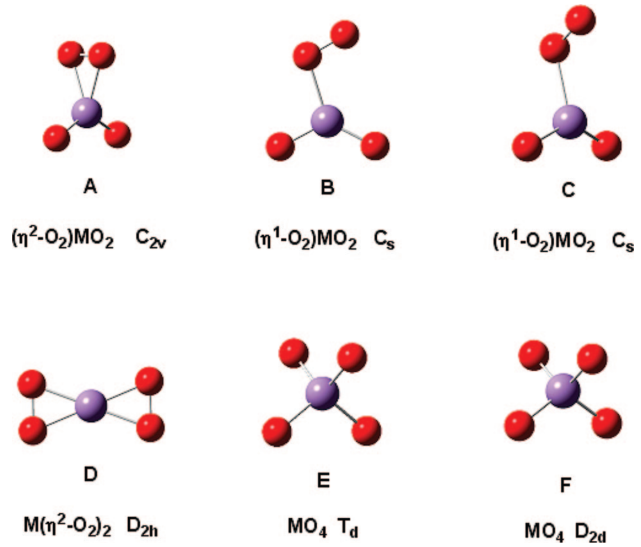

Figure 9. Optimized structures for MO_4 isomers of group VIII metals.

and the trioxide molecule were prepared via the reactions of iron monoxide with dioxygen in solid argon.[295] The (η^2-O_2)FeO complex was predicted to have a $^5B_2$ ground state with a planar C_{2v} structure, in which the O_2 fragment is side-on bonded to the iron center. The predicted bond length of the (η^2-O_2)FeO complex lies on the boundary between typical superoxo anion and peroxo dianion. Hence, it is more reasonable to consider the (η^2-O_2)FeO complex as an intermediate between superoxide and peroxide. The complex isomerizes to the more stable iron trioxide molecule upon visible light excitation. The trioxide molecule was predicted to have a $^1A_1'$ ground state with D_{3h} symmetry, in which iron possesses the +VI oxidation state.[270,287,291,295,296] It should be noted that the bond length and vibrational frequencies of FeO_3 are about the same as those of CrO_3.[202]

As for the FeO_4 species, an anion photoelectron spectroscopic study suggests that the observed FeO_4 species is due to (η^2-O_2)FeO_2.[268] Our recent matrix isolation infrared spectroscopic study on the reaction of Fe and O_2 provides evidence for the existence of two structural isomers of FeO_4, namely, the end-on bonded dioxygen−iron dioxide complex and the side-on bonded dioxygen−iron dioxide complex (Figure 9A,B).[288] These two FeO_4 isomers are interconvertible; that is, the side-on bonded complex converts to the end-on bonded isomer under near-infrared light ($\lambda > 850$ nm) excitation and vice versa with red light irradiation ($\lambda > 600$ nm), as shown in Figure 10. The end-on bonded isomer is characterized to be a superoxide complex with a planar $^3A''$ ground state, while the side-on bonded structure is a peroxide complex having a singlet ground state with a nonplanar C_{2v} symmetry. Although most pure DFT calculations predict that the tetroxide structure (T_d symmetry) without O−O bonding is more stable than the side-on bonded (η^2-O_2)FeO_2 structure,[278,297,298] ab initio and hybrid DFT calculations indicate that the tetroxide structure is less stable than the side-on structure.[299]

There is no experimental report on the FeO_5 and FeO_6 species. A bisuperoxo iron monoxide complex, $(O_2)_2FeO$, is predicted to have a singlet ground state with C_2 symmetry.[297] In a recent first-principles molecular dynamics based theoretical study, both the FeO_5 and FeO_6 species were proposed to be dioxygen adducts of iron trioxide and tetroxide.[277]

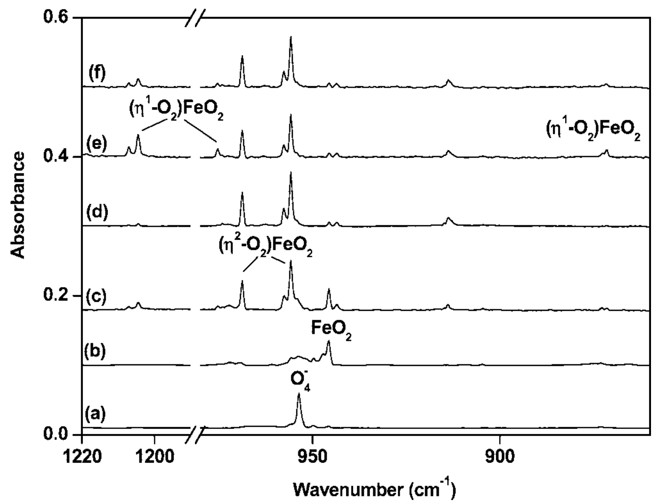

Figure 10. Infrared spectra in the 1220−1190 and 980−860 cm^{-1} regions from co-deposition of laser-evaporated Fe atoms with 1.0% O_2 in argon: (a) 1 h of sample deposition at 6 K; (b) after 15 min of broadband irradiation ($250 < \lambda < 580$ nm); (c) after annealing to 25 K; (d) after annealing to 35 K; (e) after 15 min of $\lambda > 850$ nm irradiation; (f) after 15 min of $\lambda > 600$ nm irradiation. Spectra c, e, and f are taken with six scans. Reproduced from ref 288. Copyright 2007 American Chemical Society.

Compared with the rich studies on the FeO_x system, the Ru and Os analogs have received much less attention, except for the well-known tetroxides.[300−312] The RuO molecule has been studied spectroscopically in the gas phase and in solid matrices.[261,313−315] The ground state was determined to be a $^5\Delta$ state.[70−72,261,280] No spectroscopic data is available for the osmium monoxide. DFT calculations predict that a $^5\Sigma^+$ state and a $^3\Phi$ state are very close in energy.[73,261] Both the ruthenium and osmium dioxide and trioxide molecules have been observed in solid matrices.[261,313] The RuO_2 molecule was predicted to have a $^1A_1$ ground state with a bond angle close to 150°.[78,261] From the isotopic frequencies for the ν_3 mode in solid neon, the upper and low limits of the RuO_2 bond angle were estimated to be 169° and 151°.[261] A $^3B_1$ state was predicted to be the ground state for OsO_2. The upper limit of the bond angle was estimated to be 144° in neon and 140° in argon using the most abundant ^{192}Os isotope; hence, the true angle should be around 135°.[261] The RuO_3 and OsO_3 molecules were characterized to exhibit a trioxide structure with D_{3h} symmetry.[78,261]

Two structural isomers have been observed for RuO_4 and OsO_4. It was found that the metal dioxide molecules reacted with dioxygen in solid matrices to form the dioxygen−dioxide complexes, which were characterized to have a singlet ground state with C_{2v} symmetry (Figure 9 A).[261] The complexes rearrange to the more stable tetroxide isomers upon visible light excitation.[261] The RuO_4 and OsO_4 molecules, which are the only two stable transition metal tetroxides in bulk form with the metal centers in the highest +8 oxidation state, are well-known tetrahedral molecules (Figure 9E).[316]

3.7. Co Group

Most experimental and theoretical studies suggest that cobalt monoxide has a $^4\Delta$ ground state,[24,27,28,61−65,67,69,239,317−322] while a $^4\Sigma^-$ state is predicted to be lowest in energy in a few cases.[66,68,274,323,324] An early ESR study on the reaction of cobalt atom toward dioxygen showed that the cobalt dioxide molecule is linear with a $^2\Sigma^+$ ground state.[325] No other chemically bound forms of CoO_2 than the linear dioxide structure are stabilized in solid argon. All three forms of CoO_2 (linear dioxide and side-on bonded and end-on bonded complexes) were claimed to have been observed in a matrix infrared spectroscopic study on the reaction of laser-ablated cobalt atom with dioxygen.[320] More recently, the reactivity of atomic cobalt toward dioxygen in solid noble gas matrices has been reinvestigated using infrared spectroscopy. The results showed that only the dioxide form is stabilized in the matrix and that the IR absorptions previously assigned to the end-on and side-on bonded complexes are due to other larger species.[326] The IR data of cobalt dioxide also support the linear geometry in solid matrices. Similar to the isoelectronic FeO_2^- anion,[57] theoretical calculations on cobalt dioxide require sophisticated treatment. Calculations using DFT-based methods such as BPW91 and BP86 predict a bent structure with a $^2A_1$ ground state;[77,320] B1LYP calculations give a near-linear $^6A_1$ ground state;[76,239,322] ab initio CASSCF calculations predict a linear structure with a $^2\Delta_g$ state, which is 1487 cm^{-1} below the $^2\Sigma_g^+$ state.[320] Recent CCSD(T) calculations predict a linear ground-state structure with the $^2\Sigma_g^+$ state lying lower than the $^2\Delta_g$ state, which are in good agreement with the experimental results.[326] The trioxide CoO_3 molecule is found to be thermodynamically unstable with respect to $CoO + O_2$ dissociation, but the monoxide−dioxygen complex structure, $(O_2)CoO$, is calculated to be stable with respect to dissociation.[322] It is predicted to have a $^6A_1$ ground state with C_{2v} symmetry. Two absorptions at 1090.0 and 783.0 cm^{-1} are tentatively assigned to the $(O_2)CoO$ complex.[320]

A recent investigation indicated that CoO_4 is formed following molecular diffusion by complexation of ground-state CoO_2 by dioxygen in solid matrices.[327] The CoO_4 complex is first formed in a metal-stable excited state and then spontaneously relaxes to the ground state after remaining in the dark. The ground state of CoO_4 was determined to be a $^2A_2$ state with nonplanar C_{2v} symmetry (Figure 9 A). The observed excited-state CoO_4 was characterized to have nonplanar C_s symmetry with an end-on coordinated dioxygen ligand (Figure 9C). DFT calculations suggested that the observed metal-stable state correlates to a $^4A'$ first excited state lying 0.37 eV above the ground state of CoO_4. The excited-state lifetime is estimated to be around 23 ± 2 min in argon and 15 ± 2 min in neon, indicative of a slow, spin-forbidden process.[327] Theoretical calculations at the B1LYP level of theory reveal a cobalt bisdioxygen complex structure with a $^6B_2$ ground state and nonplanar D_{2d} symmetry to be the most stable structure of CoO_4.[322] No such species has been observed experimentally.[327]

Both spectroscopic and theoretical studies suggested that the rhodium monoxide molecule has a $^4\Sigma^-$ ground state.[70,71,328−334] Experimental information on the RhO_x ($x \geq 2$) species is mainly from matrix-isolation studies.[334−336] Two structural isomers with RhO_2 stoichiometry have been identified experimentally. Matrix infrared and ESR studies indicated that the inserted rhodium dioxide molecule formed via the reaction of rhodium atom and dioxygen is linear or near linear with a doublet ground state.[325,334] Recent studies in our laboratory indicated that the side-on bonded $Rh(O_2)$ complex is the precursor for the formation of inserted dioxide molecule. The $Rh(O_2)$ complex was characterized to have a $^2A_2$ ground state with C_{2v} symmetry.[336]

Three structural isomers have been experimentally reported for RhO_4. A rhodium dioxide−dioxygen complex, $(\eta^2\text{-}O_2)RhO_2$, is formed via the reaction of rhodium dioxide with

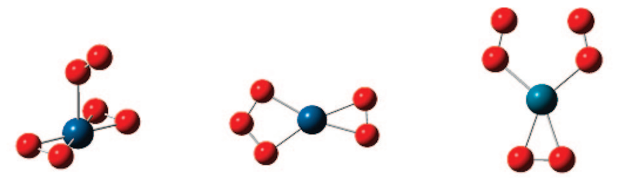

Figure 11. Optimized structures for RhO_6, CuO_5, and CuO_6.

dioxygen, which is characterized be a side-on bonded peroxide complex with C_{2v} symmetry (Figure 9A). Upon dioxygen coordination, the ORhO fragment is bent with an estimated bond angle of 110°.[334] Besides the side-on bonded RhO_4 complex, the end-on bonded $(\eta^1\text{-}O_2)RhO_2$ complex has also been observed in our recent experiments (Figure 9C).[337] Both complexes are predicted to have a doublet ground state. Similar to the FeO_4 system, the side-on and end-on bonded isomers are found to be interconvertible. The end-on bonded complex converts to the side-on bonded isomer under infrared light irradiation and back with near-infrared light ($\lambda > 850$ nm).[337] The third isomer, a bisdioxygen complex, $Rh(\eta^2\text{-}O_2)_2$, is also produced from the reaction of rhodium and dioxygen in solid argon. This complex structure is predicted to have a $^4B_{1u}$ ground state with planar D_{2h} symmetry (Figure 9 D).[336] Based on the observed O−O stretching frequency, $Rh(\eta^2\text{-}O_2)_2$ belongs to a disuperoxide complex. It is found that the $Rh(\eta^2\text{-}O_2)_2$ complex is able to weakly coordinate a third dioxygen in forming the oxygen-rich $Rh(\eta^2\text{-}O_2)_2(\eta^1\text{-}O_2)$ complex.[336] Geometric optimizations at the DFT/B3LYP level give a stable doublet $Rh(\eta^2\text{-}O_2)_2(\eta^1\text{-}O_2)$ structure with C_s symmetry (Figure 11), in which two O_2 subunits are side-on bonded and are equivalent; the third O_2 subunit is end-on bonded with the RhOO plane perpendicular to the $(O_2)_2$ plane. A stable quartet with very similar geometry is predicted to be only 0.8 kcal/mol less stable than the doublet. Xenon-doped experiments in our laboratory indicate that the $Rh(O_2)$, $Rh(\eta^2\text{-}O_2)_2$, and $Rh(\eta^2\text{-}O_2)_2(\eta^1\text{-}O_2)$ complexes are coordinated by one or two argon atoms in solid argon matrix.[336]

Investigations on the IrO_x system in the literature are quite limited. Gas-phase spectroscopic investigation failed to determine the ground state of IrO.[338] The IrO product was not observed in a gas-phase kinetic study on the reaction between Ir and O_2.[339] The vibrational fundamental of IrO is observed at 822.1 cm^{-1} in solid argon,[340] consistent with the frequency of the $^4\Sigma^-$ ground state from DFT calculations.[73,341] Matrix infrared and ESR studies imply that the iridium dioxide molecule is linear, the same as the cobalt and rhodium dioxide molecules.[325] The linear structure with a $^2\Sigma_g^+$ ground state can be reproduced by DFT/BPW91 calculations with larger 6-311+G(3d) basis set on oxygen.[341] It was found that the ground-state iridium atom reacted with O_2 to form the inserted IrO_2 spontaneously on annealing; hence, the iridium dioxygen complex is not expected to be formed.[340] The IR absorptions previously assigned to the iridium dioxygen complex[341] are due to larger iridium−oxygen species.[340]

Similar to rhodium, both the side-on and end-on bonded dioxygen−iridium dioxide complexes have been observed experimentally.[340] These IrO_4 isomers are also interconvertible. Note that the end-on bonded $(\eta^1\text{-}O_2)MO_2$ complexes with M = Fe, Rh, or Ir are characterized to have similar structure to that of the excited-state CoO_4 complex. However, these complexes are attributed to be a stable structural isomer of MO_4 instead of excited-state species. The end-on bonded complexes in the iron, rhodium, and iridium systems are found to be stable species in the dark; they rearrange to the more stable side-on bonded isomer only under photon excitation. Besides the two dioxygen metal dioxide complex structures, a third isomer with IrO_4 stoichiometry, namely, the iridium tetroxide molecule, is formed when the side-on and end-on bonded IrO_4 complexes are subjected to visible light ($\lambda > 500$ nm) irradiation. The iridium tetroxide molecule is characterized to have a doublet ground state with D_{2d} symmetry (Figure 9F), in which the iridium center is in an unusual +8 oxidation state.[340] Note that such a high oxidation state has only been observed in the Ru and Os cases.[261] So far, the highest experimentally well-established stable oxidation state of iridium is +6.[316]

3.8. Ni Group

It is now well-established that nickel monoxide possesses a $^3\Sigma^-$ ground state.[24,27−29,61−69,159,196,239,274,342−353] For PdO, a $^3\Sigma^-$ state and a $^3\Pi$ state were found to be almost isoenergetic. The relative stability of these two states strongly depends on the theoretical levels employed.[70−72,159,196,350,354−359] Anion photoelectron spectroscopic studies suggested the $^3\Sigma^-$ state to be the ground state.[342,360] Both experimental and theoretical studies confirm that the $^3\Sigma^-$ state is the ground state for PtO.[73,350,356,361−370]

Both the side-on bonded superoxide and inserted dioxide structures of NiO_2 have been characterized experimentally. The superoxide complex can be formed from the reaction of ground-state metal atom with dioxygen in solid matrices.[347,355,357,371−374] Theoretical calculations on Ni(η^2-O_2) provide contradictory results. Calculations at the CCSD(T) and CASSCF levels of theory predict a singlet ground state,[375−378] whereas DFT calculations using several functionals predict that the triplet state is more stable than the singlet state.[76,77,239,347,375,376,379] More recent DFT calculations at the PW91PW91/6-311G(3df) level with the addition of scalar relativistic effects indicate that the singlet state is slightly more stable than the triplet state by 0.1 kcal/mol.[371] The vibrational frequencies calculated for the singlet state are in much better agreement with those measured in solid argon and neon. The nickel dioxide molecule is determined to be linear with a singlet $^1\Sigma_g^+$ ground state.[77,347,371,378] The palladium dioxygen complex is the only PdO_2 isomer observed in solid matrix,[355,357,374,380] which is predicted to have a singlet ground state with C_{2v} symmetry.[355,357,380] The inserted palladium dioxide molecule has not been observed in solid matrices. However, it has been suggested to be the photodetachment product of the PdO_2^- anion from gas-phase photoelectron spectroscopic study.[342] The symmetric OPdO vibration was determined to be 680 ± 30 cm^{-1}. The ground state of palladium dioxide remains unclear. Both the linear $^3\Pi_g$ or $^3\Sigma_g^-$ states and the bent $^5A_1$ or $^3A_2$ states have been suggested as the ground state depending on the theoretical levels employed.[78,355,357,381] The PES results support a $^3\Sigma_g^+$ state for the inserted PdO_2 molecule.[342] The OPtO molecule is predicted to have the same spin state and geometry as ONiO.[355,357,368] The singlet Pt(η^2-O_2) complex with C_{2v} symmetry has been observed in a solid matrix.[355,357,372] Although the end-on bonded PtOO isomer is predicted to have a triplet ground state and is more stable than the side-on bonded complex, it is not formed in solid matrices.[357]

Both the NiO_3 and PtO_3 species, which are characterized to be metal monoxide−dioxygen complexes, have been identified in solid matrices.[347,357] It has been found that the O_2 fragment can be bound to the metal centers in either the side-on or end-on fashion. The O−O vibrational frequency for the end-on bonded complex is about 300 cm^{-1} higher than that of the side-on bonded isomer. DFT calculations indicate that the (η^1-O_2)NiO complex has a singlet ground state with planar C_s symmetry, while the side-on bonded (η^2-O_2)NiO complex has a triplet state with C_{2v} symmetry.[347] The side-on bonded (η^2-O_2)PtO complex has similar geometry and triplet ground state to those of the nickel analogs, while a $^5A'$ state is predicted to be the ground state for the end-on bonded (η^1-O_2)PtO complex.[357]

The metal disuperoxide complexes $M(O_2)_2$ with M = Ni, Pd, or Pt have also been observed from the reactions between metal atoms and dioxygen in solid matrices.[347,355,357,373,374,380] All three disuperoxide complexes exhibit strong O−O stretching vibrations around 1080 ± 30 cm^{-1}. DFT calculations indicate that these complexes have planar D_{2h} geometry (Figure 9 D). The $Ni(O_2)_2$ complex was characterized to have a triplet ground state,[347] while the $Pt(O_2)_2$ complex has a singlet ^1A_g ground state.[355,357] Our recent DFT/BPW91 calculations yielded a triplet ground state for the $Pd(O_2)_2$ complex, but single-point CCSD(T) calculations at the DFT-optimized geometries indicated that the singlet state is slightly more stable than the triplet state.[380] Besides the disuperoxide complex, a nickel dioxide−dioxygen complex, (η^2-O_2)NiO_2, which is predicted to have a singlet ground state with almost nonplanar C_{2v} symmetry, is also produced via the association reaction of nickel dioxide and O_2 in solid argon.[347]

3.9. Cu Group

The CuO molecule has a $^2\Pi$ ground state as demonstrated by numerous experimental and theoretical studies.[24,26−28,61−69,76,382−402] Due to the antibonding nature of the singly occupied 4π orbital, the Cu−O bond is significantly weakened relative to that of NiO, which results in a long CuO bond length as well as a quite low CuO vibrational fundamental.[24,383,391]

As for the CuO_2 species, two structural isomers have been observed both in the gas phase and in solid matrices.[382,383,403−408] In solid matrices, the ground-state copper atoms tend to react with O_2 to form the Cu(O_2) complex, while excited copper atoms are required for the formation of the inserted copper dioxide molecule.[383] An earlier matrix-isolation ESR experiment suggested a bent geometry for the Cu(O_2) complex with an end-on bonded O_2 ligand,[405,406] but a late theoretical interpretation indicated that the magnetic inequivalency derived from the ESR spectra may not be large enough to distinguish the coordination fashion of the O_2 molecule.[409] Although the doublet end-on bonded structure is favored at various DFT calculations, high-level ab initio calculations predict that the side-on bonded isomer is slightly more stable.[76,77,377,383,410−414] The dipole moment of the end-on bonded complex is larger than that of the side-on bonded isomer. Therefore, the end-on bonded structure is expected to be stabilized via interaction with solid argon, as also supported by high-level ab initio calculations.[414] The inserted OCuO molecule was determined to be linear based on the experimental observations.[382,383,403,404] Most theoretical calculations suggested a doublet ground state for this linear molecule.[415−417] The ν_3 mode is about 130 cm^{-1} lower than that of NiO_2, suggesting a weak bonding interaction between the copper center and two terminal oxygen atoms. Note that the inserted dioxide structure is the most stable MO_2

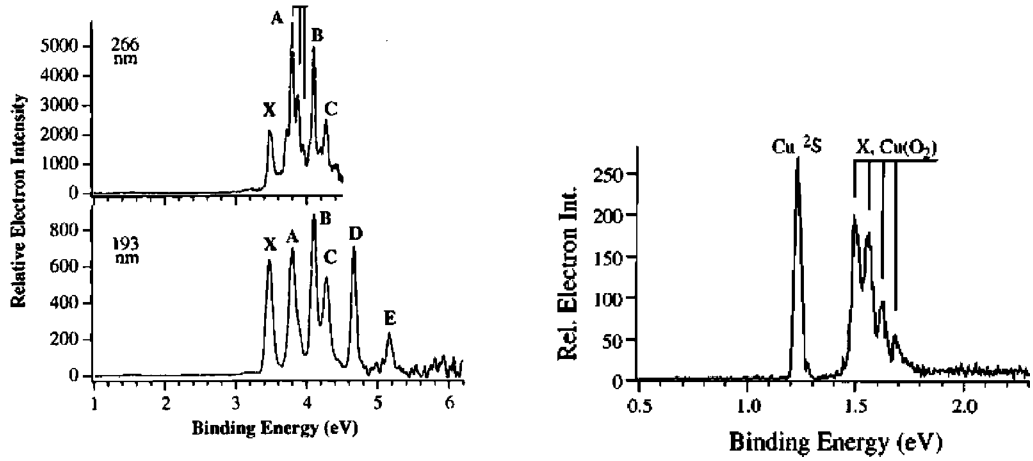

Figure 12. Photoelectron spectra of $OCuO^-$ at 266 and 193 nm (left) and $Cu(O_2)^-$ at 532 nm (right). Reproduced from refs 382 (Copyright 1997 American Chemical Society) and 403 (Copyright 1995 American Institute of Physics).

configuration for all first row transition metals except copper, which prefers a dioxygen complex structure.[77,78] The PES spectra of CuO_2^- taken at 532, 266, and 193 nm shown in Figure 12 also demonstrate the coexist of two isomers in the gas phase.[26] One isomer, constituting a very small portion of the CuO_2^- anion beam and dissociating at 532 nm, has a low electron affinity of about 1.5 eV. The second isomer, with dominating abundance, has a very high electron affinity of about 3.46 eV. These two isomers correspond to the copper dioxygen complex and the inserted copper dioxide molecule observed in matrix studies.

Two structural isomers with CuO_3 stoichiometry have been experimentally characterized.[382,383,391] An anion photoelectron spectroscopic study suggested that the observed CuO_3 species in the gas phase is due to a $(O_2)CuO$ complex.[382] A copper ozonide complex, which is the only definitive example of binary ozonide complex of the first row transition metals, was assigned in solid matrices.[383,391] Due to the extraordinary oxidizing capability of ozone, binary metal ozonide complexes known so far are limited to the alkali and alkaline earth metal ozonide complexes, which have been prepared and characterized by infrared and Raman spectroscopy.[418,419] The stable structures of the CuO_3 species have been the subject of several theoretical studies.[383,420−423] The planar $(O_2)CuO$ complex structure with a side-on bonded O_2 is predicted to be more stable than the copper ozonide complex structure. The $Cu(\eta^2\text{-}O_3)$ complex is calculated to possess a doublet ground state with planar C_{2v} symmetry, which can be described as $Cu^+(O_3)^-$. The successful isolation of the $Cu(\eta^2\text{-}O_3)$ complex may be attributed to the relative stability of the +1 oxidation state for copper and the higher energy barrier that prevents its further isomerization.

Photoelectron spectroscopic results indicate that two CuO_4 isomers coexist in the gas phase, that is, a bisdioxygen $Cu(\eta^2\text{-}O_2)_2$ complex and a copper dioxide−dioxygen complex.[382] The $Cu(\eta^2\text{-}O_2)_2$ complex was also observed in several matrix-isolation studies. Early matrix infrared studies assigned a 1110 cm^{-1} absorption in solid argon to the $Cu(\eta^2\text{-}O_2)_2$ complex with two equivalent O_2 fragments.[391,424] However this absorption was proposed to originate from the $(CuOO)(O_2)_2$ complex in a late matrix-isolation study.[383] According to our recent experimental results on the CuO_x system, the spectroscopic character of the absorption at 1110 cm^{-1} is similar to that in earlier matrix-isolation experiments, and we assert that the 1110 cm^{-1} band is due to the $Cu(\eta^2\text{-}O_2)_2$ complex.[425] Theoretical calculations suggest that the most stable configuration for the $Cu(\eta^2\text{-}O_2)_2$ complex possesses planar D_{2h} symmetry with a $^4B_{2u}$ ground state.[425] The absorption previously attributed to $(CuOO)(O_2)_2$ was reassigned to a CuO_5 complex.[425]

The CuO_5 complex has been produced via the reaction of copper atoms with O_2 or O_3 in solid argon.[425] The complex is characterized to have an $(\eta^2\text{-}O_2)Cu(\eta^2\text{-}O_3)$ structure, in which the copper center is coordinated by a O_2 ligand and an O_3 ligand. The complex is predicted to have a $^4A_1$ ground state with planar C_{2v} symmetry (Figure 11),[425] in agreement with that calculated using the spin-polarized GGA method with plane-wave basis sets.[426] However, an anion photoelectron spectroscopic study suggested that the observed CuO_5 species in the gas phase is due to an O_2 solvated $(O_2)CuO$ complex.[382]

In the case of CuO_6, an anion photoelectron spectroscopic study suggested that two isomers: a copper dioxide dioxygen complex, $OCuO(O_2)_2$ and a copper dioxygen complex, $Cu(O_2)_3$, coexist in the gas phase.[382] However, both structures are theoretically predicted not to be the global minima on the potential energy surfaces of CuO_6.[421,427] A bisozonide structure is predicted as the ground state for the CuO_6 complex using the spin-polarized GGA method with plane-wave basis sets, but isomers containing $Cu(O_2)$ building blocks are very close in energy to the bisozonide structure. Among the isomers based on the $Cu(O_2)$ unit, the structure containing one side-on and two end-on bonded O_2 units with C_{2v} symmetry lies lowest in energy.[427] Density functional calculations using the PBE functional indicate that several competitive structures exist with structures containing ozonide units being higher in energy than those with O_2 units. The structure with one side-on and two end-on bonded O_2 units (C_{2v}) is predicted to be lowest in energy.[421] Recently, an oxygen-rich CuO_6 complex bearing both side-on and end-on bonded ligands was synthesized via the reaction of Cu and O_2 in solid argon.[428] The complex was characterized to have a $^4B_1$ ground state with planar C_{2v} symmetry involving one side-on and two end-on bonded O_2 units (Figure 11), which can be formally described as a trisuperoxide $Cu^{3+}(O_2^-)_3$ complex with the copper center in its unusual +3 oxidation state. Compounds with copper in its +3 oxidation state are rare; only some copper peroxide complexes have been reported to exhibit Cu(III) character.[429]

Both the silver and gold monoxide molecules are found to have a $^2\Pi$ ground state.[71−73,196,388,400,430−446] The $Ag(O_2)$ complex is the only structure with AgO_2 stoichiometry observed in solid matrices, however, whether the O_2 ligand is side-on bonded or end-on bonded cannot be clearly identified.[405,406,430,447,448] According to the recent theoretical calculations, the end-on isomer in doublet spin state is lowest in energy for the $Ag(O_2)$ complex.[355,430,449] Earlier matrix infrared and ESR studies indicated that the $Au(O_2)$ complex is side-on bonded, but the end-on bonded isomer is predicted to be more stable.[355,430,450−453] Note that the O−O vibrational frequency of $Au(O_2)$ is sensitive to the matrix, which exhibits a large neon to argon matrix shift.[355] Besides the $Au(O_2)$ complex, the inserted AuO_2 molecule was also observed to be the reaction product of laser-ablated gold atoms and O_2.[355,430] The gold dioxide molecule is determined to have a $^2\Pi_g$ ground state with linear geometry.[355,430,440] Gold dioxide was the only AuO_2 isomer observed in the gas-phase photoelectron spectroscopic study.[440]

A silver ozonide complex, $Ag(\eta^2\text{-}O_3)$ was reported to be formed in the reactions between silver atoms and O_2 or O_3.[355,430,431] Based on the isotopic substitution experiments, an infrared absorption around 790 cm^{-1} was assigned to the ozonide complex, in which O_3 is bound to the silver center in a side-on fashion. DFT calculations suggest a doublet ground state with planar C_{2v} symmetry for this ozonide complex.[355,430] A similar ozonide complex is not formed for gold. Note that +1 is a stable oxidation state for silver but not for gold.

The AgO_4 complex is formed in solid matrices and was initially supposed to be $Ag^+(O_2)_2^-$, which involves a five-membered puckered ring,[448] similar to that of the CsO_4 complex.[454] However, recent DFT/B3LYP calculations suggested that the most stable configuration for AgO_4 is the bisdioxygen $Ag(O_2)_2$ complex with C_{2v} symmetry having a $^4B_1$ ground state. Both O_2 ligands are bound to the silver center in an end-on fashion.[355] Frequency analysis also supported reassignment of the previously observed absorptions to the bisdioxygen complex structure, which is due to a disuperoxide complex with the silver center in its +2 oxidation state. The analogous AuO_4 complex has not been observed experimentally. Theoretical calculations predict that the most stable structure is a bisdioxygen complex with planar C_{2h} symmetry having a quartet ground state.[452]

3.10. Zn Group

Group 12 of the periodic table, consisting of zinc, cadmium, and mercury, is usually considered as a post-transition metal group because the outmost shell of d orbitals is filled and does not participate significantly in chemical bonding. With the recent experimental observation of HgF_4, in which the 5d orbitals of mercury are strongly involved in bonding, mercury should be viewed as a genuine transition metal element.[455] The electronic structure of ZnO is quite similar to that of group IIA metal monoxides. The diatomic ZnO molecule has been spectroscopically studied in the gas phase as well as in solid matrices.[456−464] Theoretical calculations confirm that the ground state for zinc monoxide is $^1\Sigma^+$ with a (core)$9\sigma^2 4\pi^4$ configuration, in which the 9σ orbital is the bonding combination of Zn 4s and O $2p_\sigma$ orbtials, while the 4π orbital is largely O $2p_\pi$ orbital in character.[61−69,465−474] Spectroscopic information on cadmium monoxide is mainly from the matrix isolation studies.[463,464] An infrared absorption at 719 cm^{-1} in solid nitrogen is initially assigned to the CdO molecule,[463] but this absorption is suggested to be due to a dioxygen complex.[464] Infrared absorptions at 645.1 cm^{-1} in argon and 654.4 cm^{-1} in nitrogen are reassigned to the CdO fundamental.[464] A $^3\Pi$ state is found to be the most stable spin state using most density functionals,[71] but a $^1\Sigma^+$ state is predicted to be the ground state using high-level ab initio methods.[466,468]

The zinc and cadmium dioxide molecules have been produced in solid argon and nitrogen from the reactions of laser-ablated metal atoms with O_2.[464] Note that neither dioxide was formed in previous thermal evaporation experiments, suggesting that the laser-ablated excited-state metal atoms are responsible for the formation of these inserted products.[463] Both of the two dioxide molecules were determined to have a $^3\Sigma_g^-$ ground state with linear geometry.[76,77,464] Resolved natural zinc isotopic splittings assist in the characterization of the ZnO_2 molecule. The ZnO_2 molecule is calculated to be thermodynamically unstable; its decay with the evolution of molecular oxygen is exothermic by about 0.6 eV. Hence, its observation in solid argon suggests a barrier to decomposition. Besides the inserted dioxide molecule, a $Cd(\eta^1\text{-}O_2)$ complex with an end-on bonded O_2 ligand has also been tentatively identified in solid matrices, but DFT calculations predict that the side-on bonded isomer with a $^3B_2$ ground state is more stable than the end-on bonded complex.[464]

No gas-phase spectroscopic studies are available on mercury oxide species. A 676 cm^{-1} absorption has tentatively been assigned to the vibrational fundamental of HgO in an early matrix-isolation study.[475] However, theoretical calculations at different levels suggest that HgO has a $^3\Pi$ ground state with a vibrational fundamental around 300 cm^{-1}.[73,466,468,476−478] No spectroscopic identification of mercury dioxide has been reported, but a mercury superoxide complex was suggested to have been observed in a solid matrix.[475]

3.11. Lanthanide Group

Lanthanide metals can be classified into two groups: typical lanthanides and atypical lanthanides. Typical lanthanides exhibit a formal oxidation state of +3 and possess characteristic properties associated with rare earth metals. Due to the presence of the half-filled and filled 4f orbitals, the atypical lanthanides, Eu and Yb, exhibit a formal oxidation state of +2 and have physical properties more nearly like the alkaline earth metals. Most of the lanthanide metal monoxide molecules have been spectroscopically studied.[479−502] The vibrational fundamentals of typical lanthanide metal monoxides increase slightly along the series from Ce to Lu due to the effect of lanthanide contraction, and all are located in the narrow range of 800−830 cm^{-1} in solid argon (Table 1).[503−505] The vibrational fundamentals of atypical lanthanide metal monoxides are observed around 660 cm^{-1},[504,505] identical to the predictions given by ligand field theory.[506] From the theoretical point of view, most studies have focused on CeO, EuO, GdO, YbO and LuO,[96−99,507−515] while the other lanthanide monoxide molecules have been less investigated.[74,75,516−519] Since the bonding ability of d orbitals is larger than that of s orbitals, the 5d orbitals of lanthanide atoms are the major component in the metal−oxygen bonding for the diatomic LnO molecules; while the 4f electrons are less active due to the localized character of the 4f orbitals. Lanthanide atoms with $f^{n-1}d^1$ configurations can form relatively strong metal−oxygen bonds, and those with f^n configuration can also afford strong Ln−O bonds via f to d promotions if the energy separation is not too large. Due to the extra stability of half-filled f^7 and filled f^{14} configurations for atypical lanthanide metals, no d electrons are available for participating the Ln−O bonding, which results in the lower vibrational frequencies for EuO and YbO.[504,505] Note that these two diatomic molecules have the lowest binding energies among the lanthanide metal monoxides.[520] Following this trend, the experimentally unknown PmO molecule should absorb around 810 cm^{-1}, which is in accord with the calculated value of the $^6\Sigma^+$ ground-state PmO.[74]

Spectroscopic information on the inserted metal dioxide molecules are mainly from matrix-isolation infrared spectroscopic studies. Earlier thermal evaporation investigations have identified the dioxide molecules of Ce, Pr, and Tb,[503,521] while dioxide molecules of the remaining lanthanides except for Pm, Er, and Lu have been produced from the reactions of laser-ablated lanthanide atoms and O_2.[504,505] The dioxide molecules for Pr, Nd, Sm, Dy, and Yb were suggested to have linear geometries due to their similar oxygen isotopic ratios (about 1.049) for the antisymmetric stretching vibration (ν_3). It can be found from Table 3 that the ν_3 vibrational frequencies decrease from Ce to Ho except for Gd and Tb. Note that the infrared fundamentals of the bent CeO_2 and TbO_2 molecules are quite close to each other, suggesting a similar bonding interaction between the metal center and the oxygen atoms. Both Ce and Tb are known to form compounds with the metal centers in the +4 oxidation state.[522] Hence these two lanthanide metals can afford two Ln═O double bonds in forming the strongly bound OCeO and OTbO molecules.

3.12. Actinide Group

Due to experimental challenges faced in handling actinide metals, most spectroscopic studies are focused on thorium and uranium oxide species.[523−531] Spectroscopic and theoretical studies of the oxides of thorium and uranium have been reviewed recently.[532] The results regarding the structures and vibrational fundamentals of ground spin state thorium and uranium oxides are briefly outlined here. Thorium monoxide absorbs around 876 cm^{-1} in solid argon.[521,533] It was calculated to have a closed-shell singlet ground state.[534−537] The thorium dioxide molecule was characterized to be bent based on the matrix infrared spectra and theoretical calculations.[521,533,538−543]

Uranium monoxide was observed around 820 cm^{-1} in solid argon and 890 cm^{-1} in solid neon.[544−547] Both ab initio and DFT calculations predicted a quintet ground state for uranium monoxide,[517,548,549] whereas a triplet state was proposed to be the ground state based on group theory and atomic and molecular reactive statics.[550] The inserted uranium dioxide molecule was characterized to be a linear molecule with the antisymmetric stretching mode (ν_3) observed at 776 cm^{-1} in solid argon[544−547] and 915 cm^{-1} in solid neon.[549] The large shift in frequency from argon to neon (139 cm^{-1}) is not due to typical polarizability-based matrix effects, and a strong interaction between UO_2 and the noble gas matrix should be considered. Both DFT and high-level ab initio calculations confirm that the linear UO_2 molecule has a $^3\Phi_u$ ground state arising from a $5f^17s^1$ configuration with a ^3H_g state derived from the $5f^2$ configuration slightly higher in energy.[549,551−556] Scalar relativistic DFT and CCSD(T) calculations suggest that the uranium dioxide molecule in the ^3H_g state can be coordinated by five Ar atoms in forming the $UO_2(Ar)_5$ complex.[556] The argon−uranium interactions are far less attractive for the $^3\Phi_u$ state UO_2, largely because of repulsive interactions between the Ar atoms and the 7s-localized electron. A comparison of the calculated DFT vibrational frequencies to those observed in neon and argon matrices suggests that the large frequency change is very likely due to a change in electronic state. The calculated ν_3 mode for isolated $^3\Phi_u$ state, 919 cm^{-1}, is in excellent agreement with that observed in solid neon. The ν_3 mode for the ^3H_g state is red-shifted by 95 cm^{-1} relative to the $^3\Phi_u$ state, and the coordination of five argon atoms leads to an additional 19 cm^{-1} red shift. The energy separation between the ^3H_g and $^3\Phi_u$ states are lowered upon argon coordination, and the ^3H_g state is found to be lowest in energy if spin orbital coupling is taken into consideration (Figure 13). Hence the ground state for UO_2 molecule seems to be changed from argon to neon, in which the slightly less stable configuration can be stabilized upon argon coordination.[556] Such noble-gas-induced ground-state reversal has been observed in the CUO molecule.[39,557] However, a recent dispersed fluorescence spectroscopic study on molecular UO_2 suggested that UO_2 exists in the $^3\Phi_u$ state in solid argon, the same as that in gas phase.[529] The electronic spectra observed in solid argon were found to be identical to the recent gas-phase calculations although it cannot be determined whether the ground state of uranium dioxide is changed upon argon coordination.[558]

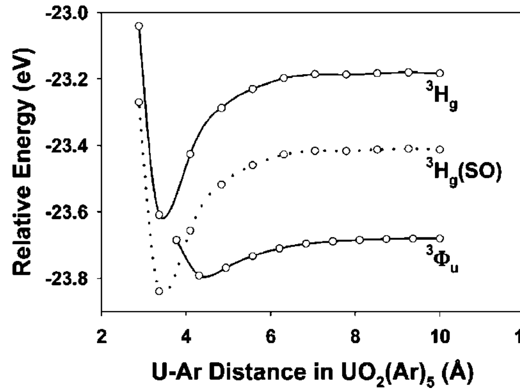

Figure 13. Calculated linear-transit potential energy curves for D_{5h} $UO_2(Ar)_5$ for the $^3\Phi_u$ and ^3H_g electronic states of UO_2. The dotted line represents a lowering of the curve for the ^3H_g state by a constant 0.23 eV to account for differential spin−orbit stabilization of the ^3H_g state. Reproduced from ref 556. Copyright 2004 American Chemical Society.

The uranium trioxide molecule has been observed in solid matrix.[544−547,549,559,560] Earlier thermal-evaporated uranium reactions propose a T-shaped structure for uranium trioxide.[559,560] However, theoretical calculations predict that uranium trioxide has a closed-shell singlet ground state with a planar Y-shaped C_{2v} structure.[549,561,562]

The radioactive plutonium monoxide and dioxide molecules have also been studied in a solid matrix. An infrared absorption around 820 cm^{-1} was assigned to PuO,[563] which is predicted to have a $^7\Pi$ ground state.[564] Plutonium dioxide absorbs at 794.3 and 786.8 cm^{-1} in solid argon and krypton.[563] Both DFT and high-level ab initio calculations suggested that plutonium dioxide has a $^5\Sigma_g^+$ ground state with a linear geometry.[564,565]

3.13. Periodic Trends on Bonding and Reactivity

Some periodic trends on the reaction mechanism can be drawn from matrix spectroscopic investigations on the reactions between transition metal atoms and dioxygen. Since only the ground-state metal atoms are trapped in solid matrices, the species observed on annealing are produced from the ground-state metal atom reactions. It is found that the ground state transition metal atoms are able to react with dioxygen to form the inserted dioxide molecules or the side-on or end-on bonded dioxygen complexes. The ground-state early transition metal atoms from the Sc group to the Cr group are found to be able to insert directly into the O−O bond of dioxygen to form metal dioxide molecules without activation energy (reaction 1; the ScO_2 molecule is not observed in solid matrices).[109,132,182,183,201,202,210]

$$M + O_2 \rightarrow OMO \quad (M = \text{Sc group through Cr group, Ru, Os, Ir}) \qquad (1)$$

The kinetics of the reactions of ground-state transition metal atoms with dioxygen have been studied in the gas phase. It has been found that most early transition metal atoms react with dioxygen via a bimolecular abstraction mechanism to form the metal monoxides.[566−568] A mechanism involving electron transfer from the neutral reactant potential energy surface to an ion pair product surface is proposed for these reactions. The oxidation reaction of the ground-state Ti(^{3}F) with the O_2 molecule has been studied theoretically.[569] An inserted fast dissociation mechanism is proposed. The reaction is predicted to proceed with the initial formation of a side-on bonded Ti(η^2-O_2) complex followed by the O−O bond breaking in forming an inserted dioxide intermediate, which dissociates readily to give TiO and O. The reaction is predicted to have a very small entrance activation barrier. In solid matrices, the internal energy of the inserted intermediate can be very effectively quenched, and therefore, the inserted dioxide molecule is trapped as the primary reaction product.

Among the late transition metal atoms, only the Ru, Os, and Ir atoms are found to be able to react with dioxygen to form the inserted dioxide molecules without activation energy.[261,313,340] Gas-phase kinetic studies also showed that the ground-state iridium atom reacted with dioxygen to form the inserted IrO_2 molecule via a termolecular reaction mechanism.[339] The relatively larger reactivity of iridium is attributed to a surface crossing with the low-lying $5d^86s^1$ electronic state. The larger reactivity of Ru with respect to iron is understandable because Ru has a $4d^75s^1$ ground-state configuration.[570] The energy separation for the $5d^76s^1$ and $5d^66s^2$ states of osmium is comparable to those of early transition metals, which makes it possible to undergo a spontaneous bimolecular abstraction reaction with O_2 in the gas phase.[571]

The other late transition metal atoms, Mn, Re, Fe, Co, Zn, and Cd, are unreactive toward dioxygen in solid matrices, and the inserted dioxide molecules are formed under UV−visible excitation or excitation under laser ablation conditions (reaction 2).[246,247,261,286,288,320,326,464] Gas-phase kinetic studies also indicate that the ground states of these metal atoms are less reactive or unreactive toward dioxygen at room temperature.[248,572−575]

$$M^* + O_2 \rightarrow OMO \quad (M = \text{Mn, Re, Fe, Co, Zn, Cd}) \qquad (2)$$

The remaining late transition metal atoms interact with dioxygen to form the side-on or end-on bonded metal dioxygen complexes spontaneously on annealing, which rearrange to the inserted isomers upon UV−visible excitation (reaction 3) except Pd and Ag.[336,347,355,357,383,430] The inserted silver and palladium dioxide molecules have not been produced in solid matrices.[355,357,430,447,448,451]

$$M + O_2 \rightarrow M(O_2) \rightarrow OMO \quad (M = \text{Ni, Pt, Cu, Au, Rh}) \qquad (3)$$

Note that all the metals that are able to form dioxygen complexes exhibit $d^{n-1}s^1$ (Rh, Pt, Cu−Au) or d^ns^0 (Pd) ground-state electronic configurations except Ni. Although Ni has a $3d^84s^2$ ground-state configuration, the first excited state with $3d^94s^1$ configuration lies only about 250 cm^{-1} higher in energy than the ground state. At the annealing temperatures (25−40 K) in solid argon, the first excited state is also populated. Gas-phase kinetic investigations also indicate that the transition metals with $d^{n-1}s^1$ configurations are more reactive than their $d^{n-1}s^2$ counterparts. Efficient depletion of the atoms of $d^{n-1}s^1$ configuration by O_2 is interpreted by an attractive interaction correlated to a stable intermediate.[574]

The reaction of ground-state nickel atoms with dioxygen to form the nickel dioxide molecule has been theoretically studied.[371] The potential energy profiles calculated at the PW91PW91/6-311G(3df) level are shown in Figure 14. The reaction starting from triplet state Ni(^{3}D) + O_2($^3\Sigma_g^-$) proceeds first on the quintet surface toward the formation of a superoxo complex ($^5B_1$). The complex, however, evolves rapidly to the $^3B_1$ state due to a favorable crossing of the two related states (denoted as P1). Since the $^3B_1$ and $^1A_1$ states are nearly isoenergetic, one can conclude that the Ni + O_2 reaction results in the superoxo cyclic complexes ($^1A_1$ and $^3B_1$) with a high exothermicity at these thermal conditions. If the internal energy is not quenched by the matrix solid, the superoxide complex can overcome a barrier height of 14 kcal/mol to reach the second minimum at the $^3B_1$ curve corresponding to a dioxide state. Intersystem crossing between the $^3B_1$ state and the second $^1A_1$ state (correlates to the $^1\Sigma_g^+$ state of dioxide) allows the system to relax toward the final product, namely, the $^1\Sigma_g^+$ dioxide. Consequently, the formation of the superoxide intermediate and dioxide product can be envisaged from the Ni(^{3}D) + O_2($^3\Sigma_g^-$) entry channel. The photochemical conversion of side-on bonded nickel superoxide complex to the nickel dioxide molecule is more complicated, which may involve some excited states. Two formation pathways of the nickel dioxide, starting from the cyclic superoxide singlet state ($^1A_1$) have been proposed based on theoretical calculations.[371]

As can be seen in Table 3, the metal dioxide molecules from the Sc group to the Fe group are bent, while those of the Co, Ni and Cu groups are linear. Among the first row transition metal dioxide molecules, the ν_3 vibrational frequencies are quite close, and all are located in the range of 1000−900 cm^{-1} characteristic of stable molecules with strong metal−oxide bonds except for ScO_2, CuO_2, and ZnO_2. Due to limited metal valence electrons available for bonding with oxygen, the ScO_2 molecule is not able to be stabilized in solid matrices, while the CuO_2 molecule is characterized to be weakly bonded with the Cu−O bonds more like that of an oxyl (−O•). The ν_1 frequencies decrease monotonically along the series from Ti to Ni. The same relationship can be found in the second row transition metal dioxides. But the ν_3 vibrational frequencies of second row metal dioxides are lower than those of the corresponding first row metal dioxides due to shell expansions. The third row transition metal dioxide ν_3 frequencies for TaO_2, WO_2, OsO_2, and IrO_2 exceed the corresponding second row fundamentals as a consequence of relativistic contraction. But the ZrO_2 and HfO_2 molecules have about the same ν_3 vibrational fundamentals due to a

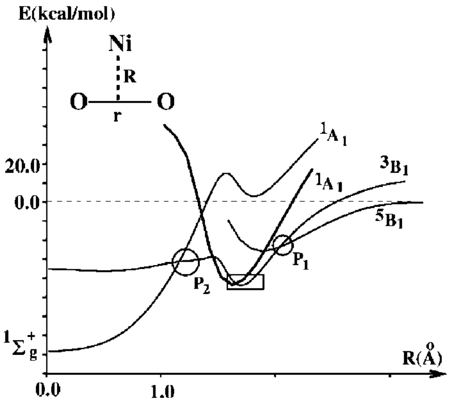

Figure 14. Potential energy profiles from the reactants (Ni(^{3}D) + O_2($^3\Sigma_g$)) to the ONiO dioxide ($^3\Sigma_g^+$). P_1 and P_2 represent intersystem crossing points. Two nearly degenerate $^3B_1$ and $^1A_1$ minima corresponding to the cyclic intermediate are shown by a rectangle. Reprinted with permission from ref 371. Copyright 2006 Royal Society of Chemistry.

Scheme 1

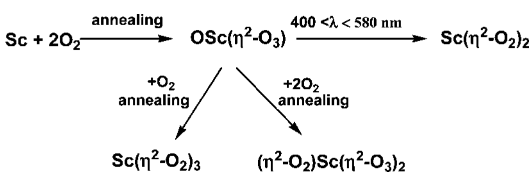

combination of lanthanide contraction and relativistic effects for hafnium.

It is found that the primary formed metal dioxide molecules or dioxygen complexes are able to react with additional dioxygen to form oxygen-rich metal dioxygen complexes in solid matrices on sample annealing, which exhibit characteristic photochemical reaction properties.

Due to limited valence electrons available for bonding, the metal dioxides of Sc and Ti groups prefer to interact with dioxygen to form high-valent dioxygen or ozonide complexes. The reactions between the Sc metal atom and dioxygen are summarized in Scheme 1. Although the scandium dioxide molecule is not produced, the experiments on the Sc + O_2 reaction in solid argon show that the ground-state scandium atoms react spontaneously with two dioxygen molecules to form the OSc(η^2-O_3) complex.[111] In the lanthanum and dioxygen reaction, an (η^2-O_2)LaO_2 complex is observed to be the precursor for the formation of the OLa(η^2-O_3) complex under near-infrared excitation.[112] The OSc(η^2-O_3) complex either isomerizes to the more stable Sc(η^2-O_2)$_2$ isomer under visible light excitation or interacts with additional dioxygen to give the even oxygen-rich Sc(η^2-O_2)$_3$ and (η^2-O_2)Sc(η^2-O_3)$_2$ clusters.[111]

The oxidation of Ti group atoms with dioxygen proceeds with the initial formation of the metal dioxide molecules, which further react with dioxygen to form the OM(η^2-O_2)(η^2-O_3) complexes.[152,153] In the case of hafnium, the OHf(η^2-O_2)(η^2-O_3) complex can be converted to the homoleptic Hf(η^2-O_2)$_3$ and Hf(η^2-O_2)$_4$ complexes, as shown in Scheme 2. The HfO_2, OHf(η^2-O_2)(η^2-O_3), Hf(η^2-O_2)$_3$ and Hf(η^2-O_2)$_4$ species all are high-valent compounds with the metal center in its formal +4 oxidation state. The results also demonstrate that the reactions from 2-fold coordinated metal dioxide to 5-fold coordinated OHf(η^2-O_2)(η^2-O_3), and to 6-fold coordinated Hf(η^2-O_2)$_3$, and finally to 8-fold coordinated Hf(η^2-O_2)$_4$ are energetically favored with increasing coordination numbers at the same oxidation state for the metal center.[153]

Scheme 2

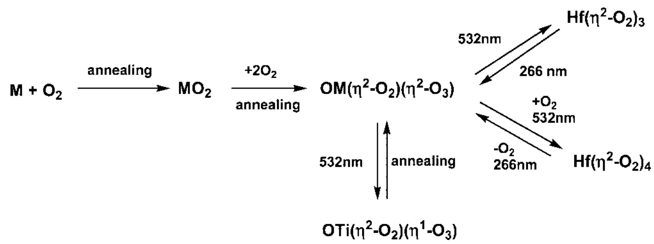

Scheme 3

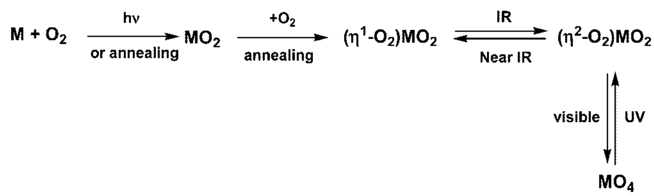

Scheme 4

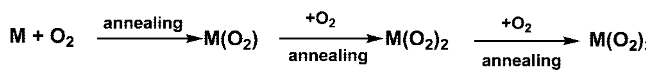

The results on Sc and Ti groups indicate that the metal oxide structures can be converted to the dioxygen complex structures via an ozonide structure intermediate.

All the metal dioxide molecules from the V group to the Co group and Ni are found to react with dioxygen spontaneously to form the metal dioxide−dioxygen complexes in solid matrices.[182,183,201,238,247,261,288,334,337,340,341] For the Cr group metals, the metal dioxide molecules prefer to coordinate two dioxygen molecules to form the disuperoxide complexes.[201,238] In selected systems (Fe, Co, Rh, Ir), both the side-on and end-on bonded complexes are formed, which are photochemically interconvertible.[288,327,337,340] In general, infrared light induces the conversion of the end-on bonded (η^1-O_2)MO_2 complex to the side-on bonded (η^2-O_2)MO_2 isomer, and vice versa with near-infrared light irradiation (Scheme 3). The metal dioxide−dioxygen complexes of Ru, Os, and Ir are also able to be rearranged to the metal tetroxide isomers.[261,340] In the case of manganese, the manganese tetroxide MnO_4 is predicted to be less stable than the (η^2-O_2)MnO_2 isomer and is not able to be stabilized in solid argon matrix.[247] However, it is found that the (η^2-O_2)MnO_2 complex interacts with another weakly coordinated dioxygen to give the (η^2-O_2)MnO_4 complex via visible light excitation, in which the manganese tetroxide is coordinated and stabilized by a side-on bonded O_2 molecule.

The primary formed side-on or end-on bonded 1:1 metal dioxygen complexes of Rh, Ni group metals, Cu, and Ag are also able to bind an additional one (Ni group, Ag) or two (Rh and Cu) dioxygen molecules to form binary oxygen-rich complexes, as illustrated in Scheme 4.[336,347,355,357,380,425,428]

4. Ionic Mononuclear Transition Metal Oxide Species

Spectroscopic investigation of molecular ions is generally more difficult than that of neutrals, because charged species are often quite reactive. Both the production and spectroscopic detection face great challenges. Laser-ablation serves as the most commonly used technique in producing charged species for gas-phase spectroscopic studies.[26] The number density of ions that are available for spectroscopic study is often low because of space charge effects or because the ions may be difficult to make in significant abundance. Thus, gas-phase investigation requires sensitive spectroscopic techniques, and conventional absorption spectroscopies are often not suitable.

Anion photon electron spectroscopy is widely used for studying molecular anions, but this technique provides spectroscopic information mainly on the neutral molecules. Only if hot bands (transitions originating from excited vibrational levels of the anion) are observed, can their energy spacings be used to determine the vibrational levels of the anions.[26] Laser-based spectroscopic techniques such as LIF, REMPI, and ZEKE, which often rely on access to a bound excited electronic state, are not suited for detecting anions, because most anions do not possess any significantly bound excited electronic states.[576] Laser ablation in conjunction with matrix isolation is a valuable tool in preparing charged species for conventional spectroscopic studies.[15] As has been discussed, laser ablation produces neutral species as well as electrons and cations, and as a result, anions can be formed by electron capture of the neutral molecules and cations can be produced by cation−molecule reactions or via photoionization by radiation in the ablation plume. Most anions bind their outmost electron less tightly than do most neutrals and cations, and therefore, they are more photosensitive. Photolysis of the initial deposited sample with filtered radiation can provide useful information in identifying the anionic species. In addition, adding a supplementary electron trapping molecule such as CCl_4 may reduce the concentration of anions and enhance the concentration of cations.[15] Knight et al. have observed that any attempts to isolate cations are unsuccessful when there is less than a 5 eV difference between the ionization energy of the matrix substrate atom and the electron affinity of the cation in question.[577] Utilizing the observed 5 eV difference, ions with an electron affinity greater than 10.8 eV (ionization energy of Ar is 15.76 eV) are not expected to be observed in an argon matrix. Neon has much higher ionization energy (21.56 eV) than argon;[578] hence, the neon matrix is the best choice for cationic species. For cationic transition metal−oxygen species, one should pay special attention, because some transition metal cationic species may interact strongly with the matrix substrate atoms, even with the lighter noble gases. Only a few transition metal oxide/dioxygen cations have been reported in solid noble gas matrices, most of which are characterized to be coordinated by one or multiple noble gas atoms. Recently developed infrared dissociation spectroscopy provides a powerful tool in studying the vibrational spectrum of free cation species in the gas phase, and some results on simple transition metal oxide cations will be discussed here.

4.1. Cations

The electronic structures of mononuclear oxide cations have been the subject of many experimental studies and theoretical calculations.[27,29,71,73,102,156,158,160,195,281,292,395,453,510,548,579−596] The vibrational frequencies of mononuclear cations are listed in Table 7. Recently, the thermochemical properties of a series of transition metal oxide cations have been summarized.[597]

In solid matrices, the singly charged monoxide cations have been reported for Sc group metals as well as lanthanide metals.[105,109,504,505] These metal monoxide cations are closed-shell species with the metal center in the most stable +3 oxidation state. An infrared absorption at 976.3 cm^{-1}, which was initially attributed to the ScO neutral[104] was reassigned to the ScO^+ cation in solid argon.[105] Note that the ground-state configuration for ScO is $8\sigma^2 3\pi^4 9\sigma^1$, in which the unpaired electron is mainly distributed in the scandium-based 3d orbital. Although the covalent interaction between scandium and oxygen is barely changed upon removal of the 9σ electron in forming the cation, the scandium and oxygen atoms are more strongly bound due to the increase in electrostatic interaction. Hence, it is expected that the Sc═O bond length will be shortened in the ScO^+ cation with the vibrational frequency blue-shifted from that of the neutral molecule.[105] This trend is followed by the YO^+ and LaO^+ cations, but with a larger cation-to-neutral shift.[109] Recent studies in this laboratory indicate that both the ScO^+ and YO^+ cations are coordinated by multiple argon atoms in solid argon matrix in forming noble gas complexes.[598] The doping experimental results show that ScO^+ coordinates up to five argon atoms, and YO^+ coordinates six argon atoms. Therefore, the ScO^+ and YO^+ cations trapped in solid argon should be regarded as the $[ScO(Ar)_5]^+$ and $[YO(Ar)_6]^+$ complexes (Figure 15). The bonding in these complexes involves the Lewis acid−base interactions, in which electron density in the Ng lone pairs is donated into the vacant orbitals of the metal center (Figure 15). The binding energies per Ar atom are computed to be several kcalories per mole, lower than that of the formal covalent bonds but are significantly higher than that of the van der Waals interactions.[598]

The niobium and tantalum monoxide cations have been characterized in solid argon and neon by Weltner and co-

Table 7. Ground Spin States and Vibrational Frequencies (cm^{-1}) for Mononuclear Transition Metal Oxide Cations in the Gas Phase and in Solid Argon Matrix

molecule	ground state	vibrational frequency[a]	experimental method[b]	ref
ScO^+	$^1\Sigma^+$	976.3 (1006.2[c])	MI-IR[c]	105
$Sc(O_2)^+$	$^1A_1$	892.9 (ν_1), 641.1 (ν_2), 624.8 (ν_3)	MI-IR	85, 105
YO^+	$^1\Sigma^+$	872.0 (899.8[c])	MI-IR	109
$Y(O_2)^+$	$^1A_1$	816.3 (ν_1), 595.3 (ν_2), 587.5 (ν_3)	MI-IR	109
LaO^+	$^1\Sigma^+$	838.2 (864.0[c])	MI-IR	109
$La(O_2)^+$	$^1A_1$	804.0 (ν_1)	MI-IR	109
LaO_2^+	$^1\Sigma_g^+$	689.3	MI-IR	109
CeO^+	$^2\Phi$	849.4 (874.8[c])	MI-IR	74, 504
PrO^+	$^3\Sigma^-$	857.4 (882.3)	MI-IR	74, 504
NdO^+	$^4\Phi$	848.3 (878.4)	MI-IR	74, 504
SmO^+	$^6\Phi$	840.0	MI-IR	74, 504
EuO^+	$^7\Sigma^-$	756.9	MI-IR	74, 504
GdO^+	$^8\Sigma^-$	844.8	MI-IR	74, 504
TbO^+	$^9\Sigma^-$	856.5 (883.7[c])	MI-IR	74, 505
DyO^+	$^8\Sigma^-$	861.2 (888.6)	MI-IR	74, 505
HoO^+	$^5\Sigma^+$	860.5 (887.9)	MI-IR	74, 505
ErO^+	$^4\Sigma^-$	861.8	MI-IR	74, 505
TmO^+	$^3\Sigma^-$	864.2	MI-IR	74, 505
YbO^+	$^2\Sigma^+$	788.7	MI-IR	74, 505
LuO^+	$^1\Sigma^+$	864.9	MI-IR	74, 505
HfO^+	$^4\Sigma^-$	1017.7[d]	ZEKE	579, 599
VO^+	$^3\Sigma^-$	1060 ± 40	PES	166
		1053 ± 5	IR-PD	606, 630
VO_2^+	$^1A_1$	1017 (ν_1), 990 (ν_3)	IR-PD	606, 630
VO_3^+	$^3A''$	1069, 1037	IR-PD	606, 630
NbO_2^+	$^1A_1$	988.0 (ν_1), 937.1 (ν_3)	MI-IR	183
TaO_2^+	$^1A_1$	993.1 (ν_1), 938.8 (ν_3)	MI-IR	183
CrO^+	$^4\Sigma^-$	640 ± 30	PES	589, 592
ThO^+	$^2\Sigma^+$	955.0[d]	ZEKE	580
UO^+		911.9[d]	ZEKE	581
UO_2^+	$^2\Phi$	921[d] (ν_1), 145.5[d] (ν_2)	ZEKE	602
		952.3 (980.1) (ν_3)	MI-IR	549

[a] The vibrational frequencies in parentheses are neon matrix values. [b] Abbreviations: MI-IR, matrix-isolation infrared spectroscopy; PES, photoelectron spectroscopy; IR-PD, infrared photon dissociation spectroscopy; ZEKE, zero-electron kinetic energy photoelectron spectroscopy. [c] Unpublished results. [d] Harmonic frequency.

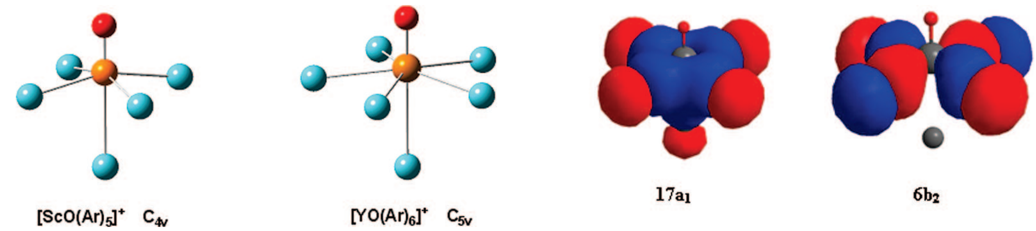

Figure 15. Optimized structures for the $[ScO(Ar)_5]^+$ and $[YO(Ar)_6]^+$ complexes and the bonding molecular orbital pictures of $[ScO(Ar)_5]^+$. Adapted from ref 598. Copyright 2005 American Chemical Society.

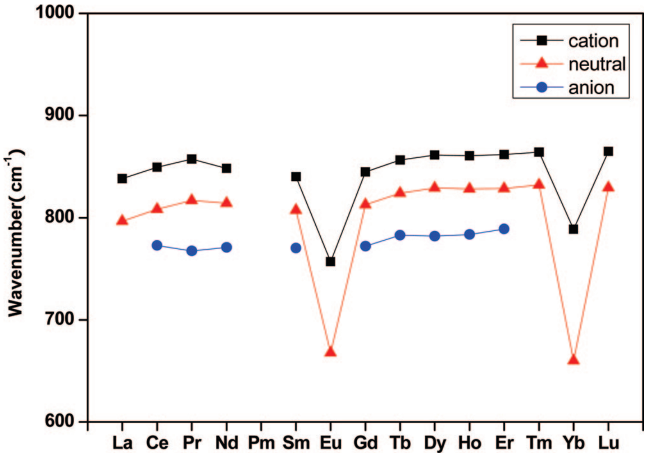

Figure 16. Plot of the vibrational fundamentals for lanthanide metal monoxide cations, neutrals, and anions in solid argon. From refs 109, 504, and 505.

workers using electron spin resonance spectroscopy. Both cations are suggested to have a $^2\Sigma$ ground state from the characteristic metal hyperfine splittings in the X band of the ESR spectra.[599]

Figure 16 presents the vibrational fundamentals of the lanthanide metal monoxide cations and neutrals in solid argon. Due to the lanthanide contraction effect, the vibrational frequencies for most lanthanide monoxide cations increase slightly from Ce to Lu with the cation-to-neutral shifts around 30−40 cm^{-1}. As found in the neutral case, the monoxide cations for Eu and Yb exhibit rather lower vibrational frequencies than those of others. Note that the frequency shifts for the EuO^+ and YbO^+ cations are about three times as large as those of the other monoxide cations. The peculiarities for these two cationic species may be related to the f^7 and f^{14} configurations of the neutral monoxide molecules, which leads to the increase in metal−oxygen interactions due to the loss of half-filled and filled shell structures upon ionization. Theoretical studies on the lanthanide monoxide cations are fewer than those of the neutrals.[102,510,518] Recently, the electronic structures and molecular properties of the complete lanthanide monoxide species have been studied using DFT methods.[74] It is found that the ground spin multiplicity for the cationic species can be obtained by −1 or +1 from that of the neutral molecules.

Several monoxide cations have been studied in the gas phase using the PFI-ZEKE and resonance-enhanced photodissociation spectroscopic methods. Rotationally or vibrationally resolved spectra were recorded for the ground states and some low-lying electronically excited states. Vibrational frequencies and anharmonicity constants for low-lying energy levels were reported. Accurate ionization energies for the neutrals were determined.[579−587]

Cationic species with more than one oxygen atom are mainly limited to those with MO_2 stoichiometry. For the Sc group metals, the cationic $M(O_2)^+$ species are formed in solid matrices, which can be regarded as peroxide cations with the metal center in the +3 oxidation state. All three cations are predicted to have a $^1A_1$ ground state with C_{2v} symmetry.[105,109] Besides the peroxide cation, a linear lanthanum dioxide cation is also formed in the reaction between La and O_2. This dioxide cation is predicted to have a $^1\Sigma_g^+$ ground state, which is about 40 kcal/mol less stable than the peroxide isomer.[109] In addition to the lanthanum dioxide cation, transition metal dioxide cations have also been reported for Nb, Ta, Pr, Nd, and U. The NbO_2^+ and TaO_2^+ cations are isovalent with the ZrO_2 and HfO_2 neutrals. Both cations are calculated to have a closed-shell singlet ground state with bent C_{2v} symmetry.[183] Their stretching vibrational frequencies are about 30 cm^{-1} higher than those of the neutrals. The two lanthanide dioxide cations, which exhibit similar O-18 isotopic ratios as the corresponding linear neutral molecules, are suggested to have linear geometry.[504] These two cations are found to undergo a larger cation-to-neutral shift than that of the NbO_2^+ and TaO_2^+ cations.

Uranium is known to form an important cationic species, namely, uranyl, UO_2^{2+}, which has been the subject of many investigations.[600] The monocharged UO_2^+ cation is observed as the cationic counterpart in the $(UO_2)^+(NO_2)^-$ and $(UO_2)^+(NO)^-$ complexes in earlier thermal reactions between neutral UO_2 and NO_2/NO.[601] In a laser ablation experiment, the uranium dioxide molecule was able to react with O_2 to give the $(UO_2)^+(O_2)^-$ complex, in which the UO_2^+ cation exhibits a similar vibrational frequency as in the $(UO_2)^+(NO_2)^-$ case.[546] The infrared absorptions at 980.1 and 952.3 cm^{-1} are assigned to the isolated UO_2^+ cation in solid neon and argon.[549] The IR inactive symmetric stretching vibration and the bending fundamental are determined to be 919 and 145 cm^{-1} from recent gas-phase PFI-ZEKE spectroscopic study.[602] Consistent with the experimental identification, the UO_2^+ cation is predicted to have a linear geometry with a $^2\Phi_u$ ground state. Recent investigations indicate that UO_2^+ coordinates up to five heavy noble gas atoms in forming complexes in solid noble gas matrices.[603] The calculated binding energies are much larger than those for the neutral $UO_2(Ng)_n$ complexes due to the combination of electron-donation and ion-induced dipole interactions. As for the bare UO_2^{2+} dication, frequency analysis reveals that it absorbs about 100 cm^{-1} higher than the singly charged cation,[549,551,604] which is much higher than that of uranyl dication observed in condensed phase.[605] Apparently, solute or anion interactions are responsible for the lower σ_u vibrations of linear UO_2^{2+} dication observed in condensed phases, and only in the gas phase can UO_2^{2+} be considered as a true dipositive cation.

The vibrational spectra of some mononuclear vanadium oxide cations have been obtained via infrared predissociation of the corresponding ion−messenger atom complexes in gas phase.[606] The vibrational frequency of the VO^+ cation is

Table 8. Ground Spin States and Vibrational Frequencies (cm^{-1}) for Transition Metal Monoxide Anions in the Gas Phase

molecule	ground state	vibrational frequency	ref
ScO^-	$^1\Sigma^+$	840 ± 60[a]	84, 89
TiO^-	$^2\Delta$	800 ± 60	115, 122
VO^-	$^3\Sigma^-$	900 ± 50	156, 165
CrO^-	$^4\Pi$[b]	885 ± 80	193, 198
MnO^-	$^5\Sigma^+$	760 ± 50	240
FeO^-	$^4\Delta$	740 ± 60	40, 63, 65, 76, 276
CoO^-	$^5\Delta(^3\Sigma^-)$[c]		63, 65, 76
NiO^-	$^2\Pi$[d]	660 ± 40[e]	63, 343
CuO^-	$^1\Sigma^+$	739 ± 25	384
ZnO^-	$^2\Sigma^+$	625 ± 40	441, 443
YO^-	$^1\Sigma^+$	740 ± 60	71, 89
ZrO^-	$^2\Delta$		71
NbO^-	$^3\Sigma^-$		71
MoO^-	$^4\Pi$	810 ± 40	71, 204
TcO^-	$^5\Sigma^+$		71
RuO^-	$^4\Delta$		71
RhO^-	$^3\Sigma^-$	730 ± 80	71, 333
PdO^-	$^2\Pi$		71, 342, 360
AgO^-	$^1\Sigma^+$	497 ± 20	71, 432
CdO^-	$^2\Sigma^+$		71
LaO^-	$^1\Sigma^+$		74, 93
HfO^-	$^4\Sigma^-$		73
TaO^-	$^3\Sigma^-$		73, 174
WO^-	$^6\Sigma^-$		73
ReO^-	$^5\Sigma^-$		73
OsO^-	$^4\Delta$		73
IrO^-	$^3\Sigma^-$		73
PtO^-	$^2\Pi$	770 ± 30	73, 342
AuO^-	$^1\Sigma^+$		73, 440, 441
HgO^-	$^2\Sigma^+$		73

[a] The vibrational frequency for the ScO^- anion is observed at 889.2 cm^{-1} in solid argon (ref 608). [b] A slightly more stable $^6\Sigma^+$ state was predicted in refs 65 and 76, and it was assigned to the ground state of the CrO^- anion in a recent photoelectron spectroscopic study (ref 197). High-level ab initio calculations suggested that the $^4\Pi$ state is lowest in energy (ref 193), in agreement with earlier photoelectron spectroscopic study (ref 198). [c] Ground state undetermined. [d] A $^4\Sigma^-$ ground state is predicted in refs 65 and 76. [e] A different value of 810 ± 50 cm^{-1} is reported in another experiment (ref 344).

observed around 1053 cm^{-1}, identical with the earlier value from photoelectron spectroscopy,[166] and a $^3\Sigma^-$ ground state is obtained from theoretical calculations.[156,158,160,163,607] Two infrared absorptions around 1000 cm^{-1} are observed for the vanadium dioxide cation, which is predicted to have a $^1A_1$ ground state with bent C_{2v} geometry.[160,163,606] The VO_3^+ cation is found to absorb at 1037 and 1069 cm^{-1}. The nonplanar C_s oxovanadium superoxide structure with a $^3A''$ ground state is found to have similar vibrational frequencies with the experimentally observed values,[163,607] although the corresponding singlet state is predicted to be more stable in some theoretical calculations.[160]

4.2. Anions

4.2.1. Monoxide Anions

The electronic structures and vibrational frequencies of most transition metal monoxide anions have been obtained from anion photoelectron spectroscopy, while matrix-isolation infrared spectroscopy has provided direct spectroscopic information on the lanthanide monoxide anions. The ground states and vibrational frequencies of transition metal monoxide anions and lanthanide metal and actinide metal monoxide anions are listed in Tables 8 and 9, respectively. Due to limited resolution, vibrational frequencies deduced from photoelectron spectra show large uncertainties. The vibrational fundamental of scandium monoxide anion is determined to be around 840 cm^{-1}

Table 9. Ground Spin States and Vibrational Frequencies (cm^{-1}) for Lanthanide Monoxide Anions in Solid Neon and Argon Matrices

molecule	ground state	vibrational frequency Ne	vibrational frequency Ar	ref
CeO^-	$^2\Phi$		772.8	74, 504
PrO^-	$^3\Sigma^-$	792.6	767.4	74, 504
NdO^-	$^4\Phi$	789.9	771.0	74, 504
PmO^-	$^5\Sigma^+$			74
SmO^-	$^6\Phi$		770.2	74, 504
EuO^-	$^7\Sigma^-$			74
GdO^-	$^8\Sigma$	[a]	772.2	74, 504
TbO^-	$^7\Sigma^-$		782.9	74, 505
DyO^-	$^6\Sigma^+$		782.0	74, 505
HoO^-	$^5\Sigma^+$		783.6	74, 505
ErO^-	$^4\Delta$		788.8	74, 505
TmO^-	$^3\Sigma^-$			74
YbO^-	$^2\Sigma^+$			74
LuO^-	$^1\Sigma^+$			74

[a] The gas-phase vibrational frequency for the GdO^- anion was determined to be 702 ± 40 cm^{-1} from anion photoelectron spectroscopy (ref 489).

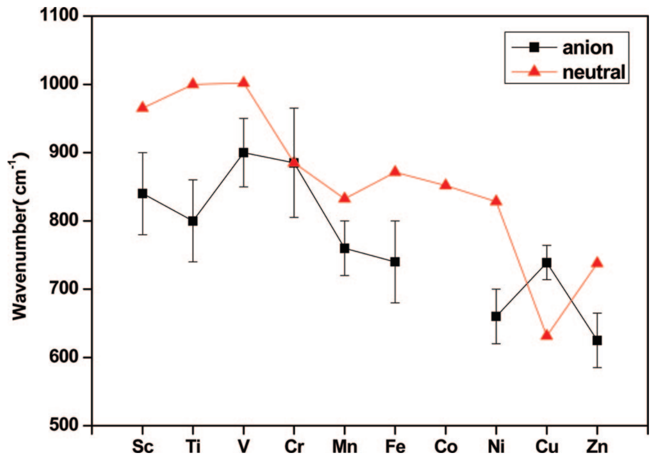

Figure 17. Plot of the vibrational fundamentals for the first row transition metal monoxide neutrals and anions. The vibrational frequencies from ScO to CuO are taken from ref 24, and the frequency for ZnO is taken from ref 456. All the vibrational frequencies for the anions are taken from Table 8.

from the hot band transitions in the photoelectron spectrum, and a $^3\Delta$ state is suggested to be lowest in energy for this anion.[89] The ScO^- anion has also been observed in solid argon with the vibrational fundamental at 889.2 cm^{-1}, which is predicted to have a $^1\Sigma^+$ ground state.[608] Figure 17 shows the vibrational fundamentals of the first row transition metal monoxide neutrals and anions. The vibrational frequencies for the ScO^-, TiO^-, VO^-, FeO^-, NiO^-, and ZnO^- anions are much lower than those of the corresponding neutral molecules.[40,115,165,343,460−462] Unlike other first row transition metal monoxide anions, the chromium and manganese monoxide anions exhibit less change in the vibrational frequencies upon electron attachment to the neutral molecules.[198,240] The additional electrons tend to occupy the nonbonding σ orbitals of both neutral CrO and MnO molecules in forming the $^4\Pi$ and $^5\Sigma^+$ state anions, which results in the similarities in vibrational frequencies between the neutral and anionic monoxide molecules. Copper monoxide anion is another special example whose vibrational fundamental lies higher than that of the neutral CuO.[384] The vibrational frequency of CuO^- anion is around 739 cm^{-1}, comparable with the value of the isoelectronic ZnO molecule.[460,461] The blue-shift in vibrational frequency

Table 10. Ground Spin States, Geometry, and Vibrational Frequencies (cm^{-1}) for Transition Metal Dioxide Anions in Solid Neon and Argon Matrices[a]

molecule	ground state	geometry	Ne ν_1	Ne ν_3	Ar ν_1	Ar ν_3	ref
ScO_2^-	$^1A_1$	bent		722.2[b]		722.5	105, 106
TiO_2^-	$^2A_1$	bent		892.2[b]		878.4	122, 132
VO_2^-	$^3A_1(^3B_1,^3B_2)$	bent	894.8[b]	907.8[b]	886.5	896.9	76, 77, 161, 182, 183
CrO_2^-	$^4B_1$	bent	847.1	918.7		906.9[b]	201
MnO_2^-	$^5B_2$	bent	781.3[b]	870.5[b]		858.3	609
FeO_2^-	$^2\Delta_g$	linear				870.6	57
CoO_2^-	$^1\Sigma_g^+$	linear		974.7		972.5	77, 610
NiO_2^-	$^4B_1(^2A_2)$	linear[c]		893.9[b]	[d]	886.8	76, 77, 347
CuO_2^-	$^3\Sigma_g^-(^3\Sigma_g^+)$	linear			[d]		76, 77, 383
ZnO_2^-	$^2\Pi_g$	linear		624.1		626	612
YO_2^-	$^1A_1$	bent		616.6[b]	702.0	618.0	109
ZrO_2^-	$^2A_1$	bent		785.8[b]		761.4	132, 146
NbO_2^-	$^1A_1$	bent	931.4[b]	878.0[b]		854.1	183
MoO_2^-	$^4B_1$	bent	883.1	837.3			201
RuO_2^-	$^2A_1$	near linear		860.6		851.8	261
RhO_2^-	$^1A_1$	near linear		898.6		893.6	337, 611
CdO_2^-	$^2\Pi_g$	linear		483.6		487.9	612
LaO_2^-	$^1A_1$	bent		569.7[b]	651.9	559.2	109
HfO_2^-	$^2A_1$	bent		770.3[b]		747.9	132, 146
TaO_2^-	$^1A_1$	bent	938.7[b]	876.6[b]		836.9	183
WO_2^-	$^2B_1$	bent	952.3	887.8	946.3	880.0	201
ReO_2^-	$^3B_1$	bent	950.8[b]	893.8		885.5	261
OsO_2^-	$^2B_1$	near linear		897.5			261
IrO_2^-	$^1\Sigma_g^+$	linear		919.9		915.7	340, 611
PtO_2^-	$^2\Pi_g$	linear		839.9[b]	[d]	836.2	611
AuO_2^-	$^3\Sigma_g^-$	linear		740.8[b]	[d]	738.2	611

[a] Only the values for the most abundant metal isotope and major site are listed. [b] Unpublished results. [c] A linear geometry was proposed for the NiO_2^- anion (ref 347). DFT/BPW91 calculations predicted a $^2A_2$ ground state with a bond angle of 170.4° (ref 77), while a $^4B_1$ state with a bond angle of 179.9° was found to be lowest in energy at the DFT/B1LYP level of theory (ref 76). [d] The symmetric OMO stretching vibrations were observed in the gas phase from anion photoelectron spectroscopy: NiO_2^- (715 ± 30, ref 342); CuO_2^- (600 ± 80, ref 382); PtO_2^- (760 ± 35, ref 342); AuO_2^- (640 ± 40, ref 440).

suggests that the CuO bond is strengthened upon electron attachment to the neutral diatomic molecule. The electronic structures of the 3d transition metal monoxide anions have been the subject of a series of theoretical studies.[28,63,65] Anions for the second and third row transition metal monoxides are less investigated.[71,73,74,89,93,136,174,204,333,342,360,432,440,441,489] The M═O vibrations for the YO^- and MoO^- anions exhibit large shifts upon electron detachment,[89,204] while the rhodium and silver monoxide anions have similar vibrational frequencies as their neutral molecules.[333,432]

Nine lanthanide monoxide anions have been characterized in solid argon, and their vibrational frequencies are about 40 cm^{-1} red-shifted from those of the neutral molecules.[504,505] The early lanthanide monoxide anions absorb around 770 cm^{-1}, while the infrared absorptions for the late lanthanide monoxide anions are about 10 cm^{-1} higher. The general trend for the change of vibrational frequencies from Ce to Er is similar to that of the neutral and cationic lanthanide monoxides as shown in Figure 16. The ground-state properties of all the lanthanide monoxide anions have been systematically studied recently using the DFT/B3LYP method.[74]

4.2.2. Dioxide Anions

Most transition metal dioxide anions have been experimentally observed. It was found that the early transition metal dioxide anions from the Sc group to the Mn group possess bent geometry[105,109,132,182,183,201,261,609] while the late transition metal dioxide anions are linear or near linear.[57,261,347,382,402,610−612] The geometric structures and vibrational frequencies of transition metal as well as lanthanide and actinide metal dioxide anions are listed in Tables 10 and 11. The antisymmetric stretching

Table 11. Ground Spin States, Experimental Bond Angles (deg), and Vibrational Frequencies (cm^{-1}) for Lanthanide and Uranium Dioxide Anions (cm^{-1}) in Solid Neon and Argon Matrices[a]

molecule	bond angle[b]	Ne ν_1	Ne ν_3	Ar ν_1	Ar ν_3
CeO_2^-	140			712.0	662.0
PrO_2^-	157		667.6	665.0	658.3
NdO_2^-	121				660.6
SmO_2^-	121			676.4	575.5
EuO_2^-	129			661.0	560.8
GdO_2^-	120			685.9	589.4
TbO_2^-	137			711.2	669.0
DyO_2^-			591.2	693.9	574.6
HoO_2^-				696.2	547
ErO_2^-	127			702.3	613.4
TmO_2^-	133				613.1
YbO_2^-	142			701.2	604.2
LuO_2^-	124				626.9
UO_2^-	180		857.2		

[a] The values for all the lanthanide dioxide anions are taken from refs 504 and 505, and the values for UO_2^- anion are taken from ref 549. [b] For lanthanide dioxide anions, angles are upper limits estimated from oxygen 16/18 isotopic ratio for ν_3; the true bond angle for bent species is probably 5° lower.

vibrational frequencies (ν_3) for the first row transition metal dioxide anions increase from Sc to Cr and from Mn to Co. The value of manganese dioxide anion is about 50 cm^{-1} lower than that of the CrO_2^- anion. In general, the ν_3 frequencies of the dioxide anions are lower than those of the corresponding neutrals. However, the cobalt dioxide anion is an exception since its ν_3 mode is blue-shifted with respect to that of neutral. Our recent matrix isolation infrared spectroscopic study reveals that the antisymmetric stretching vibration of cobalt dioxide anion at 972.5 cm^{-1} is about 30 cm^{-1} higher than that of the neutral dioxide molecule, suggesting that the CoO bonds are strengthened upon electron attachment to the neutral molecule.[610] For the second row transition metal dioxide anions, the antisymmetric stretching vibrational frequencies generally increase from left to right although the values for Nb, Mo, and Ru are close to each other. The ν_3 frequencies of the third row transition metal dioxide anions increase from La to Ir and then decrease from Ir to Au.

All the lanthanide metal dioxide anions were characterized to be bent. The ν_3 vibrational frequencies of the anions are lower than those of the corresponding neutrals. But the neutral-to-anion frequency shifts are quite small for the late lanthanide metals from Dy to Yb. The UO_2^- anion is the only actinide metal dioxide anion experimentally observed. It is characterized to be linear with a $^2\Phi_u$ ground state.[549]

The frequency shift upon electron attachment to the neutral molecules strongly depends on the nature of the frontier orbitals. Take the PtO_2^- and IrO_2^- anions as an example, the frequency difference for platinum (106.1 cm^{-1}) is much larger than that for iridium (13.3 cm^{-1}).[611] The PtO_2 neutral has a linear singlet ground state. The LUMO of neutral PtO_2 is an antibonding π orbital, which mainly consists of the O 2p orbital and Pt 5d orbital. Addition of an electron to this orbital of neutral PtO_2 results in the $^2\Pi_g$ ground-state PtO_2^- anion, in which the Pt−O bond is elongated with the stretching vibrational frequency lowered. For the IrO_2^- anion, the additional electron occupies the SOMO of neutral IrO_2 which is mainly a nonbonding orbital derived from the 5s atomic orbital of iridium. Apparently, the bond strength of IrO_2 does not change significantly upon electron attachment to this orbital, which leads to a slight decrease of the antisymmetric stretching vibrational frequency for the anion due to the increase in electrostatic interactions.

The properties of most ground-state transition metal dioxide anions have been obtained from the theoretical point of view although they are not as extensively studied as the neutrals.[76,77,105,109,132,183,197,201,240,261,440,549,609−612] In some cases, it is very difficult to determine the electronic ground state of the anions based solely upon theoretical calculations, and comparison between the experimental observations and the calculated values is essential in determining the true ground-state structure. The FeO_2^- anion provides as a good example demonstrating that theoretical calculations on such linear species require sophisticated treatment.[57] Recent studies in our laboratory indicate that calculations with single-reference methods, including various DFT and post-HF methods are unreliable for the FeO_2^- anion, which is experimentally determined to be linear. However, the state-averaged multireference MRCI method, which incorporates both the dynamic and nondynamic correlations predicts that the anion has a linear doublet ground state, consistent with the experimental observations.

4.2.3. Oxygen-Rich Anions

Trioxide anions have been observed for several systems including the V group metals, chromium, rhenium, and some rare earth metals in matrix infrared spectroscopic studies.[183,201,261,504,505] The vanadium, niobium, and tantalum trioxide anions are determined to have C_{3v} or D_{3h} structures with a closed-shell singlet ground state, in which the metal centers are in the highest +5 oxidation state.[183] The doubly degenerate M=O stretching modes are observed at 916.2, 817.1, and 807.0 cm^{-1} in solid argon. The YO_3^-, PrO_3^-, and TbO_3^- anions were suggested to have planar D_{3h} symmetry, while the GdO_3^- anion seemed to have a pyramidal structure due to the strong intermediate absorptions observed in the experiments using mixed and scrambled oxygen isotopic samples.[109,504,505] The M=O stretching vibrational frequencies for these four rare earth metal trioxide anions are more than 250 cm^{-1} lower than those of the V group trioxide anions due to the lack of enough valence electrons to afford three formal M=O double bonds. A recent vibrationally resolved photoelectron spectroscopic study revealed that the WO_3^- anion possesses a trioxide structure with three oxygen atoms atomically bound to the tungsten center, while a dioxygen−dioxide complex structure was proposed for the WO_4^- anion.[236] However, based upon a more recent PES study, the ground state of WO_4^- is found to be a tetroxide structure with C_{2v} symmetry, which comprises two W=O double bonds with the extra charge delocalized on the other two W−O units.[228]

The Mn group transition metals are known to form stable tetroxide anions with the metal centers in the highest +7 oxidation state.[316] The MnO_4^- anion has been well studied in salts and solutions. It has a tetrahedron geometry with a bond length of 1.629 ± 0.008 Å.[613] The triply degenerate antisymmetric OMnO stretching vibration is observed at 910 cm^{-1} in salts,[614] which is slightly higher than the argon matrix value of 896.9 cm^{-1}.[609] The MnO_4^- anion is unusually stable. Photoelectron spectroscopic study shows that the MnO_4 neutral has an electron affinity of 4.80 ± 0.10 eV,[249] which is significantly larger than that of atomic chlorine.[578] The ReO_4^- anion is isoelectronic with OsO_4. The triply degenerate ReO stretching vibration is observed around 907 cm^{-1}.[261]

5. Multinuclear Transition Metal Oxide Clusters

Multinuclear transition metal oxide clusters serve as building blocks for nanostructured materials and also as representative models for gas-phase studies, which can provide an understanding of the function of transition metal oxide catalysts at the molecular level. The composition of cluster ions can be determined by mass spectrometric methods, and their geometric structures can, in principle, be predicted by quantum chemical calculations. However, reliable structural assignments for transition metal oxide clusters, particularly for larger clusters are quite difficult due to the existence of many low-energy isomers and low-lying electronic states. The identification of the transition metal oxide cluster structure generally requires the confirmation by experimental data from structurally sensitive methods such as vibrational spectroscopy. Vibrational spectroscopy combined with the state-of-the-art quantum chemical calculations offers one of the most direct and generally applicable experimental approaches to structural investigation of neutral and charged transition metal oxide clusters. With the development of tunable free electron lasers, IR photodissociation spectroscopy has been successfully used to measure indirectly the vibrational absorptions of mass-selected transition metal oxide cluster ions in the gas phase. Recent progress on vibrational spectroscopic investigations of transition metal oxide cluster ions has been outlined in recent reviews[615] and will not be repeated here. But some more recent progress will be discussed. For transition metal oxide neutral clusters, anion photoelectron spectroscopy has been used to measure the electron detachment energies of anions, which can provide vibrational information on the neutral clusters in the gas phase. Due to the limited spectral resolution, vibrational frequencies can in general be resolved only for small sized clusters. Structural assignments for larger clusters are usually accomplished by combining experimental PES data with theoretical calculations. Infrared absorption spectroscopy offers another direct experimental method to investigate the vibrational frequencies of neutral multinuclear transition metal oxide clusters in solid matrices. However, matrix infrared spectroscopic experiments also face difficulties for larger multinuclear clusters owing to low concentrations and spectral congestion. It is quite difficult to determine the number of transition metal atoms involved in the clusters because the metal−metal vibrations generally lie in the far-infrared region with very low IR intensities. Nevertheless, some multinuclear transition metal oxide clusters (mainly dinuclear clusters) have been studied using matrix infrared spectroscopy. In this section, spectroscopic studies on multinuclear transition metal oxide clusters will be summarized. We will focus on small clusters with their spectral and structural information being clearly determined, in particular, dinuclear oxide clusters. The experimental vibrational frequencies of some multinuclear transition metal oxide clusters are listed in Table 12. There are a large number of studies on the reactivity of transition metal oxide clusters. These studies go beyond the scope of this review and will not be discussed here.

5.1. Sc Group

There is no experimental report on the spectroscopic study of multinuclear scandium oxide clusters except a photoionization study of scandium cluster monoxides. The photoionization efficiency spectra and ionization energies of Sc_nO (n = 5−36) are reported.[616] Density functional theory calculations on dinuclear scandium oxide clusters indicate that Sc_2O_2 has a $^3B_{1u}$ ground state with planar D_{2h} symmetry (Figure 18A).[85] Minor structural changes in the cluster are seen upon adding or removing electrons, since this involves the weakly bonding half-filled valence orbitals. Infrared absorptions at 699.1 and 647.8 cm^{-1} have been tentatively assigned to the cyclic Sc_2O_2 cluster in solid argon.[104] The Sc_2O_3 cluster has a trigonal bipyramid structure with D_{3h} symmetry (Figure 19A).[85] Mass-selected $Y_nO_m^-$ cluster anions with n = 2−10 have been investigated by photoelectron spectroscopy using 355 and 266 nm for the detachment wavelengths.[617] Electron affinities and vertical detachment energies were measured. A general trend in the observed photoelectron spectra is a shifting of threshold energies to higher binding energies with increasing cluster size n. At low electron binding energies, main spectral features are contributed from metal d-band orbitals, whereas the O 2p contribution becomes apparent with increasing oxygen content due to a higher degree of hybridization of yttrium s and d and oxygen 2p orbitals. In addition, theoretical calculations on the oxygen-deficient metal cluster monoxides of scandium and yttrium have also been reported.[618,619]

5.2. Ti Group

The dinuclear Ti_2O_2 cluster has been observed in solid matrices and was characterized to have a four-membered ring structure. It was calculated to have a closed-shell singlet ground state having a nonplanar C_{2v} geometry with a strong Ti−Ti bond (Figure 18B).[620,621] The zirconium and hafnium analogs also have a closed-shell singlet ground state but were predicted to have planar D_{2h} symmetry (Figure 18A).[620] All three M_2O_4 clusters of group IV metals have been observed in solid argon matrix.[620] These clusters are formed by the dimerization reactions between two metal dioxide molecules, which requires negligible activation energy. All these M_2O_4 clusters are characterized to have a ^1A_g ground state with nonplanar C_{2h} symmetry (Figure 20A). The clusters involve a rhombus M(μ-O)$_2$M subunit and two terminal O atoms bending out of the M(μ-O)M plane in opposite directions.[140−144,620,622−626] A comparison between the experimental PES data and theoretical calculations verifies unequivocally that the $Ti_2O_4^-$ anion has a C_{3v} structure.[135,149] The electronic structures of larger $(TiO_2)_n$ clusters have been the subject of several theoretical calculations.[141,142,627−629] The recently reported photoelectron spectra of $(TiO_2)_n^-$ (n = 3−10) clusters reveal that the band gap is strongly size-dependent for $n < 7$, but it rapidly approaches the bulk limit at $n = 7$ and remains constant up to $n = 10$. All PES features are observed to be very broad, suggesting large geometry changes between the anions and the neutral clusters due to the localized nature of the extra electron in the anions. The extra electron in the $(TiO_2)_n^-$ clusters appears to be localized in a tricoordinated Ti atom, creating a single Ti^{3+} site and making these clusters ideal molecular models for mechanistic understanding of TiO_2 surface defects and photocatalytic properties.[135]

Titanium and zirconium oxide clusters with the M_nO_{2n-1} stoichiometry have been studied using infrared photodissociation spectroscopy. Most of these clusters exhibited similar broad features in the bridged M−O−M stretching frequency region, which are assigned to the M−O stretching vibrations of the four-membered M_2O_2 rings.[46,626]

5.3. V Group

Infrared photodissociation spectroscopic investigation in the gas phase indicates that the $V_2O_2^+$ cation has a four-membered ring structure.[630] It is calculated to have a planar $^2A'$ ground state.[160b] The V_2O_2 neutral has a $^3A_1$ ground state, in which the two vanadium atoms are slightly inequivalent in forming a planar C_{2v} geometry.[631] The $V_2O_3^+$ cation and V_2O_3 neutral have nonplanar C_s symmetry (a four-membered V_2O_2 ring with an extra O atom terminally attached to a vanadium atom, Figure 19B)[630,631] The V_2O_4 cluster has been observed as the photodetachment product of the $V_2O_4^-$ anion. It is calculated to have a triplet ground state with nonplanar C_{2v} symmetry, in which no direct V−V bond is formed (Figure 20B).[160,161,631,632] The $V_2O_4^-$ anion is calculated to have a high-spin $^4B_{2g}$ ground state with planar D_{2h} symmetry (Figure 20C).[161] The IR photodissociation spectrum indicates that the $V_2O_4^+$ cation is nonplanar with the two vanadyl groups in trans positions with respect to the ring plane (Figure 20A).[630] The ground state of V_2O_5 is found to be a doubly bridged structure ($^1A_1$), where one vanadium atom has a tetrahedral coordination and the other has a trigonal-pyramidal coordination (Figure 21A).[161,631] The $V_2O_5^-$ anion is found to possess a similar doubly bridged structure with a $^2A'$ ground state. A nonplanar D_{2h} structure (Figure 21 F) is suggested to be the structure observed in anion photoelectron spectroscopic investigation of the $V_2O_6^-$ anion in the gas phase.[633] The terminal VO vibration is measured around 800 cm^{-1}, which is lower than the value of V_2O_4 cluster with two terminal VO double bonds but higher than that of cyclic V_2O_2 cluster with VO single bonds. Since each vanadium atom in the V_2O_6 cluster cannot afford two VO

Table 12. Vibrational Frequencies (cm^{-1}) for Selected Multinuclear Transition Metal Oxide Clusters

molecule	symmetry	vibrational frequency	experimental method[a]	ref
Sc_2O_2	D_{2h}	699.1, 647.8	MI-IR	104
Y_2O_2	D_{2h}	546.2	MI-IR	109
Ti_2O_2	C_{2v}	746.1, 736.2	MI-IR	620
Ti_2O_4	C_{2h}	956.8, 704.1, 679.9	MI-IR	620
Zr_2O_2	D_{2h}	701.5	MI-IR	620
Zr_2O_4	C_{2h}	870.6, 652.0, 593.4	MI-IR	620
Hf_2O_2	D_{2h}	684.2	MI-IR	620
Hf_2O_4	C_{2h}	866.4, 649.4, 591.3	MI-IR	620
$V_2O_2^+$	C_s	833, 724	IR-PD	630
$V_2O_3^+$	C_s	1044, 803, 765, 666	IR-PD	630
$V_2O_4^+$	C_s	1049, 1029, 794, 776, 594	IR-PD	630
V_2O_4	C_{2v}	1090 ± 30	PES	633
$V_2O_5^+$	C_s	1034, 911, 815, 738, 657	IR-PD	630
$V_2O_6^+$	C_1	1160, 1060, 1028, 836, 751, 673	IR-PD	630
V_2O_6	D_{2h}	800 ± 40	PES	633
$V_2O_6^-$	C_{2v}	975, 959, 930, 911, 888, 800, 775, 738, 620	IR-MPD	636b
$V_2O_7^-$	C_s	1112, 987, 965, 952, 775, 705, 627	IR-MPD	636b
$Nb_2O_6^+$	C_1	990, 790, 675, 625	IR-MPD	637
Cr_2O_2	C_s (chain)	934.4, 844.6	MI-IR	652
	D_{2h} (cyclic)	628.2	MI-IR	202
Cr_2O_3	C_s	620 ± 30, 280 ± 30	PES	650
Cr_2O_4	D_{2h}	630 ± 50	PES	650
	D_{2h}	984.1, 716.1, 642.9	MI-IR	652
Cr_2O_5	C_s	710 ± 50	PES	650
Cr_2O_6	D_{2h}	780 ± 50	PES	650
	D_{2h}	1014.8, 975.4, 704.1, 690.5	MI-IR	652
Mo_2O_2	C_s	880 ± 100, 320 ± 50	PES	653
Mo_2O_3	C_2	560 ± 30	PES	653
Mo_2O_4	C_s	970 ± 40	PES	653
W_2O	C_s	810 ± 40	PES	654
W_2O_3	C_{2v}	920 ± 50	PES	654
W_2O_4	C_1	920 ± 40	PES	654
W_2O_5	C_s	920 ± 40	PES	654
W_2O_6	D_{2h}	920 ± 40	PES	654
Mn_2O	C_{2v}	808.3	MI-IR	246
Mn_2O_2	D_{2h}	601.0, 506.8	MI-IR	246
Mn_2O_6	D_{2h}	1092.0, 683.6	MI-IR	247
Fe_2O	C_{2v}	868.6	MI-IR	270
Fe_2O_2	D_{2h}	670 ± 70	PES	268
	D_{2h}	660.6, 517.4	MI-IR	270, 320
Fe_2O_3		810 ± 100	PES	268
Fe_2O_4	D_{2h}	710 ± 60	PES	268
		861.5, 705.1	MI-IR	270
Fe_2O_5		750 ± 50	PES	268
Co_2O_2	D_{2h}	685.2, 469.5, 304.1	MI-IR	672
Co_2O_4		859.6, 540.0	MI-IR	320
Ni_2O_2	D_{2h}	650.2, 481.6	MI-IR	347
Pd_2O_2	C_{2v}	875.6	MI-IR	380
Pd_2O_4	D_{2h}	937.8	MI-IR	380
Cu_2O	C_{2v}	<200	PES	679
Cu_2O_2	D_{2h}	630 ± 30	PES	679
	C_{2v}	1096.5	MI-IR	682
	$C_{\infty v}$	955.0	MI-IR	682
Cu_2O_3	D_{3h}	640	PES	679
Cu_2O_4	D_{2h}	985.9	MI-IR	682
V_3O	C_{2v}	750 ± 20, 415 ± 15, 340 ± 15	PES	641
V_3O^-	C_{2v}	355 ± 20, 770 ± 20	PES	641
$V_3O_8^-$	C_{2v}	965, 922, 834, 680, 656	IR-MPD	636b
Nb_3O^+	C_{2v}	312 ± 1	ZEKE	639
Nb_3O	C_{2v}	710 ± 15, 320 ± 15	PES	641
Nb_3O^-	C_{2v}	300 ± 20	PES	641
$Nb_3O_8^+$	C_s	1000, 700	IR-MPD	637
Ta_3O	C_{2v}	710 ± 15, 225 ± 15	PES	641
Ta_3O^-	C_{2v}	215 ± 20	PES	641
$V_4O_{10}^+$	C_s	1032, 842	IR-MPD	638
V_4O_{10}	T_d	1028.4, 826.8, 623	MI-IR	635
$V_4O_{10}^-$	D_{2d}	990, 670, 637, 602	IR-MPD	636
$V_4O_{11}^-$	C_s	999, 990, 976, 899, 874, 824, 785, 721, 721, 684	IR-MPD	636b

[a] Abbreviations: MI-IR, matrix-isolation infrared spectroscopy; PES, photoelectron spectroscopy; IR-(M)PD, infrared (multiple) photon dissociation spectroscopy; ZEKE, zero-electron kinetic energy photoelectron spectroscopy. All the vibrational frequencies from MI-IR spectroscopy are obtained in solid argon.

double bonds due to the five valence electrons of vanadium, it is reasonable for the two terminal VO bonds in the V_2O_6 cluster to exhibit some intermediate properties with bond order roughly viewed as 1.5.[633] The observation of an O−O

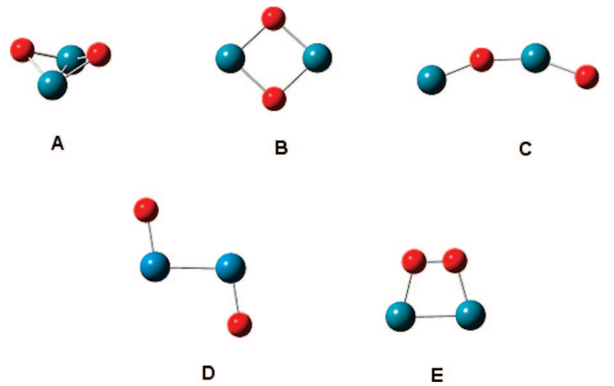

Figure 18. Experimentally observed structures for the M_2O_2 clusters.

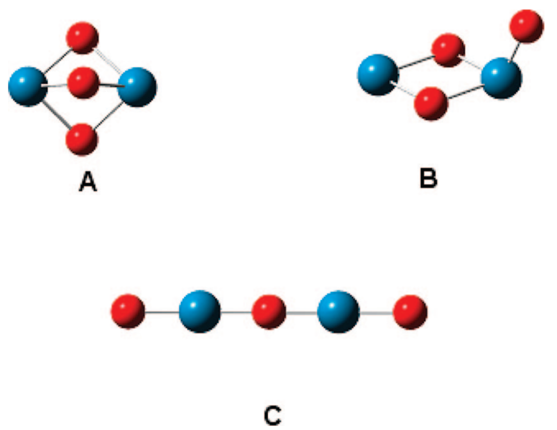

Figure 19. Experimentally observed structures for the M_2O_3 clusters.

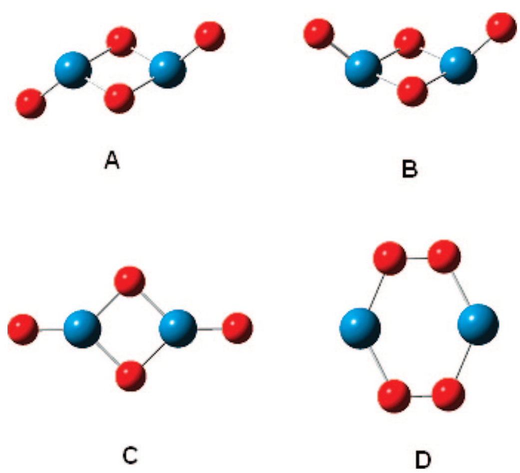

Figure 20. Experimentally observed structures for the M_2O_4 clusters.

stretching vibration at 1160 cm^{-1} in the IR photodissociation spectrum of $V_2O_6^+$ (Figure 22) indicates that $V_2O_6^+$ involves a superoxo group. In the ground state of $V_2O_6^+$, the two vanadyl groups occupy the trans position and the η^2-superoxo unit forms a three-membered ring with one of the two vanadium atoms (Figure 21E).[630] The V_2O_7 and $V_2O_7^-$ clusters are oxygen-rich species, and their ground-state structures are found to be similar to those of V_2O_6 and $V_2O_6^-$ except that one terminal oxygen atom is replaced by a peroxo O_2 unit (Figure 23A,B).[631,633]

Higher multinuclear vanadium oxide clusters have also been the subject of several gas-phase and matrix experimental studies. By condensation of the gas evaporating from a

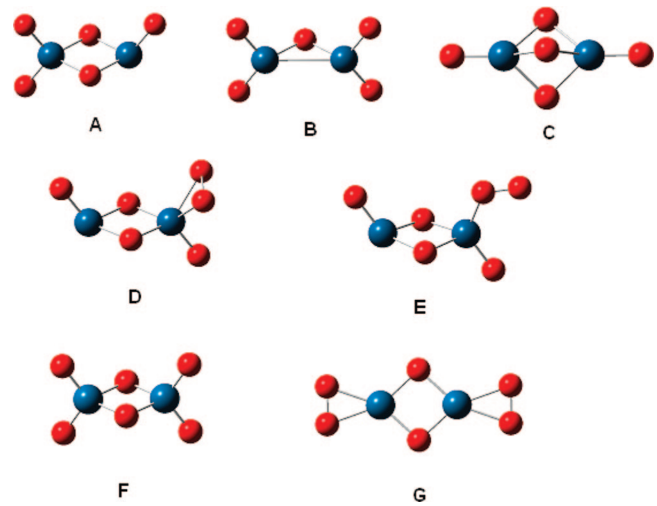

Figure 21. Experimentally observed structures for the M_2O_5 and M_2O_6 clusters.

Knudsen cell containing V_2O_5, two absorptions at 1030 and 828 cm^{-1} in solid nitrogen are assigned to the terminal V═O and bridged V−O−V stretching vibrational modes of the neutral V_4O_{10} cluster, in analogy to P_4O_{10}.[634] Very recently, the V_4O_{10} cluster has been produced and trapped in solid argon and nitrogen matrices with high concentrations and comprehensively characterized by infrared, Raman, and UV/visible spectroscopy.[635] In addition, the V_4O_8 and V_6O_{12} clusters were also suggested to be observed.

The infrared spectra of vanadium oxide anionic clusters have been studied by infrared multiple photodissociation spectroscopy.[636] Three types of anions including the open-shell $(V_2O_5)_n^-$ anion, the fully oxidized closed-shell $(V_2O_5)_nVO_3^-$ anions and the oxygen-rich $V_4O_{11}^-$ cluster. Three types of vibrational modes in the range from 600 to 1600 cm^{-1} are identified and assigned to (i) superoxo (∼1100 cm^{-1}), (ii) vanadyl (1020−870 cm^{-1}), and (iii) V−O−V and terminal V−O single bond vibrational modes (<950 cm^{-1}). Comparison of the experimental and calculated spectra favors an assignment of the closed-shell $V_3O_8^-$ anion to a C_{2v} structure consisting of a six-ring fused with a four-ring. For $V_5O_{13}^-$, two nearly isoenergetic isomers, a pyramidal C_{4v} structure and a bridged C_{2v} structure may be probed in the experiment. The spectra of the open-shell $(V_2O_5)_n^-$ clusters are distinctly different from those of closed-shell clusters. The $V_4O_{10}^-$ anion is characterized to have a tetragonal D_{2d} structure, which is minimally Jahn−Teller distorted from the T_d structure. It is found that the oxygen-rich $V_4O_{11}^-$ anion does not exhibit a caged structure derived from the exceptionally stable V_4O_{10}, but an open structure is found. It is concluded that the dinuclear and trinuclear oxide anion clusters are characterized by open structures involving four-membered V_2O_2 rings, but this motif is replaced by the less strained and more stable six- and eight-membered rings in the larger clusters.

The infrared spectra of vanadium and niobium oxide cationic clusters have been studied using mass-selected infrared photodissociation spectroscopy. The infrared spectra are obtained for the nearly stoichiometric $(Nb_2O_5)_n^+$ and $(Nb_2O_5)_nNbO_2^+$ (n = 2, 3) clusters as well as for oxygen-rich clusters of typical compositions $(Nb_2O_5)_nO^+$ and $(Nb_2O_5)_nNbO_3^+$ (n = 1−3).[637] The spectra of all examined oxide clusters exhibit two main absorption features that can be assigned to vibrations of terminal Nb═O and bridged

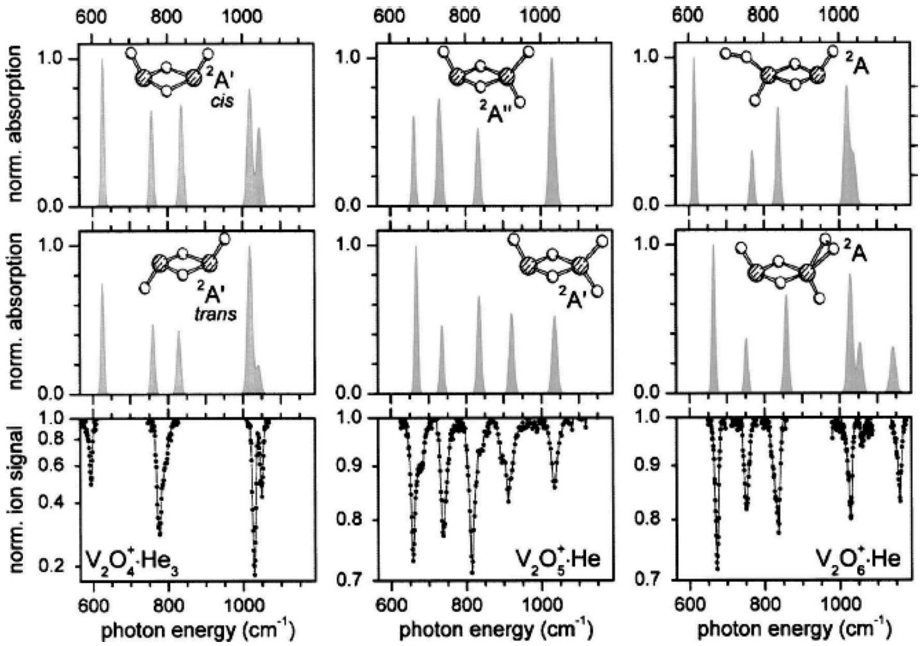

Figure 22. Experimental photodepletion spectra (solid black dots connected by black lines) of $V_2O_4^+$-He_3 (left), $V_2O_5^+$-He (center), and $V_2O_6^+$-He (right) and simulated IR spectra (gray line and gray shaded area), based on scaled B3LYP/TZVP frequencies and relative intensities of the ground state (middle row) and an energetically low-lying isomer (top row) of $V_2O_4^+$ (left), $V_2O_5^+$ (center), and $V_2O_6^+$ (right) in the region from 565 to 1190 cm^{-1}. Reprinted with permission from ref 630. Copyright 2004 American Institute of Physics.

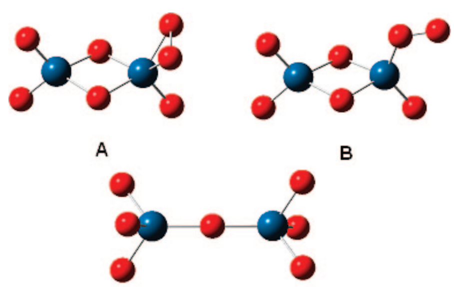

Figure 23. Experimentally observed structures for the M_2O_7 clusters.

Nb−O−Nb oxide groups. The stretching vibrations of isolated Nb═O units absorb at about 990−1000 cm^{-1}. The stretching vibrations of Nb−O−Nb bridges are found in the 700−900 cm^{-1} range, varying with cluster size and stoichiometry. Comparisons between the experimental IR spectra and calculated spectra for possible structures help to identify the gas-phase structures of the clusters. The most stable structure of $Nb_3O_8^+$ contains a peroxo η^2-O_2^{2-} unit. Fragmentation channels indicate that similar units are present in the larger $(Nb_2O_5)_nO^+$ and $(Nb_2O_5)_nNbO_3^+$ clusters. The $Nb_4O_{10}^+$ cation is assumed to have a similar structure to that of neutral V_4O_{10}, which has T_d symmetry. Theoretical calculations give a minimum structure with C_1 symmetry; however the distortion relative to T_d is small and mainly caused by the presence of one terminal single-bonded Nb−O unit, where the unpaired electron is located at the O atom. The photodissociation spectrum of $V_4O_{10}^+$ recorded by monitoring the $V_4O_8^+$ yield as a function of the excitation wavelength is very similar to that of the neutral V_4O_{10} cluster.[638] Two absorption bands at 842 and 1032 cm^{-1} are observed, which are assigned to the antisymmetric V−O−V stretching and V═O stretching vibrations of the $V_4O_{10}^+$ cation. In contrast to $Nb_4O_{10}^+$, the $V_4O_{10}^+$ cation is determined to have a structure involving a $V_4O_8^+$ ionic core weakly bound to an oxygen molecule.[638]

Multinuclear oxide clusters have also been the subject of gas-phase photoelectron spectroscopic studies. A high-resolution zero-electron kinetic energy (ZEKE) photoelectron spectroscopic study on the Nb_3O and Nb_3O^+ monoxides observed a vibrational progression in a mode with frequencies of 312 cm^{-1} in the cation and 320 cm^{-1} in the neutral.[639] Density functional theory calculations and Franck−Condon spectral simulations indicate that Nb_3O and Nb_3O^+ have low-spin, planar C_{2v} ground states with the O atom doubly bridging across the elongated bond of an isosceles Nb_3 cluster.[639,640] Vibrationally resolved 488 nm anion photoelectron spectra of V_3O, Nb_3O, and Ta_3O indicate that the neutral and anionic clusters all have planar structures with doubly bridging oxygen atoms and that the electrons in the anions occupy essentially nonbonding orbitals.[641] The metal−oxygen symmetric stretching fundamentals for both the neutral and anionic clusters are reported. The ground-state of $Nb_3O_2^-$ is found surprisingly to be a low-symmetry C_1 (^{1}A) structure, which contains a bridging and a terminal O atoms.[642] Anion photoelectron spectroscopic study on the $Ta_3O_3^-$ anion shows that the $Ta_3O_3^-$ cluster has a planar D_{3h} triangular structure.[643] Chemical-bonding analyses reveal that among the five valence molecular orbitals involved in the multicenter metal−metal bonding, there is a completely bonding δ and π orbital formed from the 5d atomic orbitals of Ta. The totally delocalized multicenter d bond renders d aromaticity for $Ta_3O_3^-$ and represents a new mode of chemical bonding. Similar PES studies have also been reported for higher clusters, but the spectra are not well vibrationally resolved.[644,645] Very high electron affinities and large HOMO−LUMO gaps are observed for the $(V_2O_5)_n$ (n = 2−4) clusters. The HOMO−LUMO gaps of $(V_2O_5)_n$ all exceed that of the band gap of the bulk oxide and are found to increase with cluster size from n = 2−4. These clusters are predicted to possess polyhedral cage structures.[645,646]

5.4. Cr Group

Combined PES and DFT studies on Cr_2O^- imply that Cr_2O^- has a high-spin ground state ($S = 9/2$) with C_{2v} symmetry.[647−651] However, the Cr_2O neutral is predicted to have a low-spin triplet ground state.[194] Two structural isomers with Cr_2O_2 stoichiometry have been characterized in solid matrices. Besides the cyclic structure, which is predicted to have a nonet ground state, a chainlike CrOCrO isomer has also been identified in a recent matrix infrared spectroscopic study.[652] The CrOCrO cluster is predicted to have a $^9A''$ ground state with bent geometry (Figure 18C). The cyclic structure is predicted to be more stable than the chainlike isomer from most theoretical studies.[647−649] The cyclic $Cr_2O_2^-$ anion is calculated to have a high-spin ground state ($S = 9/2$).[651] DFT calculations predict that $Cr_2O_3^-$ possesses C_s symmetry and a puckered four-membered ring structure with an extra oxygen atom terminally bonded to one Cr atom (Figure 19B). A high-spin state ($S = 7/2$) and a low-spin state ($S = 1/2$) are nearly degenerate with the low-spin state only 0.04 eV higher in energy.[649] The PES data imply that the experimentally observed $Cr_2O_3^-$ anion is due to a high-spin species.[650] The Cr_2O_4 cluster is formed from the barrierless dimerization of the chromium dioxide molecules in solid argon, which is characterized to have a planar D_{2h} symmetry (Figure 20C).[652] The cluster is calculated to have a $^5A_2$ ground state with the four unpaired electrons occupying the nonbonding molecular orbitals, which are largely chromium 3d in character.[652] A triplet state with nonplanar C_{2v} symmetry is proposed to be the ground state of Cr_2O_4 by earlier theoretical calculations,[647,648] but this state is predicted to be much less stable than the $^5A_2$ state planar D_{2h} structure based on recent DFT calculations.[652] The structure of Cr_2O_5 is predicted to be similar to that of Cr_2O_4 with the extra O atom bonded to one Cr atom (Figure 21A). The ground state of Cr_2O_5 is predicted to be a singlet.[647] A vibrational progression of 710 cm^{-1} in the PES spectrum is observed for the ground-state transition, which is likely due to a Cr−O stretching mode.[650] The Cr_2O_6 cluster is also formed in our recent matrix infrared spectroscopic study on the reaction of chromium atom with dioxygen.[652] The observed vibrational frequencies indicate that the Cr_2O_6 cluster involves a four-membered ring and two terminal oxygen atoms on each chromium centers. Theoretical calculations indicate that the Cr_2O_6 cluster has a closed-shell singlet ground state with nonplanar D_{2h} symmetry (Figure 21F).[232,647,652] This structure is also suggested to be the structure observed in anion photoelectron spectroscopic investigation of the $Cr_2O_6^-$ anion in gas phase.[650]

Dinuclear oxide clusters, $Mo_2O_n^-$ ($n = 2-4$) and $W_2O_n^-$ ($n = 1-6$), have also been studied by PES.[653,654] The Mo_2O_n clusters are in general similar to W_2O_n. The geometric and electronic structures of W_2O_n clusters are quite different from those of Cr_2O_n clusters for the very O-deficient systems from $n = 1-3$. The Cr_2O_n ($n = 1-3$) clusters are ferromagnetic. Although the ground state of W_2O is a triplet state, the ground states of both W_2O_2 and W_2O_3 are singlets and nonmagnetic. The structures of the two systems are also very different. Whereas in Cr_2O_n, the first two O atoms bond to both Cr atoms in a bridging manner, in W_2O_n the first two O atoms each bond only to one W atom because of the strong W−O bond strength (Figure 18D). This leaves strong W−W bonding in the O-deficient W_2O_n clusters, resulting in nonmagnetic or very weak magnetic systems. For $n = 4$ and higher, the Cr_2O_n and W_2O_n systems become similar as the magnetic coupling in the Cr systems becomes weakened due to the loss of 3d electrons to oxygen. Density functional calculations establish that the $W_2O_7^{2-}$, $W_2O_7^-$, and W_2O_7 clusters possess different global minimum structures. The dianion is predicted to have a highly symmetric structure (D_{3d}, Figure 23C), in which the two WO_3 moieties are connected by a single oxygen atom. Both the monoanion and neutral clusters are calculated to have lower symmetry (C_1) with a cyclic W_2O_2 four-membered ring. A terminal peroxo ligand bound to one tungsten center is predicted to be most stable for the neutral cluser (Figure 23A), while the isomer with a terminal oxo ligand ($-O^\bullet$) is lowest in energy in the monoanion case. The calculated electron affinities are in good agreement with the experimental values.[655] Based on photoelectron spectroscopy and density functional theory calculations,[656] the $W_2O_8^-$ anionic cluster is characterized as $[W_2O_6(O_2^-)]$, that is, a superoxide species interacting with the neutral W_2O_6 cluster. In contrast, the neutral W_2O_8 cluster is found to contain an O_2 molecule weakly interacting with the W_2O_6 cluster.

Well-resolved photoelectron spectra have been obtained for $(CrO_3)_n^-$ ($n = 3-5$) and compared with DFT calculations.[227] Unique nonplanar cyclic ring structures are firmly established for $(CrO_3)_n$ and $(CrO_3)_n^-$. The structures can be described as formed from corner-sharing tetrahedral CrO_4 units with two Cr═O μ-oxo bonds and two Cr−O bridge bonds. The structural parameters of the $(CrO_3)_n$ clusters are shown to converge rapidly to those of the CrO_3 bulk crystal. The extra electron in the $(CrO_3)_n^-$ anions is shown to be largely delocalized over all Cr centers. The $(MoO_3)_n$ and $(WO_3)_n$ clusters are predicted to have similar ring structures.[232b]

Electronic and structural properties of tritungsten oxide clusters: $W_3O_n^-$ and W_3O_n ($n = 7-11$) have been investigated using PES and density functional theory calculations.[656,657] Detachment features due to W 5d and O 2p features are observed in $W_3O_7^-$ and $W_3O_8^-$ with the 5d feature at lower electron binding energies and the O 2p features at very high electron binding energies.[657] A large energy gap is observed in the PES spectrum of the stoichiometric W_3O_9 cluster. High electron binding energies (>7.0 eV) are observed for $W_3O_{10}^-$, suggesting that the W_3O_{10} neutral cluster is an unusually strong oxidizing agent. The calculation results show that W_3O_9 is a D_{3h} cluster with a W_3O_3 six-membered ring and two terminal W═O units on each W site. The structure of W_3O_8 can be viewed as removing a terminal O atom from W_3O_9, whereas that of W_3O_7 can be viewed as removing two terminal O atoms from W_3O_9. The O-rich cluster W_3O_{10} can be viewed with replacing a terminal O atom in W_3O_9 by an O_2 unit. The $W_3O_{11}^-$ anionic cluster is characterized as $[W_3O_9(O_2^-)]$, a superoxide species interacting with the neutral W_3O_9 cluster. The neutral W_3O_{11} cluster is found to contain an O_2 molecule weakly interacting with the W_3O_9 cluster.[656] The $M_3O_9^-$ and $M_3O_9^{2-}$ clusters (M = Mo and W) are characterized to involve a single, fully delocalized metal−metal bond and may be considered as a new class of d-orbital aromatic molecules.[658]

Recent photoelectron spectrosocopic and theoretical studies on the $W_4O_x^-$ ($x \leq 6$) clusters reveal that tungsten oxide clusters undergo a transition from metal-like to semiconductor-like behavior with oxygen uptake at $x = 5$. The oxygen atoms are bound to the W_4 cluster in either terminal or bridged fashions for both neutral and anionic $W_4O_x^-$ ($x = 1-4$) clusters, while the tetrahedral W_4 core is changed to ringlike structure with fewer metal−metal bonds in the W_4O_5 case.[659] The structural and spectral properties of some multinuclear clusters have also been theoretically reported.[660]

5.5. Mn Group

The Mn_2O cluster is identified to possess high-spin state with ferromagnetic feature.[661] The Mn_2O_2 cluster is regarded as a building block for bulk manganese oxide.[241] The Mn_2O_2 cluster can be formed via the reaction of manganese dimer with dioxygen in solid argon and is characterized to have a rhombic structure.[246,247] It is predicted to have a high-spin ferromagnetic ground state with the unpaired electrons mainly distributed on the manganese atoms. Unlike the bare Mn_2 dimer, which is considered as a weakly bound van der Waals system, the Mn−Mn interaction is enhanced in the rhombus Mn_2O_2 cluster.[241] The distance between two manganese centers is predicted to be 2.56 Å, about 0.9 Å shorter than that of the manganese dimer.[662] The Mn_2O_6 cluster has been spectroscopically characterized in solid argon matrix, which is determined to be a bisdioxygen complex of cyclic Mn_2O_2 cluster.[247] The cluster is predicted to have a $^{11}B_{1u}$ ground state with planar D_{2h} symmetry, in which the Mn_2O_2 core is coordinated by two equivalent O_2 molecules in a side-on fashion (Figure 21G). Based on the observed O−O stretching frequency and predicted O−O bond length, the two O_2 subunits are due to superoxide ligands. Hence, the Mn_2O_6 cluster can be described as $[(O_2^-)_2(Mn_2O_2)^{2-}]$, a disuperoxide complex.

There is no experimental report on spectroscopic study of multinuclear manganese oxide clusters except a photoelectron spectroscopic study on the Mn_5O and Mn_6O clusters. The results show that while the O atom occupies either a bridge or hollow site in Mn_5, it prefers a hollow site in Mn_6 clusters.[663]

5.6. Fe Group

It is found that the ground-state iron dimer reacts with dioxygen directly to form the cyclic Fe_2O_2 cluster without activation energy.[270,320] A slightly distorted rhombus structure with triplet state is found to be lowest in energy using density functional methods.[320] However, subsequent B3LYP calculations indicate that the cyclic Fe_2O_2 cluster has a planar D_{2h} structure with a $^7B_{2u}$ ground state, which is also confirmed by single-point CCSD(T) calculations. The existence of an effective Fe−Fe bonding is confirmed by NBO and Bader analyses.[664] The Fe_2O_4 cluster has also been observed in solid argon from the dimerization reaction of the corresponding metal dioxide molecules.[270] Spectroscopically, only some small iron oxide clusters have been studied by PES in the gas phase.[665,666] The PES spectra for the Fe_2O_x ($x = 1-5$) series are quite similar. Isomers are observed for the $Fe_2O_x^-$ series when $x > 1$. These isomers are proposed to be complexes involving O_2 or O_3 units.[268a] The Fe_2O cluster is determined to have C_{2v} triangle structure. But the ground-state geometry of the Fe_2O^- anion changes drastically from that of the neutral. The anion is predicted to have a linear Fe−O−Fe structure.[667] The ground state of $Fe_2O_3^-$ anion has a four-membered ring structure with an extra oxygen atom terminally bonded to one Fe atom (Figure 19B). The $Fe_2O_4^-$ anion has a planar structure (Figure 20C), while in the neutral the two terminal O atoms are placed in a trans position with respect to the Fe_2O_2 ring (Figure 20A).[667] The structural and magnetic properties of tri- and tetranuclear anionic clusters, $Fe_3O_m^-$ ($m = 1-5$) and $Fe_4O_m^-$ ($m = 1-6$) are theoretically predicted by means of the first-principles molecular dynamics based on the density functional theory.[668] The structural and electronic structures of some neutral multinuclear iron oxide clusters have also been theoretically predicted.[669−671] First-principles electronic structure calculations show that small Fe_nO_n ($n = 2-5$) clusters form single highly stable rings; starting at Fe_6O_6, these elementary rings begin to assemble into nano columnar structures to form stable Fe_nO_n ($n = 6-12$) towers. The rings and the empty towers can be further stabilized by capping O atoms at the ends, leading to Fe_nO_{n+1} and Fe_nO_{n+2} sequences.[669] A very recent DFT calculation on both cage and noncage structures of $(Fe_2O_3)_n$ ($n = 2-6$ and 10) clusters shows that all the cage structures are stable, but the global minima are the noncage clusters for most cases.[670]

5.7. Co Group

The cyclic Co_2O_2 cluster has been identified using matrix infrared spectroscopy.[320] Recent thermal evaporation experiments suggest that photoexcitation is required for the formation of the Co_2O_2 cluster.[672] DFT calculations reveal that a $^5B_{1g}$ state is less stable than a ^7A_u state by 27 kcal/mol although the calculated frequencies for the former state seem to be more similar to the experimental values.[320] In a recent combined DFT and high-level ab initio theoretical study, a ^1A_g state was predicted to be the ground state for the planar D_{2h} Co_2O_2 cluster. Its properties are better described by meta-GGA functional TPSS. Wave functional based ab initio calculations result in a number of closely spaced electronic states for this rhombus cluster, but the closed-shell singlet state is still a bit more stable.[673] The Co_2O_4 cluster has also been observed in solid argon from the dimerization of the coblat dioxide molecules.[320] It is suggested to have a similar structure to the other M_2O_4 clusters, but detailed information on the electronic and geometric structure requires further theoretical study.

Anion photoelectron spectroscopy of mass-selected $Co_nO_m^-$ clusters ($n = 4-20$; $m = 0-2$) was performed at photon energies of 3.49 and 4.66 eV.[674] Main PES spectral features are contributed from Co 3d-derived orbitals throughout the complete series. The additional oxygen atoms indicate a minor influence toward the electronic structure. With increasing oxygen content, electron affinities shift to higher values. The experimental values are well reproduced by the DFT/B3LYP calculations.[675] There are no experimental reports on spectroscopic study of rhodium and iridium oxide clusters. The infrared vibrational spectra of low-lying isomers of rhodium oxide clusters have been predicted using density functional theory.[676]

5.8. Ni Group

The cyclic Ni_2O_2 cluster has been identified in solid matrices.[347,677] Based on the unrestricted hybrid DFT calculations with a broken symmetry approach, an open shell singlet state, the vibrational frequencies of which were in good agreement with the experimental values, was predicted to be lowest in energy. Although a short Ni−Ni bond length was predicted for the D_{2h} Ni_2O_2 cluster, no direct bonding interactions were found between the two nickel centers.[677] The most recent MRCI calculations gave a ^1A_g ground state for this cluster species, which correlates with the density functional results.[678]

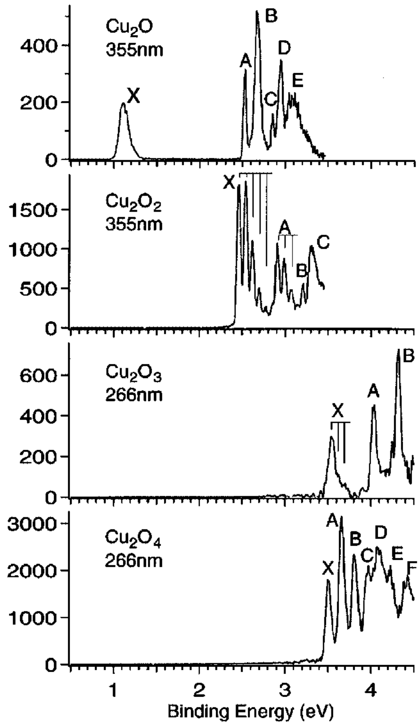

Figure 24. Photoelectron spectra of $Cu_2O_x^-$ ($x = 1-4$). The ground states of the neutral clusters are labeled "X", and their low-lying electronic excited states are labeled with the alphabet. The vertical lines indicate the resolved vibrational structures. Reprinted with permission from ref 679. Copyright 1996 American Physical Society.

It was found that the palladium dimer interacts with dioxygen to form the $Pd_2(O_2)$ complex under visible light excitation, in which the dioxygen molecule is predicted to be side-on bonded to the metal dimer with a planar C_{2v} symmetry (Figure 18E).[380] The Pd_2O_4 cluster, which was characterized to be a bisdioxygen complex, has also been experimentally observed. It was predicted to have a singlet ground state with planar D_{2h} symmetry (Figure 20D).[380]

The structures of platinum oxide clusters have been studied using density functional methods. Clusters with Pt_xO_x ($x > 2$) stoichiometry prefer to form closed ring-like structures with a bridged oxygen atom bound to two platinum atoms, which roughly form two-dimensional structures. The Pt_xO_{2x} clusters are found to possess nearly one-dimensional structures with periodical cyclic Pt_2O_2 subunits. All of these structures are quite different from that of bulk platinum oxide.[368]

5.9. Cu Group

A PES study indicated that the Cu_2O cluster exhibits a large HOMO–LUMO gap (Figure 24), suggesting a closed-shell nature for this simple triatomic cluster.[679] Theoretical calculations revealed that the Cu_2O cluster possesses a bent C_{2v} geometry with the central oxygen atom bound to two copper atoms,[679,680] which can serve as the building block for the formation of larger copper oxide clusters via the active oxygen site.[681] The cationic cluster is predicted to be more bent than the anionic and neutral ones.[680]

Three structural isomers with Cu_2O_2 stoichiometry have been experimentally characterized. Matrix isolation experiments show that the copper dimer is able to react with dioxygen in forming a $Cu_2(O_2)$ complex, which is characterized to be a side-on bonded superoxide complex with a Cu–Cu bond (Figure 18E).[682] Upon near-infrared excitation, the $Cu_2(O_2)$ complex isomerizes to a CuOCuO cluster, in which both oxygen atoms are atomically bound to the copper centers.[682] An anion photoelectron spectroscopic study revealed that the cyclic Cu_2O_2 cluster is experimentally observed (Figure 18A).[679] Recent theoretical studies predicted that the linear or near linear CuOCuO structure is the most stable isomer with Cu_2O_2 stoichiometry.[680] For Cu_2O_3, two isomers with close energies are predicted: a D_{3h} bipyramid (Figure 19A) and a C_{2v} bent structure with an O–Cu–O–Cu–O atomic arrangement. The D_{3h} isomer was proposed to be the observed structure in the gas-phase PES experiment.[679] However, recent DFT calculations suggested that the calculated electron affinity of a linear isomer (Figure 19C) is in better agreement with the experimental value.[680] A matrix-isolation infrared study indicated that the Cu_2O_4 cluster is a side-on bonded dicopper bis-superoxide complex, which was predicted to have a $^3B_{3u}$ ground state with a planar D_{2h} symmetry (Figure 20D). The Cu–Cu distance in the Cu_2O_4 complex was computed to be quite long, indicating no direct bonding interaction between the two copper atoms.[682] The dicopper bis-superoxide structure is also proposed as the photodetachment product of the corresponding anion in the gas phase.[679] Vibrationally resolved PES studies on larger $Cu_xO_2^-$ clusters ($x = 6-11$) indicate that O_2 molecularly adsorbs on the Cu_x^- anionic clusters.[683]

The Au_2O^- anion is characterized to have a near linear doublet ground state with direct Au–Au bond.[684] Recent time-resolved photoelectron spectroscopic study on Au_2O^- suggests the existence of a long-lived excited state with the lifetime being more than 100 ps.[685] The PES spectrum of the Au_4O^- anionic cluster was also recorded.[684] The calculation results showed that the geometric structure of Au_4^- is significantly modified upon the chemisorption of atomic oxygen.[684]

Dioxygen adsorption on silver and gold anionic clusters has been studied using vibrationally resolved photoelectron spectroscopy. The results have been summarized in a recent review.[686] In general, the odd-numbered silver and gold anionic clusters were unreactive toward dioxygen, while the even-numbered clusters interacted with dioxygen to form $M_xO_2^-$ clusters (M = Ag, Au). PES investigations on these $M_xO_2^-$ anionic clusters showed that O_2 molecularly adsorbs on the metal clusters,[684,687] in agreement with theoretical predictions.[449,452,688−690] Besides the molecularly adsorbed clusters, dissociative adsorption species were also reported. For $Au_4O_2^-$ anionic cluster, the dissociative oxide isomer can be prepared by using atomic oxygen reagent.[691] The formation of dissociative oxide clusters was predicted to be thermodynamically favored but kinetically hindered due to the existence of a high energy barrier.[692,693]

Most theoretical calculations indicate that O_2 adsorbs molecularly on small gold clusters such as Au_3 and Au_5.[452,689,692] But dissociative adsorption is predicted to be more favorable for larger Au_x clusters with $x > 3$ in a recent theoretical study, and the geometric structures of gold clusters are strongly distorted upon O_2 adsorption.[693] For both the neutral and anionic Au_{24} clusters, density functional calculations indicated that O_2 prefers to adsorb on the tubelike gold clusters molecularly in the side-on fashion. The binding energy between neutral Au_{24} and O_2 is comparable to that of small neutral odd-numbered gold clusters.[694] The oxide products from O_2 dissociative adsorption on both Au_{32} (I_h) and Au_{32} (C_1) clusters are predicted to be more stable than the molecularly adsorbed isomers, although the Au_{32} (I_h) cluster is found to be highly inert chemically.[695]

6. Summary

Transition metal oxides and dioxygen complexes are potential intermediates or products during the oxidation of metal atoms or clusters and are of major importance in a wide range of catalytic and biological processes. Spectroscopic and theoretical investigations of these species are therefore of considerable interest and are reviewed and summarized.

Matrix infrared spectroscopy has provided a powerful technique for the investigation of transition metal oxide molecules and their cations and anions. The formation of subject species can be integrated over time to accumulate a sufficient number density in the matrix to afford the measurement of a suitable vibrational spectrum. Isotopic substitution is straightforward and important for the identification of subject species. Laser ablation provides a convenient source of transition metal atoms, cations, and electrons for the synthetic preparation of the subject species, and a source of excitation when such activation is needed to promote the reaction with oxygen molecules. The forming matrix is unique in that it quenches reaction energies and allows triatomic molecules such as MO_2 to be stabilized where the gas-phase reaction provides only MO diatomic molecules. Doping of the sample with an electron-trapping molecule such as CCl_4 aids in the identification of cations and anions. The condensing matrix allows for the formation of further oxygen-rich MO_x ($x \geq 3$) complexes between initial products and additional reagent molecules, which reveal rich structure and bonding properties.

Molecular spectroscopies such as laser-induced fluorescence (LIF), resonance-enhanced multiple photon ionization spectroscopy (REMPI), pulsed-field ionization zero kinetic energy (PFI-ZEKE) photoelectron spectroscopy, and rotational spectroscopy offer precise and detailed measurements of vibrational or rotational transitions of simple transition metal oxide molecules in the gas phase. Photoelectron spectroscopy is another quite powerful method, which provides direct information on the electron affinities, low-lying electronic states, and vibrational frequencies of size-selected transition metal−oxygen molecules and small clusters in the gas phase. Although the vibrational assignment is less accurate due to limited resolution compared with other spectroscopic methods, PES is a versatile and convenient method in gas phase studies, which complements the extensively used matrix-isolation infrared spectroscopic investigations.

Spectral and structural assignments for sized transition metal oxide clusters are quite difficult due to the existence of many low-energy isomers and low-lying electronic states. With the development of tunable IR lasers, infrared photon dissociation spectroscopy has recently been successfully used to measure the vibrational spectra of some mass-selected transition metal oxide clusters in the gas phase, which can provide reliable structural assignments for these cluster species. The well-resolved vibrational spectroscopic data combined with the state-of-the-art quantum chemical calculations may provide a very powerful and applicable approach to motivate further detailed understanding of the geometric and electronic structures and bonding and reactivity of more complicated oxygen-rich transition metal oxygen complexes as well as transition metal oxide clusters.

7. Acknowledgments

The authors gratefully acknowledge financial support from the National Basic Research Program of China (Grant Nos. 2004CB719501 and 2007CB815203) and the National Natural Science Foundation of China (Grant No. 20773030).

8. References

(1) (a) Rao, C. N. R.; Raveau, B. *Transition Metal Oxides*; VCH: New York, 1995. (b) Rao, C. N. R. *Annu. Rev. Phys. Chem.* **1989**, *40*, 291. (c) Cox, P. A. *Transition Metal Oxides: An Introduction to their Electronic Structure and Properties*; Clarendon: Oxford, U.K., 1992.

(2) (a) Kieber-Emmons, M. T.; Riordan, C. G. *Acc. Chem. Res.* **2007**, *40*, 618. (b) Cramer, C. J.; Tolman, W. B. *Acc. Chem. Res.* **2007**, *40*, 601. (c) Chufán, E. E.; Puiu, S. C.; Karlin, K. D. *Acc. Chem. Res.* **2007**, *40*, 563. (d) Korendovych, I. V.; Kryatov, S. V.; Rybak-Akimova, E. V. *Acc. Chem. Res.* **2007**, *40*, 510.

(3) (a) Mirica, L. M.; Ottenwaelder, X.; Stack, T. D. P. *Chem. Rev.* **2004**, *104*, 1013. (b) Costas, M.; Mehn, M. P.; Jensen, M. P.; Que, L., Jr. *Chem. Rev.* **2004**, *104*, 939. (c) Crans, D. C.; Smee, J. J.; Gaidamauskas, E.; Yang, L. Q. *Chem. Rev.* **2004**, *104*, 849. (d) Lewis, E. A.; Tolman, W. B. *Chem. Rev.* **2004**, *104*, 1047.

(4) (a) Solomon, E. I.; Tuczek, F.; Root, D. E.; Brown, C. A. *Chem. Rev.* **1994**, *94*, 827. (b) Pecoraro, V. L.; Baldwin, M. J.; Gelasco, A. *Chem. Rev.* **1994**, *94*, 807. (c) Kitajima, N.; Moro-oka, Y. *Chem. Rev.* **1994**, *94*, 737. (d) Momenteau, M.; Reed, C. A. *Chem. Rev.* **1994**, *94*, 659. (e) Bytheway, I.; Hall, M. B. *Chem. Rev.* **1994**, *94*, 639. (f) Butler, A.; Clague, M. J.; Meister, E. *Chem. Rev.* **1994**, *94*, 625. (g) Dickman, M. H.; Pope, M. T. *Chem. Rev.* **1994**, *94*, 569.

(5) (a) Lanci, M. P.; Brinkley, D. W.; Stone, K. L.; Smirnov, V. V.; Roth, J. P. *Angew. Chem., Int. Ed.* **2005**, *44*, 7273. (b) Smirnov, V. V.; Brinkley, D. W.; Lanci, M. P.; Karlin, K. D.; Roth, J. P. *J. Mol. Catal. A* **2006**, *251*, 100. (c) Karlin, K. D.; Tolman, W. B.; Kaderli, S.; Zuberbühler, A. D. *J. Mol. Catal. A* **1997**, *117*, 215.

(6) Jena, P.; Castleman, A. W., Jr. *Proc. Natl. Acad. Sci. U.S.A.* **2006**, *103*, 10560.

(7) Lai, X.; Goodman, D. W. *J. Mol. Catal. A* **2000**, *162*, 1647.

(8) (a) Pramann, A.; Rademann, K. *Int. J. Mass Spectrom.* **2001**, *209*, 1. (b) Optiz-Coutureau, J.; Fielicke, A.; Kaiser, B.; Rademann, K. *Phys. Chem. Chem. Phys.* **2001**, *3*, 3034. (c) Justes, D. R.; Mitrić, R.; Moore, N. A.; Bonačić-Kautecký, V.; Castleman, A. W., Jr. *J. Am. Chem. Soc.* **2003**, *125*, 6289. (d) Kimble, M. L.; Castleman, A. W., Jr.; Mitrić, R.; Bürgel, C.; Bonačić-Kautecký, V. *J. Am. Chem. Soc.* **2004**, *126*, 2526. (e) Fialko, E. F.; Kikhtenko, A. V.; Goncharov, V. B.; Zamaraev, K. I. *J. Phys. Chem. B* **1997**, *101*, 5772.

(9) (a) Zemski, K. A.; Justes, D. R.; Castleman, A. W., Jr. *J. Phys. Chem. B* **2002**, *106*, 6136. (b) Bell, R. C.; Zemski, K. A.; Castleman, A. W., Jr. *J. Cluster Sci.* **1999**, *10*, 509. (c) Johnson, G. E.; Mitrić, R.; Bonačić-Koutecký, V.; Castleman, A. W., Jr. *Chem. Phys. Lett.* **2009**, *475*, 1.

(10) (a) Feyel, S.; Schröder, D.; Schwarz, H. *Eur. J. Inorg. Chem.* **2008**, 4961. (b) Feyel, S.; Scharfenberg, L.; Daniel, C.; Hartl, H.; Schröder, D.; Schwarz, H. *J. Phys. Chem. A* **2007**, *111*, 3278. (c) Feyel, S.; Schröder, D.; Schwarz, H. *J. Phys. Chem. A* **2006**, *110*, 2647. (d) Schröder, D.; Schwarz, H. *Top. Organomet. Chem.* **2007**, *22*, 1. (e) Zhang, X. G.; Armentrout, P. B. *J. Phys. Chem. A* **2003**, *107*, 8915. (f) Sievers, M. R.; Armentrout, P. B. *Int. J. Mass Spectrom.* **1999**, *185/186/187*, 117. (g) Sievers, M. R.; Armentrout, P. B. *Inorg. Chem.* **1999**, *38*, 397. (h) Sievers, M. R.; Armentrout, P. B. *Int. J. Mass Spectrom.* **1998**, *179/180*, 103. (i) Sievers, M. R.; Armentrout, P. B. *J. Phys. Chem. A* **1998**, *102*, 10754. (j) Schröder, D.; Schwarz, H.; Clemmer, D. E.; Chen, Y.; Armentrout, P. B.; Baranov, V.; Bohme, D. K. *Int. J. Mass Spectrom. Ion Processes* **1997**, *161*, 175. (k) Chen, Y. M.; Clemmer, D. E.; Armentrout, P. B. *J. Am. Chem. Soc.* **1994**, *116*, 7815.

(11) (a) Reed, Z. D.; Duncan, M. A. *J. Phys. Chem. A* **2008**, *112*, 5354. (b) Molek, K. S.; Anfuso-Cleary, C.; Duncan, M. A. *J. Phys. Chem. A* **2008**, *112*, 9238. (c) Molek, K. S.; Reed, Z. D.; Ricks, A. M.; Duncan, M. A. *J. Phys. Chem. A* **2007**, *111*, 8080. (d) Molek, K. S.; Jaeger, T. D.; Duncan, M. A. *J. Chem. Phys.* **2005**, *123*, 144313.

(12) (a) Xie, Y.; Dong, F.; Heinbuch, S.; Rocca, J. J.; Bernstein, E. R. *J. Chem. Phys.* **2009**, *130*, 114306. (b) Dong, F.; Heinbuch, S.; Xie, Y.; Rocca, J. J.; Bernstein, E. R. *J. Phys. Chem. A* **2009**, *113*, 3029. (c) Dong, F.; Heinbuch, S.; Xie, Y.; Bernstein, E. R.; Rocca, J. J.; Wang, Z. C.; Ding, X. L.; He, S. G. *J. Am. Chem. Soc.* **2009**, *131*, 1057. (d) Xue, W.; Wang, Z. C.; He, S. G.; Xie, Y.; Bernstein, E. R. *J. Am. Chem. Soc.* **2008**, *130*, 15879. (e) He, S. G.; Xie, Y.; Dong, F.; Heinbuch, S.; Jakubikova, E.; Rocca, J. J.; Bernstein, E. R. *J. Phys. Chem. A* **2008**, *112*, 11067. (f) Dong, F.; Heinbuch, S.; Xie, Y.; Rocca, J. J.; Bernstein, E. R.; Wang, Z. C.; Deng, K.; He, S. G. *J. Am. Chem. Soc.* **2008**, *130*, 1932.

(13) Andrews, L.; Moskovits, M. *Chemistry and Physics of Matrix-Isolated Species*; North-Holland: Amsterdam, The Netherlands, 1989.
(14) Moskovits, M.; Ozin, G. A. *Matrix Cryochemistry Using Transition Metal Atoms. Cryochemistry*; Wiley: New York, 1976.
(15) (a) Zhou, M. F.; Andrews, L.; Bauschlicher, C. W., Jr. *Chem. Rev.* **2001**, *101*, 1931. (b) Andrews, L.; Citra, A. *Chem. Rev.* **2002**, *102*, 885.
(16) (a) Wang, G. J.; Zhou, M. F. *Int. Rev. Phys. Chem.* **2008**, *27*, 1. (b) Andrews, L. *Chem. Soc. Rev.* **2004**, *33*, 123. (c) Andrews, L.; Cho, H. G. *Organometallics* **2006**, *25*, 4040.
(17) (a) Himmel, H. J.; Downs, A. J.; Greene, T. M. *Chem. Rev.* **2002**, *102*, 4191. (b) Himmel, H. J.; Reiher, M. *Angew. Chem., Int. Ed.* **2006**, *45*, 6264.
(18) (a) Khriachtchev, L.; Räsänen, M.; Gerber, R. B. *Acc. Chem. Res.* **2009**, *42*, 183. (b) Gerber, R. B. *Annu. Rev. Phys. Chem.* **2004**, *55*, 55.
(19) Mascetti, J.; Galan, F.; Pàpai, I. *Coord. Chem. Rev.* **1999**, *190*–*192*, 557.
(20) (a) Perutz, R. N. *Chem. Rev.* **1985**, *85*, 77. (b) Perutz, R. N. *Chem. Rev.* **1985**, *85*, 97.
(21) (a) Jacox, M. E. *Chem. Phys.* **1994**, *189*, 149. (b) Jacox, M. E. *J. Phys. Chem. Ref. Data* **1998**, *27*, 115. (c) Jacox, M. E. *J. Phys. Chem. Ref. Data* **2003**, *32*, 1.
(22) (a) Jacox, M. E. *Chem. Soc. Rev.* **2002**, *31*, 108. (b) Jacox, M. E. *Acc. Chem. Res.* **2004**, *37*, 727. (c) Jacox, M. E. *Int. J. Mass Spectrom.* **2007**, *267*, 268.
(23) Beattie, I. R. *Angew. Chem., Int. Ed.* **1999**, *38*, 3294.
(24) Merer, A. J. *Annu. Rev. Phys. Chem.* **1989**, *40*, 407.
(25) Huber, K. P.; Herzberg, G. *Constants of Diatomic Molecules*; Van Nostrand-Reinhold: New York, 1979.
(26) Wang, L. S. Photodetachment Photoelectron Spectroscopy of Transition Metal Oxide Species. In *Photoionization and Photodetachment*; Ng, C. Y., Ed.; Advanced Series in Physical Chemistry, Vol. 10. World Scientific: Singapore, 2000; Chapter 16.
(27) Harrison, J. F. *Chem. Rev.* **2000**, *100*, 679.
(28) (a) Gutsev, G. L.; Andrews, L.; Bauschlicher, C. W., Jr. Structure and chemical bonding of 3d-metal anions. In *Theoretical Prospects of Negative Ions*; Kalcher, J., Ed.; Research Signpost: Trivandrum, India, 2002, pp 43–60. (b) Langhoff, S. R.; Bauschlicher, C. W., Jr. *Annu. Rev. Phys. Chem.* **1988**, *39*, 181.
(29) Kretzschmar, I.; Schröder, D.; Schwarz, H.; Armentrout, P. B. The binding in neutral and cationic 3d and 4d transition-metal monoxides and sulfides. In *Advances in Metal and Semiconductor Clusters*; Elsevier Science: Amsterdam, 2001; Vol. 5, pp 347–395.
(30) (a) Ozin, G. A. *Acc. Chem. Res.* **1977**, *10*, 21. (b) Ozin, G. A.; Vander Voet, A. *Acc. Chem. Res.* **1973**, *6*, 313.
(31) Bondybey, V. E.; Smith, A. M.; Agreiter, J. *Chem. Rev.* **1996**, *96*, 2113.
(32) Cramer, C. J.; Tolman, W. B.; Theopold, K. H.; Rheingold, A. L. *Proc. Natl. Acad. Sci. U.S.A.* **2003**, *100*, 3635.
(33) Akita, M.; Moro-oka, Y. *Catal. Today* **1998**, *44*, 183.
(34) Gubelmann, M. H.; Williams, A. F. *Struct. Bonding (Berlin)* **1983**, *55*, 1.
(35) Vaska, L. *Acc. Chem. Res.* **1976**, *9*, 175.
(36) Valentine, J. S. *Chem. Rev.* **1973**, *73*, 235.
(37) (a) Andrews, L.; Liang, B. Y.; Li, J.; Bursten, B. E. *J. Am. Chem. Soc.* **2003**, *125*, 3126. (b) Liang, B. Y.; Andrews, L.; Li, J.; Bursten, B. E. *J. Am. Chem. Soc.* **2002**, *124*, 9016.
(38) Zhao, Y. Y.; Gong, Y.; Zhou, M. F. *J. Phys. Chem. A* **2006**, *110*, 10777.
(39) (a) Andrews, L.; Liang, B. Y.; Li, J.; Bursten, B. E. *New. J. Chem.* **2004**, *28*, 289. (b) Liang, B. Y.; Andrews, L.; Li, J.; Bursten, B. E. *Inorg. Chem.* **2004**, *43*, 882. (c) Liang, B. Y.; Andrews, L.; Li, J.; Bursten, B. E. *Chem.*—*Eur. J.* **2003**, *9*, 4781.
(40) (a) Engelking, P. C.; Lineberger, W. C. *J. Chem. Phys.* **1977**, *66*, 5054. (b) Andersen, T.; Lykke, K. R.; Neumark, D. M.; Lineberger, W. C. *J. Chem. Phys.* **1987**, *86*, 1858.
(41) (a) Hotop, H.; Lineberger, W. C. *J. Chem. Phys.* **1973**, *58*, 2379. (b) Stevens, A. E.; Feigerle, C. S.; Lineberger, W. C. *J. Chem. Phys.* **1983**, *78*, 5420. (c) Leopold, D. G.; Lineberger, W. C. *J. Chem. Phys.* **1986**, *85*, 51.
(42) Wang, L. S.; Chen, H. S.; Fan, J. *J. Chem. Phys.* **1995**, *102*, 9480.
(43) (a) Weltner, W., Jr. *Magnetic Atoms and Molecules*; Scientific and Academic Edition: New York, 1983. (b) Van Zee, R. J.; Li, S. *J. Phys. Chem.* **1995**, *99*, 6277.
(44) Van Zee, R. J.; Brown, C. M.; Zeringue, K. J.; Weltner, W., Jr. *Acc. Chem. Res.* **1980**, *13*, 237.
(45) Duncan, M. A. *Int. Rev. Phys. Chem.* **2003**, *22*, 407.
(46) (a) Oomens, J.; Sartakov, B. G.; Meijer, G.; von Helden, G. *Int. J. Mass Spectrom.* **2006**, *254*, 1. (b) von Helden, G.; van Heijnsbergen, D.; Meijer, G. *J. Phys. Chem. A* **2003**, *107*, 1671.
(47) Hirota, E. *Annu. Rep. Prog. Chem., Sect. C* **2000**, *96*, 95.
(48) Bernath, P. F. *Annu. Rep. Prog. Chem., Sect. C* **2000**, *96*, 177.
(49) Demtroder, W. *Laser Spectroscopy*; Springer-Verlag: Berlin, 2002.
(50) (a) Schlag, E. W. *ZEKE Spectroscopy*; Cambridge University Press: Cambridge, U.K., 1998. (b) Cockett, M. C. R. *Chem. Soc. Rev.* **2005**, *34*, 935.
(51) (a) Head-Gordon, M.; Pople, J. A.; Frisch, M. J. *Chem. Phys. Lett.* **1988**, *153*, 503. (b) Frisch, M. J.; Head-Gordon, M.; Pople, J. A. *Chem. Phys. Lett.* **1990**, *166*, 275. (c) Pople, J. A.; Seeger, R.; Krishnan, R. *Int. J. Quantum Chem. Symp.* **1976**, *10*, 1. (d) Pople, J. A.; Seeger, R.; Krishnan, R. *Int. J. Quantum Chem. Symp.* **1977**, *11*, 149. (e) Krishnan, R.; Pople, J. A. *Int. J. Quantum Chem.* **1978**, *14*, 91.
(52) Pople, J. A.; Gordon, M. H.; Raghavachari, K. *J. Chem. Phys.* **1987**, *87*, 5968.
(53) Sousa, S. F.; Fernandes, P. A.; Ramos, M. J. *J. Phys. Chem. A* **2007**, *111*, 10439.
(54) Zhao, Y.; Truhlar, D. G. *Acc. Chem. Res.* **2008**, *41*, 157.
(55) (a) Hegarty, D.; Robb, M. A. *Mol. Phys.* **1979**, *38*, 1795. (b) Eade, R. H. E.; Robb, M. A. *Chem. Phys. Lett.* **1981**, *83*, 362. (c) Schlegel, H. B.; Robb, M. A. *Chem. Phys. Lett.* **1982**, *93*, 43. (d) Bernardi, F.; Bottini, A.; McDougall, J. J. W.; Robb, M. A.; Schlegel, H. B. *Faraday Symp. Chem. Soc.* **1984**, *19*, 137.
(56) (a) Burton, P. G.; Buenker, R. J.; Bruna, P. J.; Peyerimhoff, S. D. *Chem. Phys. Lett.* **1983**, *95*, 379. (b) Bauschlicher, C. W., Jr.; Taylor, P. R. *J. Chem. Phys.* **1987**, *86*, 858. (c) Shavitt, I.; Brown, F. B.; Burton, P. G. *Int. J. Quantum Chem.* **1987**, *31*, 507.
(57) Li, Z. H.; Gong, Y.; Fan, K. N.; Zhou, M. F. *J. Phys. Chem. A* **2008**, *112*, 13641.
(58) Pyykkö, P. *Chem. Rev.* **1988**, *88*, 563.
(59) Pepper, M.; Bursten, B. E. *Chem. Rev.* **1991**, *91*, 719.
(60) Piechota, J.; Suffczynski, M. *Z. Phys. Chem.* **1997**, *200*, 39.
(61) Baranowska, A.; Siedlecka, M.; Sadlej, A. J. *Theor. Chem. Acc.* **2007**, *118*, 959.
(62) Jensen, K. P.; Roos, B. O.; Ryde, U. *J. Chem. Phys.* **2007**, *126*, 14103.
(63) Dai, B.; Deng, K. M.; Yang, J. L.; Zhu, Q. S. *J. Chem. Phys.* **2003**, *118*, 9608.
(64) (a) Gutsev, G. L.; Andrews, L.; Bauschlicher, C. W., Jr. *Theor. Chem. Acc.* **2003**, *109*, 298. (b) Bauschlicher, C. W., Jr.; Maitre, P. *Theor. Chim. Acta* **1995**, *90*, 189.
(65) Gutsev, G. L.; Rao, B. K.; Jena, P. *J. Phys. Chem. A* **2000**, *104*, 5374.
(66) Bridgeman, A. J.; Rothery, J. *J. Chem. Soc., Dalton Trans.* **2000**, 211.
(67) Bakalbassis, E. G.; Stiakaki, M. A. D.; Tsipis, A. C.; Tsipis, C. A. *Chem. Phys.* **1996**, *205*, 389.
(68) (a) Anderson, A. B.; Hong, S. Y.; Smialek, J. L. *J. Phys. Chem.* **1987**, *91*, 4250. (b) Anderson, A. B.; Grimes, R. W.; Hong, S. Y. *J. Phys. Chem.* **1987**, *91*, 4245.
(69) Dolg, M.; Wedig, U.; Stoll, H.; Preuss, H. *J. Chem. Phys.* **1987**, *86*, 2123.
(70) Siegbahn, P. E. M. *Chem. Phys. Lett.* **1993**, *201*, 15.
(71) Song, P.; Guan, W.; Yao, C.; Su, Z. M.; Wu, Z. J.; Feng, J. D.; Yan, L. K. *Theor. Chem. Acc.* **2007**, *117*, 407.
(72) Kharat, B.; Deshmukh, S. B.; Chaudhari, A. *Int. J. Quantum Chem.* **2009**, *109*, 1103.
(73) Yao, C.; Guan, W.; Song, P.; Su, Z. M.; Feng, J. D.; Yan, L. K.; Wu, Z. J. *Theor. Chem. Acc.* **2007**, *117*, 115.
(74) Wu, Z. J.; Guan, W.; Meng, J.; Su, Z. M. *J. Cluster Sci.* **2007**, *18*, 444.
(75) Dolg, M.; Stoll, H. *Theor. Chim. Acta* **1989**, *75*, 369.
(76) Uzunova, E. L.; Mikosch, H.; Nikolov, G. St. *J. Chem. Phys.* **2008**, *128*, 094307.
(77) Gutsev, G. L.; Rao, B. K.; Jena, P. *J. Phys. Chem. A* **2000**, *104*, 11961.
(78) Siegbahn, P. E. M. *J. Phys. Chem.* **1993**, *97*, 9096.
(79) (a) Wilson, E. B., Jr.; Decius, J. C.; Cross, P. C. *Molecular Vibratons*; McGraw-Hill: New York, 1955. (b) Herzberg, G. *Molecular Spectra and Molecular Structure. II. Infrared and Raman Spectra of Polyatomic Molecules*; Van Nostrand: Princeton, NJ, 1945.
(80) Allavena, M.; Rysnik, R.; White, D.; Calder, V.; Mann, D. E. *J. Chem. Phys.* **1969**, *50*, 3399.
(81) (a) Brabson, G. D.; Mielke, Z.; Andrews, L. *J. Phys. Chem.* **1991**, *95*, 79. (b) Thorwirth, S.; McCarthy, M. C.; Gottlieb, C. A.; Thaddeus, P.; Gupta, H.; Stanton, J. F. *J. Chem. Phys.* **2005**, *123*, 054326.
(82) (a) Weltner, W., Jr.; McLeod, D., Jr.; Kasai, P. H. *J. Chem. Phys.* **1967**, *46*, 3172. (b) Kasai, P. H.; Weltner, W., Jr. *J. Chem. Phys.* **1965**, *43*, 2553.
(83) Knight, L. B.; Kaup, J. G.; Petzoldt, B.; Ayyad, R.; Ghanty, T. K.; Davidson, E. R. *J. Chem. Phys.* **1999**, *110*, 5658.
(84) Gonzales, J. M.; King, R. A.; Schaefer, H. F., III. *J. Chem. Phys.* **2000**, *113*, 567.
(85) Johnson, J. R. T.; Panas, I. *Chem. Phys.* **1999**, *248*, 161.
(86) Mattar, S. M. *J. Phys. Chem.* **1993**, *97*, 3171.
(87) Jeung, G. H.; Koutecký, J. *J. Chem. Phys.* **1988**, *88*, 3747.

(88) Bauschlicher, C. W., Jr.; Langhoff, S. R. *J. Chem. Phys.* **1986**, *85*, 5936.
(89) Wu, H. B.; Wang, L. S. *J. Phys. Chem. A* **1998**, *102*, 9129.
(90) Howard, J. A.; Histed, M.; Mile, B.; Hampson, C. A.; Morris, H. *J. Chem. Soc., Faraday Trans.* **1991**, *87*, 3189.
(91) Hoeft, J.; Törring, T. *Chem. Phys. Lett.* **1993**, *215*, 367.
(92) Suenram, R. D.; Lovas, F. J.; Fraser, G. T.; Matsumura, K. *J. Chem. Phys.* **1990**, *92*, 4724.
(93) Klingeler, R.; Lüttgens, G.; Pontius, N.; Rochow, R.; Bechthold, P. S.; Neeb, M.; Eberhardt, W. *Eur. Phys. J., D* **1999**, *9*, 263.
(94) Törring, T.; Zimmermann, K.; Hoeft, J. *Chem. Phys. Lett.* **1988**, *151*, 520.
(95) Langhoff, S. R.; Bauschlicher, C. W., Jr. *J. Chem. Phys.* **1988**, *89*, 2160.
(96) (a) Cao, X.; Dolg, M. *THEOCHEM* **2002**, *581*, 139. (b) Cao, X.; Dolg, M. *J. Chem. Phys.* **2001**, *115*, 7348. (c) Küchle, W.; Dolg, M.; Stoll, H. *J. Phys. Chem. A* **1997**, *101*, 7128.
(97) Wang, S. G.; Schwarz, W. H. E. *J. Phys. Chem.* **1995**, *99*, 11687.
(98) (a) Wang, S. G.; Pan, D. K.; Schwarz, W. H. E. *J. Chem. Phys.* **1995**, *102*, 9296. (b) Cao, X.; Liu, W.; Dolg, M. *Sci. Chin., Ser. B* **2002**, *45*, 91.
(99) Kotzian, M.; Rösch, N.; Zerner, M. C. *Theor. Chim. Acta* **1992**, *81*, 201.
(100) Todorova, T. K.; Infante, I.; Gagliardi, L.; Dyke, J. M. *J. Phys. Chem. A* **2008**, *112*, 7825.
(101) Schamps, J.; Bencheikh, M.; Barthelat, J.-C.; Field, R. W. *J. Chem. Phys.* **1995**, *103*, 8004.
(102) Márquez, A.; Capitán, M. J.; Odriozola, J. A.; Sanz, J. F. *Int. J. Quantum Chem.* **1994**, *52*, 1329.
(103) Clemmer, D. E.; Dalleska, N. F.; Armentrout, P. B. *Chem. Phys. Lett.* **1992**, *190*, 259.
(104) Chertihin, G. V.; Andrews, L.; Rosi, M.; Bauschlicher, C. W., Jr. *J. Phys. Chem. A* **1997**, *101*, 9085.
(105) Bauschlicher, C. W., Jr.; Zhou, M. F.; Andrews, L.; Johnson, J. R. T.; Panas, I.; Snis, A.; Roos, B. O. *J. Phys. Chem. A* **1999**, *103*, 5463.
(106) Lee, E. P. F.; Mok, D. K. W.; Chau, F. T.; Dyke, J. M. *J. Comput. Chem.* **2008**, *30*, 337.
(107) Rosi, M.; Bauschlicher, C. W.; Chertihin, G. V.; Andrews, L. *Theor. Chem. Acc.* **1998**, *99*, 106.
(108) Kim, S. J.; Crawford, T. D. *J. Phys. Chem. A* **2004**, *108*, 3097.
(109) Andrews, L.; Zhou, M. F.; Chertihin, G. V.; Bauschlicher, C. W., Jr. *J. Phys. Chem. A* **1999**, *103*, 6525.
(110) Lee, E. P. F.; Dyke, J. M.; Mok, D. K. W.; Chau, F. T. *J. Phys. Chem. A* **2008**, *112*, 4511.
(111) Gong, Y.; Ding, C. F.; Zhou, M. F. *J. Phys. Chem. A* **2007**, *111*, 11572.
(112) Gong, Y.; Ding, C. F.; Zhou, M. F. *J. Phys. Chem. A* **2009**, *113*, 8569.
(113) Stösser, G.; Schnöckel, H. *Angew. Chem., Int. Ed.* **2005**, *44*, 4261.
(114) (a) Flemmig, B.; Wolczanski, P. T.; Hoffmann, R. *J. Am. Chem. Soc.* **2005**, *127*, 1278. (b) Venter, G. A.; Raubenheimer, H. G.; Dillen, J. *J. Phys. Chem. A* **2007**, *111*, 8193.
(115) Wu, H. B.; Wang, L. S. *J. Chem. Phys.* **1997**, *107*, 8221.
(116) Loock, H.; Simard, B.; Wallin, S.; Linton, C. *J. Chem. Phys.* **1998**, *109*, 8980.
(117) Gustavson, T.; Amiot, C.; Vergès, J. *J. Mol. Spectrosc.* **1991**, *145*, 56.
(118) (a) Namiki, K. I.; Saito, S.; Robinson, J. S.; Steimle, T. C. *J. Mol. Spectrosc.* **1998**, *191*, 176. (b) Steimle, T. C.; Shirley, J. E.; Jung, K. Y.; Russon, L. R.; Scurlock, C. T. *J. Mol. Spectrosc.* **1990**, *144*, 27. (c) Steimle, T. C.; Shirley, J. E. *J. Chem. Phys.* **1989**, *91*, 8000.
(119) Dyke, J. M.; Gravenor, B. W.; Josland, G. D.; Lewis, R. A.; Morris, A. *Mol. Phys.* **1984**, *53*, 465.
(120) Powell, D.; Brittain, R.; Vala, M. *Chem. Phys.* **1981**, *58*, 355.
(121) Gallaher, T. N.; DeVore, T. C. *High Temp. Sci.* **1979**, *11*, 123.
(122) Walsh, M. B.; King, R. A.; Schaefer, H. F., III. *J. Chem. Phys.* **1999**, *110*, 5224.
(123) Bauschlicher, C. W., Jr.; Langhoff, S. R.; Komornicki, A. *Theor. Chim. Acta* **1990**, *77*, 263.
(124) Bauschlicher, C. W.; Bagus, P. S.; Nelin, C. J. *Chem. Phys. Lett.* **1983**, *101*, 229.
(125) Beaton, S. A.; Gerry, M. C. L. *J. Chem. Phys.* **1999**, *110*, 10715.
(126) Simard, B.; Mitchell, S. A.; Humphries, M. R.; Umphries, M. R.; Hackett, P. A. *J. Mol. Spectrosc.* **1988**, *129*, 186.
(127) Lauchlan, L. J.; Brom, J. M., Jr.; Broida, H. P. *J. Chem. Phys.* **1976**, *65*, 2672.
(128) Weltner, W., Jr.; McLeod, D., Jr. *Nature* **1965**, *206*, 87.
(129) (a) Edvinsson, G.; Nylén, Ch. *Phys. Scr.* **1971**, *3*, 261. (b) Jonsson, J.; Edvinsson, G.; Taklif, A. G. *J. Mol. Spectrosc.* **1995**, *172*, 299.
(130) Hammer, P. D.; Davis, S. P. *Astrophys. J.* **1980**, *237*, L51.
(131) Weltner, W., Jr.; McLeod, D., Jr. *J. Phys. Chem.* **1965**, *69*, 3488.
(132) Chertihin, G. V.; Andrews, L. *J. Phys. Chem.* **1995**, *99*, 6356.
(133) McIntyre, N. S.; Thompson, K. R.; Weltner, W., Jr. *J. Phys. Chem.* **1971**, *75*, 3243.
(134) Brünken, S.; Müller, H. S. P.; Menten, K. M.; McCarthy, M. C.; Thaddeus, P. *Astrophys. J.* **2008**, *676*, 1367.
(135) Zhai, H. J.; Wang, L. S. *J. Am. Chem. Soc.* **2007**, *129*, 3022.
(136) Thomas, O. C.; Xu, S.; Lippa, T. P.; Bowen, K. H. *J. Cluster Sci.* **1999**, *10*, 525.
(137) Zheng, W.; Bowen, K. H., Jr.; Li, J.; Dabkowska, I.; Gutowski, M. *J. Phys. Chem. A* **2005**, *109*, 11521.
(138) (a) Lesarri, A.; Suenram, R. D.; Brugh, D. *J. Chem. Phys.* **2002**, *117*, 9651. (b) Brugh, D. J.; Suenram, R. D.; Stevens, W. J. *J. Chem. Phys.* **1999**, *111*, 3526.
(139) Grein, F. *J. Chem. Phys.* **2007**, *126*, 034313.
(140) Li, S.; Dixon, D. A. *J. Phys. Chem. C* **2008**, *112*, 6646.
(141) Woodley, S. M.; Hamad, S.; Mejias, J. A.; Catlow, C. R. A. *J. Mater. Chem.* **2006**, *16*, 1927.
(142) Qu, Z. W.; Kroes, G. J. *J. Phys. Chem. B.* **2006**, *110*, 8998.
(143) Albaret, T.; Finocchi, F.; Noguera, C. *Appl. Surf. Sci.* **1999**, *144*, 672.
(144) (a) Hagfeldt, A.; Bergström, R.; Siegbahn, H. O. G.; Lunell, S. *J. Phys. Chem.* **1993**, *97*, 12725. (b) Bergström, R.; Lunell, S.; Eriksson, L. A. *Int. J. Quantum Chem.* **1996**, *59*, 427.
(145) Ramana, M. V.; Phillips, D. H. *J. Chem. Phys.* **1988**, *88*, 2637.
(146) (a) Mok, D. K. W.; Chau, F. T.; Dyke, J. M.; Lee, E. P. F. *Chem. Phys. Lett.* **2008**, *458*, 11. (b) Mok, D. K. W.; Lee, E. P. F.; Chau, F. T.; Dyke, J. M. *Phys. Chem. Chem. Phys.* **2008**, *10*, 7270.
(147) Gong, Y.; Zhou, M. F. *J. Phys. Chem. A* **2008**, *112*, 9758.
(148) Gong, Y.; Zhou, M. F. *Chin. J. Chem. Phys.* **2009**, *22*, 113.
(149) Albaret, T.; Finocchi, F.; Noguera, C. *J. Chem. Phys.* **2000**, *113*, 2238.
(150) Jeong, K. S.; Chang, Ch.; Sedlmayr, E.; Sülzle, D. *J. Phys. B* **2000**, *33*, 3417.
(151) (a) Zhou, M. F.; Andrews, L. *J. Phys. Chem. A* **1999**, *103*, 5259. (b) Zhou, M. F.; Andrews, L. *J. Am. Chem. Soc.* **2000**, *122*, 1531.
(152) Gong, Y.; Zhou, M. F.; Tian, S. X.; Yang, J. L. *J. Phys. Chem. A* **2007**, *111*, 6127.
(153) Gong, Y.; Zhou, M. F. *J. Phys. Chem. A* **2007**, *111*, 8973.
(154) (a) Wight, C. A.; Ault, B. S.; Andrews, L. *J. Chem. Phys.* **1976**, *65*, 1244. (b) Andrews, L.; Ault, B. S.; Grzybowski, J. M.; Allen, R. O. *J. Chem. Phys.* **1975**, *62*, 2461.
(155) (a) Bayot, D.; Devillers, M. *Coord. Chem. Rev.* **2006**, *250*, 2610. (b) Bortolini, O.; Conte, V. *J. Inorg. Biochem.* **2005**, *99*, 1549.
(156) Miliordos, E.; Mavridis, A. *J. Phys. Chem. A* **2007**, *111*, 1953.
(157) (a) Broclawik, E.; Borowski, T. *Chem. Phys. Lett.* **2001**, *339*, 433. (b) Broclawik, E. *Catal. Today* **1995**, *23*, 379. (c) Broclawik, E. *Theor. Comput. Chem.* **1995**, *2*, 349. (d) Broclawik, E.; Salahub, D. R. *J. Mol. Catal.* **1993**, *82*, 117.
(158) Pykavy, M.; Van Wüllen, C. *J. Phys. Chem. A* **2003**, *107*, 5566.
(159) Rakowitz, F.; Marian, C. M.; Seijo, L.; Wahlgren, U. *J. Chem. Phys.* **1999**, *110*, 3678.
(160) (a) Calatayud, M.; Berski, S.; Beltran, A.; Andres, J. *Theor. Chem. Acc.* **2002**, *108*, 12. (b) Calatayud, M.; Silvi, B.; Andres, J.; Beltran, A. *Chem. Phys. Lett.* **2001**, *333*, 493. (c) Calatayud, M.; Andres, J.; Beltran, A.; Silvi, B. *Theor. Chem. Acc.* **2001**, *105*, 299.
(161) Vyboishchikov, S. F.; Sauer, J. *J. Phys. Chem. A* **2000**, *104*, 10913.
(162) Jakubikova, E.; Rappé, A. K.; Bernstein, E. R. *J. Phys. Chem. A* **2007**, *111*, 12938.
(163) Bande, A.; Lüchow, A. *Phys. Chem. Chem. Phys.* **2008**, *10*, 3371.
(164) Knight, L. B., Jr.; Babb, R.; Ray, M.; Banisaukas, T. J., III; Russon, L.; Dailey, R. S.; Davidson, E. R. *J. Chem. Phys.* **1996**, *105*, 10237.
(165) Wu, H. B.; Wang, L. S. *J. Chem. Phys.* **1998**, *108*, 5310.
(166) Dyke, J. M.; Gravenor, B. W. J.; Hastings, M. P.; Morris, A. *J. Phys. Chem.* **1985**, *89*, 4613.
(167) Kasai, P. H. *J. Chem. Phys.* **1968**, *49*, 4979.
(168) Dolg, M.; Stoll, H.; Preuss, H.; Pitzer, R. M. *J. Phys. Chem.* **1993**, *97*, 5852.
(169) Osanai, Y.; Sekiya, M.; Noro, T.; Koga, T. *Mol. Phys.* **2003**, *101*, 65.
(170) Vala, M.; Brittain, R. D.; Powell, D. *Chem. Phys.* **1985**, *93*, 147.
(171) Dyke, J. M.; Ellis, A. M.; Feher, M.; Morris, A.; Paul, A. J.; Stevens, J. C. *J. Chem. Soc., Faraday Trans. 2* **1987**, *83*, 1555.
(172) Wu, Z. J.; Kawazoe, Y.; Meng, J. *THEOCHEM* **2006**, *764*, 123.
(173) Manke, K. J.; Vervoort, T. R.; Kuwata, K. T.; Varberg, T. D. *J. Chem. Phys.* **2008**, *128*, 104302.
(174) Zheng, W.; Li, X.; Eustis, S.; Bowen, K. *Chem. Phys. Lett.* **2008**, *460*, 68.
(175) Al-Khalili, A.; Hallsten, U.; Launila, O. *J. Mol. Spectrosc.* **1999**, *198*, 230.
(176) Brittain, R.; Powell, D.; Kreglewski, M.; Vala, M. *Chem. Phys.* **1980**, *54*, 71.
(177) Weltner, W., Jr.; McLeod, D., Jr. *J. Chem. Phys.* **1965**, *42*, 882.
(178) Cheetham, C. J.; Barrow, R. F. *Trans. Faraday Soc.* **1967**, *63*, 1835.
(179) Matsuda, Y.; Bernstein, E. R. *J. Phys. Chem. A* **2005**, *109*, 3803.

(180) Sambrano, J. R.; Andrés, J.; Beltrán, A.; Sensato, F.; Longo, E. *Chem. Phys. Lett.* **1998**, *287*, 620.
(181) Gershikov, A. G.; Spiridonov, V. P.; Prikhod'ko, A. Ya.; Erokhin, E. V. *High Temp. Sci.* **1981**, *14*, 17.
(182) Chertihin, G. V.; Bare, W. D.; Andrews, L. *J. Phys. Chem. A* **1997**, *101*, 5090.
(183) Zhou, M. F.; Andrews, L. *J. Phys. Chem. A* **1998**, *102*, 8251.
(184) Chen, M. H.; Wang, X. F.; Qin, Q. Z. *Appl. Surf. Sci.* **2000**, *156*, 16.
(185) Brom, J. M., Jr.; Durham, C. H., Jr.; Weltner, W., Jr. *J. Chem. Phys.* **1974**, *61*, 970.
(186) Green, D. W.; Korfmacher, W.; Gruen, D. M. *J. Chem. Phys.* **1973**, *58*, 404.
(187) Chen, M. H.; Wang, X. F.; Zhang, L. N.; Yu, M.; Qin, Q. Z. *Chem. Phys.* **1999**, *242*, 81.
(188) Zhao, Y. Y.; Gong, Y.; Chen, M. H.; Zhou, M. F. *J. Phys. Chem. A* **2006**, *110*, 1845.
(189) Zhao, Y. Y.; Zheng, X. M.; Zhou, M. F. *Chem. Phys.* **2008**, *351*, 13.
(190) Almond, M. J.; Atkins, R. W. *J. Chem. Soc., Dalton Trans.* **1994**, 835.
(191) (a) Wells, J. R.; Weitz, E. *J. Am. Chem. Soc.* **1992**, *114*, 2783. (b) Sun, X. Z.; George, M. W.; Kazarian, S. G.; Nikiforov, S. M.; Poliakoff, M. *J. Am. Chem. Soc.* **1996**, *118*, 10525. (c) Ball, G. E.; Darwish, T. A.; Geftakis, S.; George, M. W.; Lawes, D. J.; Portius, P.; Rourke, J. P.; Bergman, R. G. *Proc. Natl. Acad. Sci. U.S.A.* **2005**, *102*, 1853.
(192) Stevens, F.; Carmichael, I.; Callens, F.; Waroquier, M. *J. Phys. Chem. A* **2006**, *110*, 4846.
(193) Bauschlicher, C. W., Jr.; Gutsev, G. L. *J. Chem. Phys.* **2002**, *116*, 3659.
(194) Veliah, S.; Xiang, K. H.; Pandey, R.; Recio, J. M.; Newsam, J. M. *J. Phys. Chem. B* **1998**, *102*, 1126.
(195) Jasien, P. G.; Stevens, W. J. *Chem. Phys. Lett.* **1988**, *147*, 72.
(196) Bauschlicher, C. W., Jr.; Nelin, C. J.; Bagus, P. S. *J. Chem. Phys.* **1985**, *82*, 3265.
(197) Gutsev, G. L.; Jena, P.; Zhai, H. J.; Wang, L. S. *J. Chem. Phys.* **2001**, *115*, 7935.
(198) Wenthold, P. G.; Gunion, R. F.; Lineberger, W. C. *Chem. Phys. Lett.* **1996**, *258*, 101.
(199) Steimle, T. C.; Nachman, D. F.; Shirley, J. E.; Bauschlicher, C. W., Jr.; Langhoff, S. R. *J. Chem. Phys.* **1989**, *91*, 2049.
(200) (a) Cheung, A. S. C.; Zyrnicki, W.; Merer, A. J. *J. Mol. Spectrosc.* **1984**, *104*, 315. (b) Hocking, W. H.; Merer, A. J.; Milton, D. J.; Jones, W. E.; Krishnamurthy, G. *Can. J. Phys.* **1980**, *58*, 516. (c) Barnes, M.; Hajigeorgiou, P. G.; Merer, A. J. *J. Mol. Spectrosc.* **1993**, *160*, 289.
(201) Zhou, M. F.; Andrews, L. *J. Chem. Phys.* **1999**, *111*, 4230.
(202) Chertihin, G. V.; Bare, W. D.; Andrews, L. *J. Chem. Phys.* **1997**, *107*, 2798.
(203) Kuzyakov, Y. Y.; Moskvitina, E. N.; Filippova, E. N. *Spectrosc. Lett.* **1997**, *30*, 1057.
(204) Gunion, R. F.; Dixon-Warren, St. J.; Lineberger, W. C. *J. Chem. Phys.* **1996**, *104*, 1765.
(205) Hamrick, Y. M.; Taylor, S.; Morse, M. D. *J. Mol. Spectrosc.* **1991**, *146*, 274.
(206) Broclawik, E.; Salahub, D. R. *Int. J. Quantum Chem.* **1994**, *52*, 1017.
(207) Langhoff, S. R.; Bauschlicher, C. W., Jr.; Pettersson, L. G. M.; Siegbahn, P. E. M. *Chem. Phys.* **1989**, *132*, 49.
(208) Bates, J. K.; Gruen, D. M. *J. Mol. Spectrosc.* **1979**, *78*, 284.
(209) Ram, R. S.; Liévin, J.; Li, G.; Hirao, T.; Bernath, P. F. *Chem. Phys. Lett.* **2001**, *343*, 437.
(210) Bare, W. D.; Souter, P. F.; Andrews, L. *J. Phys. Chem. A* **1998**, *102*, 8279.
(211) Samoilova, A. N.; Efremov, Yu. M.; Gurvich, L. V. *J. Mol. Spectrosc.* **1981**, *86*, 1.
(212) Weltner, W., Jr.; McLeod, D., Jr. *J. Mol. Spectrosc.* **1965**, *17*, 276.
(213) Nelin, C. J.; Bauschlicher, C. W., Jr. *Chem. Phys. Lett.* **1985**, *118*, 221.
(214) Lorenz, M.; Bondybey, V. E. *Chem. Phys.* **1999**, *241*, 127.
(215) (a) Almond, M. J.; Hahne, M. *J. Chem. Soc., Dalton Trans.* **1988**, 2255. (b) Darling, J. H.; Garton Sprenger, M. B.; Ogden, J. S. *Symp. Faraday Soc.* **1974**, *8*, 74.
(216) (a) Almond, M. J.; Crayston, J. A.; Downs, A. J.; Poliakoff, M.; Turner, J. J. *Inorg. Chem.* **1986**, *25*, 19. (b) Almond, M. J.; Downs, A. J. *J. Chem. Soc., Dalton Trans.* **1988**, 809.
(217) Wenthold, P. G.; Jonas, K.-L.; Lineberger, W. C. *J. Chem. Phys.* **1997**, *106*, 9961.
(218) Grein, F. *Chem. Phys.* **2008**, *343*, 231.
(219) Sniatynsky, R.; Cedeño, D. L. *THEOCHEM* **2004**, *711*, 123.
(220) Li, G. L.; Xu, W. G.; Li, Q. S. *THEOCHEM* **2000**, *498*, 61.
(221) Martínez, A. *J. Phys. Chem. A* **1998**, *102*, 1381.
(222) Murugan, P.; Kumar, V.; Kawazoe, Y.; Ota, N. *Chem. Phys. Lett.* **2006**, *423*, 202.
(223) Oliveira, J. A.; De Almeida, W. B.; Duarte, H. A. *Chem. Phys. Lett.* **2003**, *372*, 650.
(224) Hewett, W. D., Jr.; Newton, J. H.; Weltner, W., Jr. *J. Phys. Chem.* **1975**, *79*, 2640.
(225) Davico, G. E.; Schwartz, R. L.; Ramond, T. M.; Lineberger, W. C. *J. Phys. Chem. A* **1999**, *103*, 6167.
(226) Green, D. W.; Ervin, K. M. *J. Mol. Spectrosc.* **1981**, *89*, 145.
(227) Zhai, H. J.; Li, S.; Dixon, D. A.; Wang, L. S. *J. Am. Chem. Soc.* **2008**, *130*, 5167.
(228) Zhai, H. J.; Kiran, B.; Cui, L. F.; Li, X.; Dixon, D. A.; Wang, L. S. *J. Am. Chem. Soc.* **2004**, *126*, 16134.
(229) Walter, C. W.; Hertzler, C. F.; Devynck, P.; Smith, G. P.; Peterson, J. R. *J. Chem. Phys.* **1991**, *95*, 824.
(230) Neikirk, D. L.; Fagerli, J. C.; Smith, M. L.; Mosman, D.; Devore, T. C. *J. Mol. Struct.* **1991**, *244*, 165.
(231) Iorns, T. V.; Stafford, F. E. *J. Am. Chem. Soc.* **1966**, *88*, 4819.
(232) (a) Li, S.; Dixon, D. A. *J. Phys. Chem. A* **2007**, *111*, 11908. (b) Li, S.; Dixon, D. A. *J. Phys. Chem. A* **2006**, *110*, 6231.
(233) Sun, Q.; Rao, B. K.; Jena, P.; Stolcic, D.; Kim, Y. D.; Ganteför, G.; Castleman, A. W., Jr. *J. Chem. Phys.* **2004**, *121*, 9417.
(234) Tsipis, A. C. *Phys. Chem. Chem. Phys.* **2000**, *2*, 1357.
(235) Tsipis, A. C.; Tsipis, C. A. *J. Phys. Chem. A* **2000**, *104*, 859.
(236) Stolcic, D.; Kim, Y. D.; Ganteför, G. *J. Chem. Phys.* **2004**, *120*, 5.
(237) Chen, Z. Y.; Yang, J. L. *Chin. J. Chem. Phys.* **2007**, *20*, 78.
(238) Zhao, Y. Y.; Su, J.; Gong, Y.; Li, J.; Zhou, M. F. *J. Phys. Chem. A* **2008**, *112*, 8606.
(239) Uzunova, E. L.; Nikolov, G. St.; Mikosch, H. *ChemPhysChem* **2004**, *5*, 192.
(240) Gutsev, G. L.; Rao, B. K.; Jena, P.; Li, X.; Wang, L. S. *J. Chem. Phys.* **2000**, *113*, 1473.
(241) (a) Nayak, S. K.; Jena, P. *J. Am. Chem. Soc.* **1999**, *121*, 644. (b) Nayak, S. K.; Jena, P. *Phys. Rev. Lett.* **1998**, *81*, 2970.
(242) Namiki, K.; Saito, S. *J. Chem. Phys.* **1997**, *107*, 8848.
(243) Ferrante, R. F.; Wilkerson, J. L.; Graham, W. R. M.; Weltner, W., Jr. *J. Chem. Phys.* **1977**, *67*, 5904.
(244) Gordon, R. M.; Merer, A. J. *Can. J. Phys.* **1980**, *58*, 642.
(245) (a) Pinchemel, B.; Schamps, J. *Chem. Phys.* **1976**, *18*, 481. (b) Pinchemel, B.; Schamps, J. *Can. J. Phys.* **1975**, *53*, 431.
(246) Chertihin, G. V.; Andrews, L. *J. Phys. Chem. A* **1997**, *101*, 8547.
(247) Gong, Y.; Wang, G. J.; Zhou, M. F. *J. Phys. Chem. A* **2008**, *112*, 4936.
(248) Brown, C. E.; Mitchell, S. A.; Hackett, P. A. *J. Phys. Chem.* **1991**, *95*, 1062.
(249) Gutsev, G. L.; Rao, B. K.; Jena, P.; Wang, X. B.; Wang, L. S. *Chem. Phys. Lett.* **1999**, *312*, 598.
(250) Gutsev, G. L.; Rao, B. K.; Jena, P. *J. Phys. Chem. A* **1999**, *103*, 10819.
(251) Zhou, M. F.; Zeng, A. H.; Wang, Y.; Kong, Q. Y.; Wang, Z. X.; Schleyer, P. V. R. *J. Am. Chem. Soc.* **2003**, *125*, 11512.
(252) (a) Griffiths, J. E.; Sunder, W. A.; Falconer, W. E. *Spectrochim. Acta* **1975**, *31A*, 1207. (b) Edwards, A. J.; Falconer, W. E.; Griffiths, J. E.; Sunder, W. A.; Vasile, M. J. *J. Chem. Soc., Dalton Trans.* **1974**, 1129.
(253) Zhou, M. F.; Zhao, Y. Y.; Gong, Y.; Li, J. *J. Am. Chem. Soc.* **2006**, *128*, 2504.
(254) Beckers, H.; Garcia, P.; Willner, H.; Argüello, G. A.; Cobos, C. J.; Francisco, J. S. *Angew. Chem., Int. Ed.* **2007**, *46*, 3754.
(255) Viggiano, A. A.; Henchman, M. J.; Dale, F.; Deakyne, C. A.; Paulson, J. F. *J. Am. Chem. Soc.* **1992**, *114*, 4299.
(256) Kuznetsov, S. V.; Korobov, M. V.; Sidorov, L. N.; Shipachev, V. A.; Mitkin, V. N. *Int. J. Mass Spectrom. Ion Processes* **1989**, *87*, 13.
(257) Bartlett, N. *Proc. Chem. Soc.* **1962**, 218.
(258) Gancheff, J.; Kremer, C.; Kremer, E.; Ventura, O. N. *THEOCHEM* **2002**, *580*, 107.
(259) (a) Balfour, W. J.; Ram, R. S. *J. Mol. Spectrosc.* **1983**, *100*, 164. (b) Balfour, W. J.; Orth, F. B. *J. Mol. Spectrosc.* **1980**, *84*, 424.
(260) Roberts, M. A.; Alfonzo, C. G.; Manke, K. J.; Ames, W. M.; Ron, D. B.; Varberg, T. D. *Mol. Phys.* **2007**, *105*, 917.
(261) Zhou, M. F.; Citra, A.; Liang, B. Y.; Andrews, L. *J. Phys. Chem. A* **2000**, *104*, 3457.
(262) Pramann, A.; Rademann, K. *Chem. Phys. Lett.* **2001**, *343*, 99.
(263) Metz, R. B.; Nicolas, C.; Ahmed, M.; Leone, S. R. *J. Chem. Phys.* **2005**, *123*, 114313.
(264) Chestakov, D. A.; Parker, D. H.; Baklanov, A. V. *J. Chem. Phys.* **2005**, *122*, 084302.
(265) Son, H. S.; Lee, K.; Shin, S. K.; Ku, J. K. *Chem. Phys. Lett.* **2000**, *320*, 658.
(266) Drechsler, G.; Boesl, U.; Bässmann, C.; Schlag, E. W. *J. Chem. Phys.* **1997**, *107*, 2284.
(267) Allen, M. D.; Ziurys, L. M.; Brown, J. M. *Chem. Phys. Lett.* **1996**, *257*, 130.

(268) (a) Wu, H. B.; Desai, S. R.; Wang, L. S. *J. Am. Chem. Soc.* **1996**, *118*, 5296. (b) Wu, H. B.; Desai, S. R.; Wang, L. S. *J. Am. Chem. Soc.* **1996**, *118*, 7434.
(269) Fan, J.; Wang, L. S. *J. Chem. Phys.* **1995**, *102*, 8714.
(270) Chertihin, G. V.; Saffel, W.; Yustein, J. T.; Andrews, L.; Neurock, M.; Ricca, A.; Bauschlicher, C. W., Jr. *J. Phys. Chem.* **1996**, *100*, 5261.
(271) Kröckertskothen, T.; Knöckel, H.; Tiemann, E. *Mol. Phys.* **1987**, *62*, 1031.
(272) (a) Cheung, A. S. C.; Gordon, R. M.; Merer, A. J. *J. Mol. Spectrosc.* **1981**, *87*, 289. (b) Cheung, A. S.-C.; Lee, N.; Lyyra, A. M.; Merer, A. J.; Taylor, A. W. *J. Mol. Spectrosc.* **1982**, *95*, 213. (c) Taylor, A. W.; Cheung, A. S.-C.; Merer, A. J. *J. Mol. Spectrosc.* **1985**, *113*, 487. (d) Barnes, M.; Fraser, M. M.; Hajigeorgiou, P. G.; Merer, A. J.; Rosner, S. D. *J. Mol. Spectrosc.* **1995**, *170*, 449. (e) Steimle, T. C.; Nachman, D. F.; Shirley, J. E.; Merer, A. J. *J. Chem. Phys.* **1989**, *90*, 5360.
(273) Harris, S. M.; Barrow, R. F. *J. Mol. Spectrosc.* **1980**, *84*, 334.
(274) Green, D. W.; Reedy, G. T.; Kay, J. G. *J. Mol. Spectrosc.* **1979**, *78*, 257.
(275) West, J. B.; Broida, H. P. *J. Chem. Phys.* **1975**, *62*, 2566.
(276) (a) Hendrickx, M. F. A.; Anam, K. R. *J. Phys. Chem. A* **2009**, *113*, 8746. (b) Neumark, D. M.; Lineberger, W. C. *J. Phys. Chem. A,* published online August 28, 2009, doi:10.1021/jp906974n.
(277) Shiroishi, H.; Oda, T.; Hamada, I.; Fujima, N. *Eur. Phys. J., D* **2003**, *24*, 85.
(278) Gutsev, G. L.; Khanna, S. N.; Rao, B. K.; Jena, P. *J. Phys. Chem. A* **1999**, *103*, 5812.
(279) Glukhovtser, M. N.; Bach, R. D.; Nagel, C. J. *J. Phys. Chem. A* **1997**, *101*, 316.
(280) Krauss, M.; Stevens, W. J. *J. Chem. Phys.* **1985**, *82*, 5584.
(281) Blyholder, G.; Head, J.; Ruette, F. *Inorg. Chem.* **1982**, *21*, 1539.
(282) Bagus, P. S.; Preston, H. J. T. *J. Chem. Phys.* **1973**, *59*, 2986.
(283) Abramowitz, S.; Acquista, N.; Levin, I. W. *Chem. Phys. Lett.* **1977**, *50*, 423.
(284) Chang, S.; Blyholder, G.; Fernandez, J. *Inorg. Chem.* **1981**, *20*, 2813.
(285) Fanfarillo, M.; Downs, A. J.; Green, T. M.; Almond, M. J. *Inorg. Chem.* **1992**, *31*, 2973.
(286) Andrews, L.; Chertihin, G. V.; Ricca, A.; Bauschlicher, C. W., Jr. *J. Am. Chem. Soc.* **1996**, *118*, 467.
(287) Yamada, Y.; Sumino, H.; Okamura, Y.; Shimasaki, H.; Tominaga, T. *Appl. Radiat. Isot.* **2000**, *52*, 157.
(288) Gong, Y.; Zhou, M. F.; Andrews, L. *J. Phys. Chem. A* **2007**, *111*, 12001.
(289) Grein, F. *Int. J. Quantum Chem.* **2009**, *109*, 549.
(290) Cao, Z.; Duran, M.; Solà, M. *Chem. Phys. Lett.* **1997**, *274*, 411.
(291) Lyne, P. D.; Mingos, D. M. P.; Ziegler, T.; Downs, A. J. *Inorg. Chem.* **1993**, *32*, 4785.
(292) García-Sosa, A. T.; Castro, M. *Int. J. Quantum Chem.* **2000**, *80*, 307.
(293) Kellogg, C. B.; Irikura, K. K. *J. Phys. Chem. A* **1999**, *103*, 1150.
(294) Plane, J. M. C.; Rollason, R. J. *Phys. Chem. Chem. Phys.* **1999**, *1*, 1843.
(295) Gong, Y.; Zhou, M. F. *J. Phys. Chem. A* **2008**, *112*, 10838.
(296) Rollason, R. J.; Plane, J. M. C. *Phys. Chem. Chem. Phys.* **2000**, *2*, 2335.
(297) Atanasov, M. *Inorg. Chem.* **1999**, *38*, 4942.
(298) Gutsev, G. L.; Khanna, S. N.; Rao, B. K.; Jena, P. *Phys. Rev. A* **1999**, *59*, 3681.
(299) Cao, Z.; Wu, W.; Zhang, Q. *THEOCHEM* **1999**, *489*, 165.
(300) Carbonniere, P.; Ciofini, I.; Adamo, C.; Pouchan, C. *Chem. Phys. Lett.* **2006**, *429*, 52.
(301) Hohm, U.; Maroulis, G. *J. Chem. Phys.* **2004**, *121*, 10411.
(302) Pershina, V.; Bastug, T.; Fricke, B.; Varga, S. *J. Chem. Phys.* **2001**, *115*, 792.
(303) Nakajima, T.; Koga, K.; Hirao, K. *J. Chem. Phys.* **2000**, *112*, 10142.
(304) Bridgeman, A. J.; Cavigliasso, G. *Polyhedron* **2001**, *20*, 2269.
(305) Ujaque, G.; Maseras, F.; Lledós, A. *Int. J. Quantum Chem.* **2000**, *77*, 544.
(306) Stückl, A. C.; Daul, C. A.; Güdel, H. U. *J. Chem. Phys.* **1997**, *107*, 4606.
(307) Pyykkö, P.; Li, J.; Bastug, T.; Fricke, B.; Kolb, D. *Inorg. Chem.* **1993**, *32*, 1525.
(308) (a) Bursten, B. E.; Green, J. C.; Kaltsoyannis, N. *Inorg. Chem.* **1994**, *33*, 2315. (b) Green, J. C.; Guest, M. F.; Hillier, I. H.; Jarrett-Sprague, S. A.; Kaltsoyannis, N.; MacDonald, M. A.; Sze, K. H. *Inorg. Chem.* **1992**, *31*, 1588. (c) Green, J. C.; Kaltsoyannis, N.; Sze, K. H.; MacDonald, M. A. *Chem. Phys. Lett.* **1990**, *175*, 359.
(309) Gulliver, D. J.; Levason, W. *Coord. Chem. Rev.* **1982**, *46*, 1.
(310) Green, D. W.; Kay, J. G.; Zimmerman, G. L.; Balko, B. *J. Mol. Spectrosc.* **1989**, *138*, 62.
(311) Grinter, R.; Zimmerman, R. L.; Dunn, T. M. *J. Mol. Spectrosc.* **1984**, *107*, 12.
(312) Beattie, I. R.; Blayden, H. E.; Crocombe, R. A.; Jones, P. J.; Ogden, J. S. *J. Raman Spectrosc.* **1976**, *4*, 313.
(313) Kay, J. G.; Green, D. W.; Duca, K.; Zimmerman, G. L. *J. Mol. Spectrosc.* **1989**, *138*, 49.
(314) Scullman, R.; Thelin, B. *J. Mol. Spectrosc.* **1975**, *56*, 64.
(315) Raziunas, V.; Macur, G.; Katz, S. *J. Chem. Phys.* **1965**, *43*, 1010.
(316) Riedel, S.; Kaupp, M. *Coord. Chem. Rev.* **2009**, *253*, 606.
(317) McLamarrah, S. K.; Sheridan, P. M.; Ziurys, L. M. *Chem. Phys. Lett.* **2005**, *414*, 301.
(318) Danset, D.; Manceron, L. *J. Phys. Chem. A* **2003**, *107*, 11324.
(319) Namiki, K. C.; Saito, S. *J. Chem. Phys.* **2001**, *114*, 9390.
(320) Chertihin, G. V.; Citra, A.; Andrews, L.; Bauschlicher, C. W., Jr. *J. Phys. Chem. A* **1997**, *101*, 8793.
(321) (a) Clouthier, D. J.; Huang, G.; Merer, A. J.; Friedman-Hill, E. J. *J. Chem. Phys.* **1993**, *99*, 6336. (b) Adam, A. G.; Azuma, Y.; Barry, J. A.; Huang, G.; Lyne, M. P. J.; Merer, A. J.; Schröder, J. O. *J. Chem. Phys.* **1987**, *86*, 5231.
(322) Uzunova, E. L.; Nikolov, G. St.; Mikosch, H. *J. Phys. Chem. A* **2002**, *106*, 4104.
(323) Piechota, J.; Suffczynski, M. *Phys. Rev. A* **1993**, *48*, 2679.
(324) DeVore, T. C.; Gallaher, T. N. *J. Chem. Phys.* **1979**, *71*, 474.
(325) Van Zee, R. J.; Hamrick, Y. M.; Li, S.; Weltner, W., Jr. *J. Phys. Chem.* **1992**, *96*, 7247.
(326) Danset, D.; Alikhani, M. E.; Manceron, L. *J. Phys. Chem. A* **2005**, *109*, 97.
(327) Danset, D.; Alikhani, M. E.; Manceron, L. *J. Phys. Chem. A* **2005**, *109*, 105.
(328) Suo, B.; Han, H.; Lei, Y.; Zhai, G.; Wang, Y.; Wen, Z. *J. Chem. Phys.* **2009**, *130*, 094304.
(329) Stevens, F.; Van Speybroeck, V.; Carmichael, I.; Callens, F.; Waroquier, M. *Chem. Phys. Lett.* **2006**, *421*, 281.
(330) Mains, G. J.; White, J. M. *J. Phys. Chem.* **1991**, *95*, 112.
(331) Gengler, J.; Ma, T.; Adam, A. G.; Steimle, T. C. *J. Chem. Phys.* **2007**, *126*, 134304.
(332) (a) Heuff, R. F.; Fougere, S. G.; Balfour, W. J. *J. Mol. Spectrosc.* **2005**, *231*, 99. (b) Jensen, R. H.; Fougere, S. G.; Balfour, W. J. *Chem. Phys. Lett.* **2003**, *370*, 106.
(333) Li, X.; Wang, L. S. *J. Chem. Phys.* **1998**, *109*, 5264.
(334) Citra, A.; Andrews, L. *J. Phys. Chem. A* **1999**, *103*, 4845.
(335) (a) Hanlan, A. J. L.; Ozin, G. A. *Inorg. Chem.* **1977**, *16*, 2848. (b) Hanlan, A. J. L.; Ozin, G. A. *Inorg. Chem.* **1977**, *16*, 2857.
(336) Yang, R.; Gong, Y.; Zhou, H.; Zhou, M. F. *J. Phys. Chem. A* **2007**, *111*, 64.
(337) Riedel, S.; Gong, Y.; Zhou, M. F.; Kaupp, M. Unpublished results.
(338) Jansson, K.; Scullman, R. *J. Mol. Spectrosc.* **1972**, *43*, 208.
(339) Campbell, M. L. *J. Phys. Chem. A* **1997**, *101*, 9377.
(340) Gong, Y.; Zhou, M. F.; Kaupp, M.; Riedel, S. *Angew. Chem., Int. Ed.* **2009**, doi: 10.1002/anie.200902733.
(341) Citra, A.; Andrews, L. *J. Phys. Chem. A* **1999**, *103*, 4182.
(342) Ramond, T. M.; Davico, G. E.; Hellberg, F.; Svedberg, F.; Salen, P.; Söderqvist, P.; Lineberger, W. C. *J. Mol. Spectrosc.* **2002**, *216*, 1.
(343) Moravec, V. D.; Jarrold, C. C. *J. Chem. Phys.* **1998**, *108*, 1804.
(344) Wu, H.; Wang, L. S. *J. Chem. Phys.* **1997**, *107*, 16.
(345) Namiki, K.; Saito, S. *Chem. Phys. Lett.* **1996**, *252*, 347.
(346) Srdanov, V. I.; Harris, D. O. *J. Chem. Phys.* **1988**, *89*, 2748.
(347) Citra, A.; Chertihin, G. V.; Andrews, L.; Neurock, M. *J. Phys. Chem. A* **1997**, *101*, 3109.
(348) Hwang, D. Y.; Mebel, A. M. *J. Phys. Chem. A* **2002**, *106*, 520.
(349) Doll, K.; Dolg, M.; Fulde, P.; Stoll, H. *Phys. Rev. B* **1997**, *55*, 10282.
(350) Chung, S. C.; Krüger, S.; Pacchioni, G.; Rösch, N. *J. Chem. Phys.* **1995**, *102*, 3695.
(351) Bridgeman, A. J. *J. Chem. Soc., Dalton Trans.* **1996**, 4555.
(352) Bauschlicher, C. W., Jr. *Chem. Phys.* **1985**, *93*, 399.
(353) Walch, S. P.; Goddard, W. A., III. *J. Am. Chem. Soc.* **1978**, *100*, 1338.
(354) Hwang, D. Y.; Mebel, A. M. *J. Phys. Chem. A* **2002**, *106*, 12072.
(355) Wang, X. F.; Andrews, L. *J. Phys. Chem. A* **2001**, *105*, 5812.
(356) Dedieu, A. *Chem. Rev.* **2000**, *100*, 543.
(357) Bare, W. D.; Citra, A.; Chertihin, G. V.; Andrews, L. *J. Phys. Chem. A* **1999**, *103*, 5456.
(358) (a) Broclawik, E.; Yamauchi, R.; Endou, A.; Kubo, M.; Miyamoto, A. *Int. J. Quantum Chem.* **1997**, *61*, 673. (b) Broclawik, E.; Yamauchi, R.; Eudou, A.; Kubo, M.; Miyamoto, A. *J. Chem. Phys.* **1996**, *104*, 4098.
(359) Schwerdtfeger, P.; McFeaters, J. S.; Moore, J. J.; McPherson, D. M.; Cooney, R. P.; Bowmaker, G. A.; Dolg, M.; Andrae, D. *Langmuir* **1991**, *7*, 116.
(360) Klopcic, S. A.; Moravec, V. D.; Jarrold, C. C. *J. Chem. Phys.* **1999**, *110*, 10216.
(361) Liu, H.; O'Brien, L. C.; Shaji, S.; O'Brien, J. J. *J. Mol. Spectrosc.* **2009**, *253*, 73.

(362) Citir, M.; Metz, R. B.; Belau, L.; Ahmed, M. *J. Phys. Chem. A* **2008**, *112*, 9584.
(363) Cooke, S. A.; Gerry, M. C. L. *Phys. Chem. Chem. Phys.* **2005**, *7*, 2453.
(364) Okabayashi, T.; Yamazaki, E.; Tanimoto, M. *J. Mol. Spectrosc.* **2005**, *229*, 283.
(365) Steimle, T. C.; Jung, K. Y.; Li, B. Z. *J. Chem. Phys.* **1995**, *103*, 1767.
(366) Jansson, K.; Scullman, R. *Ber. Bunsen-Ges.* **1978**, *82*, 92.
(367) (a) Sassenberg, U.; Scullman, R. *Phys. Scr.* **1983**, *28*, 139. (b) Sassenberg, U.; Scullman, R. *J. Mol. Spectrosc.* **1977**, *68*, 331.
(368) (a) Xu, Y.; Shelton, W. A.; Schneider, W. F. *J. Phys. Chem. B* **2006**, *110*, 16591. (b) Xu, Y.; Shelton, W. A.; Schneider, W. F. *J. Phys. Chem. A* **2006**, *110*, 5839.
(369) Hwang, D. Y.; Mebel, A. M. *Chem. Phys. Lett.* **2002**, *365*, 140.
(370) Kirchner, E. J. J.; Baerends, E. J.; van Slooten, U.; Kleyn, A. W. *J. Chem. Phys.* **1992**, *97*, 3821.
(371) Allouti, F.; Manceron, L.; Alikhani, M. E. *Phys. Chem. Chem. Phys.* **2006**, *8*, 448.
(372) Danset, D.; Manceron, L.; Andrews, L. *J. Phys. Chem. A* **2001**, *105*, 7205.
(373) Huber, H.; Ozin, G. A. *Can. J. Chem.* **1972**, *50*, 3746.
(374) Huber, H.; Klotzbücher, W.; Ozin, G. A.; Vander Voet, A. *Can. J. Chem.* **1973**, *51*, 2722.
(375) Song, J.; Aprá, E.; Khait, Y. G.; Hoffmann, M. R.; Kowalski, K. *Chem. Phys. Lett.* **2006**, *428*, 277.
(376) Bauschlicher, C. W., Jr. *J. Phys. Chem. A* **2004**, *108*, 2871.
(377) Bauschlicher, C. W., Jr.; Langhoff, S. R.; Partridge, H.; Sodupe, M. *J. Phys. Chem.* **1993**, *97*, 856.
(378) Blomberg, M. R. A.; Siegbahn, P. E. M.; Strich, A. *Chem. Phys.* **1985**, *97*, 287.
(379) Deng, K.; Yang, J. L.; Zhu, Q. S. *J. Chem. Phys.* **2003**, *118*, 6868.
(380) Yang, R.; Gong, Y.; Zhou, M. F. *Chem. Phys.* **2007**, *340*, 134.
(381) Campbell, M. L.; Plane, J. M. C. *J. Phys. Chem. A* **2003**, *107*, 3747.
(382) Wu, H. B.; Desai, S. R.; Wang, L. S. *J. Phys. Chem. A* **1997**, *101*, 2103.
(383) Chertihin, G. V.; Andrews, L.; Bauschlicher, C. W., Jr. *J. Phys. Chem. A* **1997**, *101*, 4026.
(384) Polak, M. L.; Gilles, M. K.; Ho, J.; Lineberger, W. C. *J. Phys. Chem.* **1991**, *95*, 3460.
(385) O'Brien, L. C.; Kubicek, R. L.; Wall, S. J.; Koch, D. E.; Friend, R. J.; Brazier, C. R. *J. Mol. Spectrosc.* **1996**, *180*, 365.
(386) (a) Steimle, T.; Namiki, K.; Saito, S. *J. Chem. Phys.* **1997**, *107*, 6109. (b) Steimle, T. C.; Chang, W. L.; Nachman, D. F. *Chem. Phys. Lett.* **1988**, *153*, 534. (c) Gerry, M. C. L.; Merer, A. J.; Sassenberg, U.; Steimle, T. C. *J. Chem. Phys.* **1987**, *86*, 4754.
(387) (a) Appelblad, O.; Lagerqvist, A.; Renhorn, I.; Field, R. W. *Phys. Scr.* **1980**, *22*, 603. (b) Appelblad, O.; Lagerqvist, A. *Phys. Scr.* **1974**, *10*, 307.
(388) Griffiths, M. J.; Barrow, R. F. *J. Chem. Soc., Faraday Trans. 2* **1977**, *73*, 943.
(389) (a) Thompson, K. R.; Easley, W. C.; Knight, L. B. *J. Phys. Chem.* **1973**, *77*, 49.
(390) Shirk, J. S.; Bass, A. M. *J. Chem. Phys.* **1970**, *52*, 1894.
(391) Tevault, D. E.; Mowery, R. L.; De Marco, R. A.; Smardzewski, R. R. *J. Chem. Phys.* **1981**, *74*, 4342.
(392) Ferrão, L. F. A.; Roberto-Neto, O.; Machado, F. B. C. *Int. J. Quantum Chem.* **2008**, *108*, 2512.
(393) Midda, S.; Bera, N. C.; Bhattacharyya, I.; Das, A. K. *THEOCHEM* **2006**, *761*, 17.
(394) Xian, H.; Cao, Z. X.; Xu, X.; Lu, X.; Zhang, Q. E. *Chem. Phys. Lett.* **2000**, *326*, 485.
(395) Daoudi, A.; Touimi, B. A.; Flament, J. P.; Berthier, G. *J. Mol. Spectrosc.* **1999**, *194*, 8.
(396) (a) Hippe, D.; Peyerimhoff, S. D. *Mol. Phys.* **1992**, *76*, 293. (b) Hippe, D.; Peyerimhoff, S. D. *J. Chem. Phys.* **1992**, *96*, 3503.
(397) (a) Langhoff, S. R.; Bauschlicher, C. W., Jr. *Chem. Phys. Lett.* **1986**, *124*, 241. (b) Bagus, P. S.; Nelin, C. J.; Bauschlicher, C. W., Jr. *J. Chem. Phys.* **1983**, *79*, 2975.
(398) Madhavan, P. V.; Newton, M. D. *J. Chem. Phys.* **1985**, *83*, 2337.
(399) Basch, H.; Osman, R. *Chem. Phys. Lett.* **1982**, *93*, 51.
(400) Igel, G.; Wedig, U.; Dolg, M.; Fuentealba, P.; Preuss, H.; Stoll, H.; Frey, R. *J. Chem. Phys.* **1984**, *81*, 2737.
(401) Schamps, J.; Pinchemel, B.; Lefebvre, Y.; Raseev, G. *J. Mol. Spectrosc.* **1983**, *101*, 344.
(402) Den Boer, D. H. W.; Kaleveld, E. W. *Chem. Phys. Lett.* **1980**, *69*, 389.
(403) Wu, H. B.; Desai, S. R.; Wang, L. S. *J. Chem. Phys.* **1995**, *103*, 4363.
(404) (a) Caspary, N.; Savchenko, E. V.; Thoma, A.; Lammers, A.; Bondybey, V. E. *Low Temp. Phys.* **2000**, *26*, 744. (b) Bondybey, V. E.; English, J. H. *J. Phys. Chem.* **1984**, *88*, 2247.
(405) Kasai, P. H.; Jones, P. M. *J. Phys. Chem.* **1986**, *90*, 4239.
(406) Howard, J. A.; Sutcliffe, R.; Mile, B. *J. Phys. Chem.* **1984**, *88*, 4351.
(407) Ozin, G. A.; Mitchell, S. A.; Garćia-Prieto, J. *J. Am. Chem. Soc.* **1983**, *105*, 6399.
(408) Tevault, D. E. *J. Chem. Phys.* **1982**, *76*, 2859.
(409) Mattar, S. M.; Ozin, G. A. *J. Phys. Chem.* **1988**, *92*, 3511.
(410) Güell, M.; Luis, J. M.; Rodríguez-Santiago, L.; Sodupe, M.; Solà, M. *J. Phys. Chem. A* **2009**, *113*, 1308.
(411) Mochizuki, Y.; Nagashima, U.; Yamamoto, S.; Kashiwagi, H. *Chem. Phys. Lett.* **1989**, *164*, 225.
(412) (a) Pouillon, Y.; Massobrio, C.; Celino, M. *Comput. Mater. Sci.* **2000**, *17*, 539. (b) Pouillon, Y.; Massobrio, C. *Chem. Phys. Lett.* **2000**, *331*, 290.
(413) Hrušák, J.; Koch, W.; Schwarz, H. *J. Chem. Phys.* **1994**, *101*, 3898.
(414) Hasegawa, J.; Pierloot, K.; Roos, B. O. *Chem. Phys. Lett.* **2001**, *335*, 503.
(415) Deng, K.; Yang, J. L.; Yuan, L. F.; Zhu, Q. S. *J. Chem. Phys.* **1999**, *111*, 1477.
(416) Mochizuki, Y.; Tanaka, K.; Kashiwagi, H. *Chem. Phys.* **1991**, *151*, 11.
(417) Ha, T. K.; Nguyen, M. T. *J. Phys. Chem.* **1985**, *89*, 5569.
(418) (a) Andrews, L.; Prochaska, E. S.; Ault, B. S. *J. Chem. Phys.* **1978**, *69*, 556. (b) Spiker, R. C., Jr.; Andrews, L. *J. Chem. Phys.* **1973**, *59*, 1851. (c) Andrews, L. *J. Am. Chem. Soc.* **1973**, *95*, 4487.
(419) Bates, J. B.; Brooker, M. H.; Boyd, G. E. *Chem. Phys. Lett.* **1972**, *16*, 391.
(420) Pouillon, Y.; Massobrio, C. *Appl. Surf. Sci.* **2004**, *226*, 306.
(421) Baruah, T.; Zope, R. R.; Pederson, M. R. *Phys. Rev. A* **2004**, *69*, 023201.
(422) Cao, Z. X.; Solà, M.; Xian, H.; Duran, M.; Zhang, Q. E. *Int. J. Quantum Chem.* **2001**, *81*, 162.
(423) Deng, K.; Yang, J. L.; Zhu, Q. S. *J. Chem. Phys.* **2000**, *113*, 7867.
(424) Darling, J. H.; Garton-Sprenger, M. B.; Ogden, J. S. *Faraday Symp. Chem. Soc.* **1973**, *7*, 75.
(425) Gong, Y.; Zhou, M. F. *Phys. Chem. Chem. Phys.* **2009**, *11*, doi: 10.1039/b909999a.
(426) Massobrio, C.; Pouillon, Y. *J. Chem. Phys.* **2003**, *119*, 8305.
(427) Pouillon, Y.; Massobrio, C. *Chem. Phys. Lett.* **2002**, *356*, 469.
(428) Gong, Y.; Wang, G. J.; Zhou, M. F. *J. Phys. Chem. A* **2009**, *113*, 5355.
(429) (a) Reynolds, A. M.; Gherman, B. F.; Cramer, C. J.; Tolman, W. B. *Inorg. Chem.* **2005**, *44*, 6989. (b) Aboelella, N. W.; Kryatov, S. V.; Gherman, B. F.; Brennessel, W. W.; Young, V. G., Jr.; Sarangi, R.; Rybak-Akimova, E. V.; Hodgson, K. O.; Hedman, B.; Solomon, E. I.; Cramer, C. J.; Tolman, W. B. *J. Am. Chem. Soc.* **2004**, *126*, 16896.
(430) Citra, A.; Andrews, L. *THEOCHEM* **1999**, *489*, 95.
(431) Tevault, D. E.; DeMarco, R. A.; Smardzewski, R. R. *J. Chem. Phys.* **1981**, *75*, 4168.
(432) Andrews, D. H.; Gianola, A. J.; Lineberger, W. C. *J. Chem. Phys.* **2002**, *117*, 4074.
(433) Steimle, T.; Tanimoto, M.; Namiki, K.; Saito, S. *J. Chem. Phys.* **1998**, *108*, 7616.
(434) (a) O'Brien, L. C.; Wall, S. J.; Henry, G. L. *J. Mol. Spectrosc.* **1998**, *191*, 218. (b) O'Brien, L. C.; Wall, S. J.; Sieber, M. K. *J. Mol. Spectrosc.* **1997**, *183*, 57.
(435) (a) Bojović, V.; Antić-Jovanović, A.; Stoiljković, M. M.; Miletić, M.; Peĉić, D. S. *Spectrosc. Lett.* **1999**, *32*, 875. (b) Vujisić, B. R.; Savović, J. J.; Bojović, V.; Peŝić, D. S. *Spectrosc. Lett.* **1993**, *26*, 1529.
(436) Griffiths, M. J.; Barrow, R. F. *J. Phys. B* **1977**, *10*, 925.
(437) Bauschlicher, C. W., Jr.; Partridge, H.; Langhoff, S. R. *Chem. Phys.* **1990**, *148*, 57.
(438) Hay, P. J.; Martin, R. L. *J. Chem. Phys.* **1985**, *83*, 5174.
(439) Andzelm, J.; Radzio, E.; Salahub, D. R. *J. Chem. Phys.* **1985**, *83*, 4573.
(440) Zhai, H. J.; Bürgel, C.; Bonacic-Koutecky, V.; Wang, L. S. *J. Am. Chem. Soc.* **2008**, *130*, 9156.
(441) Ichino, T.; Gianola, A. J.; Andrews, D. H.; Lineberger, W. C. *J. Phys. Chem. A* **2004**, *108*, 11307.
(442) (a) O'Brien, L. C.; Oberlink, A. E.; Roos, B. O. *J. Phys. Chem. A* **2006**, *110*, 11954. (b) O'Brien, L. C.; Hardimon, S. C.; O'Brien, J. J. *J. Phys. Chem. A* **2004**, *108*, 11302.
(443) Okabayashi, T.; Koto, F.; Tsukamoto, K.; Yamazaki, E.; Tanimoto, M. *Chem. Phys. Lett.* **2005**, *403*, 223.
(444) Wu, Z. J. *J. Phys. Chem. A* **2005**, *109*, 5951.
(445) Okumura, M.; Kitagawa, Y.; Haruta, M.; Yamaguchi, K. *Chem. Phys. Lett.* **2001**, *346*, 163.
(446) Schwerdtfeger, P.; Dolg, M.; Schwarz, W. H. E.; Bowmaker, G. A.; Boyd, P. D. W. *J. Chem. Phys.* **1989**, *91*, 1762.
(447) Tevault, D. E.; Smardzewski, R. R.; Urban, M. W.; Nakamoto, K. *J. Chem. Phys.* **1982**, *77*, 577.
(448) McIntosh, D.; Ozin, G. A. *Inorg. Chem.* **1977**, *16*, 59.
(449) Zhou, J.; Li, Z. H.; Wang, W. N.; Fan, K. N. *Chem. Phys. Lett.* **2006**, *421*, 448.

(450) Kasai, P. H. *J. Phys. Chem.* **1990**, *94*, 3539.
(451) McIntosh, D.; Ozin, G. A. *Inorg. Chem.* **1976**, *15*, 2869.
(452) Ding, X. L.; Li, Z. Y.; Yang, J. L.; Hou, J. G.; Zhu, Q. S. *J. Chem. Phys.* **2004**, *120*, 9594.
(453) Tielens, F.; Gracia, L.; Polo, V.; Andrés, J. *J. Phys. Chem. A* **2007**, *111*, 13255.
(454) Andrews, L.; Hwang, J. T.; Trindle, C. *J. Phys. Chem.* **1973**, *77*, 1065.
(455) Wang, X. F.; Andrews, L.; Riedel, S.; Kaupp, M. *Angew. Chem., Int. Ed.* **2007**, *46*, 8371.
(456) Zack, L. N.; Pulliam, R. L.; Ziurys, L. M. *J. Mol. Spectrosc.* **2009**, *256*, 186.
(457) Cannavo, D.; Knopp, G.; Radi, P.; Beaud, P.; Tulej, M.; Bodek, P.; Gerber, T.; Wokaun, A. *J. Mol. Struct.* **2006**, *782*, 67.
(458) Clemmer, D. E.; Dalleska, N. F.; Armentrout, P. B. *J. Chem. Phys.* **1991**, *95*, 7263.
(459) Wikde, B. G. *J. Chem. Phys.* **1983**, *78*, 6036.
(460) Kim, J. H.; Li, X.; Wang, L. S.; de Clercq, H. L.; Fancher, C. A.; Thomas, O. C.; Bowen, K. H. *J. Phys. Chem. A* **2001**, *105*, 5709.
(461) Moravec, V. D.; Klopcic, S. A.; Chatterjee, B.; Jarrold, C. C. *Chem. Phys. Lett.* **2001**, *341*, 313.
(462) Fancher, C. A.; de Clercq, H. L.; Thomas, O. C.; Robinson, D. W.; Bowen, K. H. *J. Chem. Phys.* **1998**, *109*, 8426.
(463) Prochaska, E. S.; Andrews, L. *J. Chem. Phys.* **1980**, *72*, 6782.
(464) Chertihin, G. V.; Andrews, L. *J. Chem. Phys.* **1997**, *106*, 3457.
(465) Boughdiri, S.; Tangour, B.; Teichteil, C.; Barthelat, J. C.; Leininger, T. *Chem. Phys. Lett.* **2008**, *462*, 18.
(466) Chambaud, G.; Guitou, M.; Hayashi, S. *Chem. Phys.* **2008**, *352*, 147.
(467) von Szentpály, L. *J. Phys. Chem. A* **2008**, *112*, 12695.
(468) Peterson, K. A.; Shepler, B. C.; Singleton, J. M. *Mol. Phys.* **2007**, *105*, 1139.
(469) Kullie, O.; Zhang, H.; Kolb, J.; Kolb, D. *J. Chem. Phys.* **2006**, *125*, 244303.
(470) Erhart, P.; Juslin, N.; Goy, O.; Nordlund, K.; Müller, R.; Albe, K. *J. Phys. (Paris)* **2006**, *18*, 6585.
(471) Gusarov, A. V.; Iorish, V. S. *Russ. J. Phys. Chem.* **2006**, *80*, 1864.
(472) Bauschlicher, C. W., Jr.; Partridge, H. *J. Chem. Phys.* **1998**, *109*, 8430.
(473) Bauschlicher, C. W., Jr.; Langhoff, S. R. *Chem. Phys. Lett.* **1986**, *126*, 163.
(474) Boldyrev, A. I.; Simons, J. *Mol. Phys.* **1997**, *92*, 365.
(475) Butler, R.; Katz, S.; Snelson, A.; Stephens, J. B. *J. Phys. Chem.* **1979**, *83*, 2578.
(476) Cremer, D.; Kraka, E.; Filatov, M. *ChemPhysChem* **2008**, *9*, 2510.
(477) Shepler, B. C.; Peterson, K. A. *J. Phys. Chem. A* **2003**, *107*, 1783.
(478) Hu, A.; Otto, P.; Ladik, J. *THEOCHEM* **1999**, *468*, 163.
(479) Kaledin, L. A.; McCord, J. E.; Heaven, M. C. *J. Mol. Spectrosc.* **1995**, *170*, 166.
(480) (a) Linton, C.; Dulick, M.; Field, R. W.; Carette, P.; Leyland, P. C.; Barrow, R. F. *J. Mol. Spectrosc.* **1983**, *102*, 441. (b) Linton, C.; Dulick, M.; Field, R. W.; Carette, P.; Barrow, R. F. *J. Chem. Phys.* **1981**, *74*, 189. (c) Linton, C.; Dulick, M.; Field, R. W. *J. Mol. Spectrosc.* **1979**, *78*, 428.
(481) Childs, W. J.; Azuma, Y.; Goodman, G. L. *J. Mol. Spectrosc.* **1990**, *144*, 70.
(482) (a) Shenyavskaya, E. A.; Kaledin, L. A. *J. Mol. Spectrosc.* **1982**, *91*, 22. (b) Shenyavskaya, E. A.; Egorova, I. V.; Lupanov, V. N. *J. Mol. Spectrosc.* **1973**, *47*, 355.
(483) (a) Dulick, M.; Field, R. W.; Beaufils, J. C.; Schamps, J. *J. Mol. Spectrosc.* **1981**, *87*, 278. (b) Dulick, M.; Field, R. W.; Beaufils, J. C. *J. Mol. Spectrosc.* **1981**, *87*, 268. (c) Dulick, M.; Field, R. W. *J. Mol. Spectrosc.* **1985**, *113*, 105.
(484) Linton, C.; Ma, T.; Wang, H.; Steimle, T. C. *J. Chem. Phys.* **2008**, *129*, 124310.
(485) (a) Effantin, C.; Bernard, A.; Crozet, P.; Ross, A. J.; d'Incan, J. *J. Mol. Spectrosc.* **2005**, *231*, 154. (b) Linton, C.; Effantin, C.; Crozet, P.; Ross, A. J.; Shenyavskaya, E. A.; d'Incan, J. *J. Mol. Spectrosc.* **2004**, *225*, 132. (c) Shenyavskaya, E. A.; Bernard, A.; Verges, J. *J. Mol. Spectrosc.* **2003**, *222*, 240.
(486) (a) Kaledin, L. A.; Shenyavskaya, E. A.; Kovacs, I. *Acta Phys. Hung.* **1983**, *54*, 189. (b) Kaledin, L. A.; Shenyavskaya, E. A. *Opt. Spekt.* **1979**, *47*, 1015.
(487) (a) Bujin, G.; Linton, C. *J. Mol. Spectrosc.* **1991**, *147*, 120. (b) Bujin, G.; Linton, C. *J. Mol. Spectrosc.* **1989**, *137*, 114. (c) Linton, C.; Bujin, G.; Rana, R. S.; Gray, J. A. *J. Mol. Spectrosc.* **1987**, *126*, 370.
(488) Linton, C.; James, A. M.; Simard, B. *J. Chem. Phys.* **1993**, *99*, 9420.
(489) Klingeler, R.; Pontius, N.; Lüttgens, G.; Bechthold, P. S.; Neeb, M.; Eberhardt, W. *Phys. Rev. A* **2002**, *65*, 032502.
(490) Kaledin, L. A.; Erickson, M. G.; Heaven, M. C. *J. Mol. Spectrosc.* **1994**, *165*, 323.
(491) Carette, P.; Hocquet, A.; Douay, M.; Pinchemel, B. *J. Mol. Spectrosc.* **1987**, *124*, 243.
(492) Yadav, B. R.; Rai, S. B.; Rai, D. K. *J. Mol. Spectrosc.* **1981**, *89*, 1.
(493) Van Zee, R. J.; Ferrante, R. F.; Zeringue, K. J.; Weltner, W., Jr. *J. Chem. Phys.* **1981**, *75*, 5297.
(494) Kulikov, A. N.; Kaledin, L. A.; Kobylianskii, A. I.; Gurvich, L. V. *Can. J. Phys.* **1984**, *62*, 1855.
(495) Kaledin, L. A.; Shenyavskaya, E. A. *J. Mol. Spectrosc.* **1981**, *90*, 590.
(496) (a) Linton, C.; Simard, B. *J. Chem. Phys.* **1992**, *96*, 1698. (b) Linton, C.; Gaudet, D. M.; Schall, H. *J. Mol. Spectrosc.* **1986**, *115*, 58.
(497) (a) Chen, J.; Steimle, T. C.; Linton, C. *J. Mol. Spectrosc.* **2005**, *232*, 105. (b) Linton, C.; Liu, Y. C. *J. Mol. Spectrosc.* **1988**, *131*, 367. (c) Liu, Y. C.; Linton, C.; Schall, H.; Field, R. W. *J. Mol. Spectrosc.* **1984**, *104*, 72.
(498) Kaledin, L. A.; Shenyavskaya, E. A. *J. Mol. Spectrosc.* **1989**, *133*, 469.
(499) Melville, T. C.; Gordon, I.; Tereszchuk, K. A.; Coxon, J. A.; Bernath, P. F. *J. Mol. Spectrosc.* **2003**, *218*, 235.
(500) Steimle, T. C.; Goodridge, D. M.; Linton, C. *J. Chem. Phys.* **1997**, *107*, 3723.
(501) (a) McDonald, S. A.; Rice, S. F.; Field, R. W.; Linton, C. *J. Chem. Phys.* **1990**, *93*, 7676. (b) Linton, C.; McDonald, S.; Rice, S.; Dulick, M.; Liu, Y. C.; Field, R. W. *J. Mol. Spectrosc.* **1983**, *101*, 332.
(502) Bernard, A.; Effantin, C. *Can. J. Phys.* **1986**, *64*, 246.
(503) Weltner, W., Jr.; DeKock, R. L. *J. Phys. Chem.* **1971**, *75*, 514.
(504) Willson, S. P.; Andrews, L. *J. Phys. Chem. A* **1999**, *103*, 3171.
(505) Willson, S. P.; Andrews, L. *J. Phys. Chem. A* **1999**, *103*, 6972.
(506) Field, R. W. *Ber. Bunsen-Ges. Phys. Chem.* **1982**, *86*, 771.
(507) Sekiya, M.; Noro, T.; Miyoshi, E.; Osanai, Y.; Koga, T. *J. Comput. Chem.* **2006**, *27*, 463.
(508) Dolg, M.; Stoll, H.; Preuss, H. *J. Chem. Phys.* **1989**, *90*, 1730.
(509) Dai, D.; Li, L.; Ren, J.; Whangbo, M. H. *J. Chem. Phys.* **1998**, *108*, 3479.
(510) Todorova, T. K.; Infante, I.; Gagliardi, L.; Dyke, J. M. *Int. J. Quantum Chem.* **2009**, *109*, 2068.
(511) Kotzian, M.; Rösch, N. *J. Mol. Spectrosc.* **1991**, *147*, 346.
(512) (a) Liu, W. J.; Hong, G. Y.; Dai, D. D.; Li, L. M.; Dolg, M. *Theor. Chem. Acc.* **1997**, *96*, 75. (b) Dolg, M.; Stoll, H.; Preuss, H. *Chem. Phys.* **1990**, *148*, 219.
(513) Sakai, Y.; Nakai, T.; Mogi, K.; Miyoshi, E. *Mol. Phys.* **2003**, *101*, 117.
(514) (a) Dolg, M.; Liu, W.; Kalvoda, S. *Int. J. Quantum Chem.* **2000**, *76*, 359. (b) Dolg, M.; Stoll, H.; Preuss, H. *Chem. Phys. Lett.* **1990**, *174*, 208.
(515) (a) Dolg, M.; Stoll, H.; Flad, H. J.; Preuss, H. *J. Chem. Phys.* **1992**, *97*, 1162. (b) Liu, W.; Dolg, M.; Li, L. *J. Chem. Phys.* **1998**, *108*, 2886.
(516) Allouche, A. R.; Aubert-Frécon, M.; Umanskiy, S. Ya. *J. Chem. Phys.* **2006**, *124*, 184317.
(517) Boudreaux, E. A.; Baxter, E. *Int. J. Quantum Chem.* **2002**, *90*, 629.
(518) Paulovič, J.; Gagliardi, L.; Dyke, J. M.; Hirao, K. *J. Chem. Phys.* **2004**, *120*, 9998.
(519) Dulick, M.; Murad, E.; Barrow, R. F. *J. Chem. Phys.* **1986**, *85*, 385.
(520) Gibson, J. K. *J. Phys. Chem. A* **2003**, *107*, 7891.
(521) Gabelnick, S. D.; Reedy, G. T.; Chasanov, M. G. *J. Chem. Phys.* **1974**, *60*, 1167.
(522) Hu, Z.; Kaindl, G.; Müller, B. G. *J. Alloys Compd.* **1997**, *246*, 177.
(523) Goncharov, V.; Han, J.; Kaledin, L. A.; Heaven, M. C. *J. Chem. Phys.* **2005**, *122*, 204311.
(524) (a) Edvinsson, G.; Lagerqvist, A. *Phys. Scr.* **1984**, *30*, 309. (b) von Bornstedt, A.; Edvinsson, G.; Lagerqvist, A.; Renhorn, I. *Phys. Scr.* **1979**, *20*, 599.
(525) Han, J.; Kaledin, L. A.; Goncharov, V.; Komissarov, A. V.; Heaven, M. C. *J. Am. Chem. Soc.* **2003**, *125*, 7176.
(526) (a) Kaledin, L. A.; Heaven, M. C. *J. Mol. Spectrosc.* **1997**, *185*, 1. (b) Kaledin, L. A.; McCord, J. E.; Heaven, M. C. *J. Mol. Spectrosc.* **1994**, *164*, 27. (c) Heaven, M. C.; Nicolai, J. P.; Riley, S. J.; Parks, E. K. *Chem. Phys. Lett.* **1985**, *119*, 229.
(527) Allen, G. C.; Baerends, E. J.; Vernooijs, P.; Dyke, J. M.; Ellis, A. M.; Feher, M.; Morris, A. *J. Chem. Phys.* **1988**, *89*, 5363.
(528) Han, J.; Goncharov, V.; Kaledin, L. A.; Komissarov, A. V.; Heaven, M. C. *J. Chem. Phys.* **2004**, *120*, 5155.
(529) Lue, C. J.; Jin, J.; Ortiz, M. J.; Rienstra-Kiracofe, J. C.; Heaven, M. C. *J. Am. Chem. Soc.* **2004**, *126*, 1812.
(530) Abramowitz, S.; Acquista, N. *J. Phys. Chem.* **1972**, *76*, 648.
(531) Abramowitz, S.; Acquista, N.; Thompson, K. R. *J. Phys. Chem.* **1971**, *75*, 2283.
(532) Heaven, M. C. *Phys. Chem. Chem. Phys.* **2006**, *8*, 4497.
(533) (a) Kushto, G. P.; Andrews, L. *J. Phys. Chem. A* **1999**, *103*, 4836. (b) Souter, P. F.; Kushto, G. P.; Andrews, L.; Neurock, M. *J. Phys. Chem. A* **1997**, *101*, 1287.
(534) Paulovič, J.; Nakajima, T.; Hirao, K.; Lindh, R.; Malmqvist, P. A. *J. Chem. Phys.* **2003**, *119*, 798.
(535) Seijo, L.; Barandiarán, Z.; Harguindey, E. *J. Chem. Phys.* **2001**, *114*, 118.

(536) Watanabe, Y.; Matsuoka, O. *J. Chem. Phys.* **1997**, *107*, 3738.
(537) Marian, C. M.; Wahlgren, U.; Gropen, O.; Pyykkö, P. *THEOCHEM* **1988**, *46*, 339.
(538) Zhou, M. F.; Andrews, L. *J. Chem. Phys.* **1999**, *111*, 11044.
(539) Jackson, V. E.; Craciun, R.; Dixon, D. A.; Peterson, K. A.; de Jong, W. A. *J. Phys. Chem. A* **2008**, *112*, 4095.
(540) Straka, M.; Dyall, K. G.; Pyykkö, P. *Theor. Chem. Acc.* **2001**, *106*, 393.
(541) Dyall, K. G. *Mol. Phys.* **1999**, *96*, 511.
(542) Pyykkö, P.; Laakkonen, L. J.; Tatsumi, K. *Inorg. Chem.* **1989**, *28*, 1801.
(543) Wadt, W. R. *J. Am. Chem. Soc.* **1981**, *103*, 6053.
(544) Gabelnick, S. D.; Reedy, G. T.; Chasanov, M. G. *J. Chem. Phys.* **1973**, *58*, 4468.
(545) Carstens, D. H. W.; Gruen, D. M.; Kozlowski, J. F. *High Temp. Sci.* **1972**, *4*, 436.
(546) Hunt, R. D.; Andrews, L. *J. Chem. Phys.* **1993**, *98*, 3690.
(547) Sankaran, K.; Sundararajan, K.; Viswanathan, K. S. *Bull. Mater. Sci.* **1999**, *22*, 785.
(548) Paulovič, J.; Gagliardi, L.; Dyke, J. M.; Hirao, K. *J. Chem. Phys.* **2005**, *122*, 144317.
(549) Zhou, M. F.; Andrews, L.; Ismail, N.; Marsden, C. *J. Phys. Chem. A* **2000**, *104*, 5495.
(550) Wang, H. Y.; Zhu, Z. H.; Gao, T.; Fu, Y. B.; Wang, X. L.; Sun, Y. *Mol. Phys.* **2000**, *98*, 875.
(551) Majumdar, D.; Balasubramanian, K.; Nitsche, H. *Chem. Phys. Lett.* **2002**, *361*, 143.
(552) Van Wezenbeek, E. M.; Baerends, E. J.; Snijders, J. G. *Theor. Chim. Acta* **1991**, *81*, 139.
(553) Fleig, T.; Jensen, H. J. A.; Olsen, J.; Visscher, L. *J. Chem. Phys.* **2006**, *124*, 104106.
(554) Infante, I.; Eliav, E.; Vilkas, M. J.; Ishikawa, Y.; Kaldor, U.; Visscher, L. *J. Chem. Phys.* **2007**, *127*, 124308.
(555) Gagliardi, L.; Roos, B. O.; Malmqvist, P.; Dyke, J. M. *J. Phys. Chem. A* **2001**, *105*, 10602.
(556) Li, J.; Bursten, B. E.; Andrews, L.; Marsden, C. J. *J. Am. Chem. Soc.* **2004**, *126*, 3424.
(557) (a) Li, J.; Bursten, B. E.; Liang, B. Y.; Andrews, L. *Science* **2002**, *295*, 2242. (b) Andrews, L.; Liang, B. Y.; Li, J.; Bursten, B. E. *Angew. Chem., Int. Ed.* **2000**, *39*, 4565.
(558) Gagliardi, L.; Heaven, M. C.; Krogh, J. W.; Roos, B. O. *J. Am. Chem. Soc.* **2005**, *127*, 86.
(559) Gabelnick, S. D.; Reedy, G. T.; Chasanov, M. G. *J. Chem. Phys.* **1973**, *59*, 6397.
(560) Green, D. W.; Reedy, G. T.; Gabelnick, S. D. *J. Chem. Phys.* **1980**, *73*, 4207.
(561) Privalov, T.; Schimmelpfennig, B.; Wahlgren, U.; Grenthe, I. *J. Phys. Chem. A* **2002**, *106*, 11277.
(562) Pyykkö, P.; Li, J.; Runeberg, N. J. *J. Phys. Chem.* **1994**, *98*, 4809.
(563) Green, D. W.; Reedy, G. T. *J. Chem. Phys.* **1978**, *69*, 544.
(564) La Macchia, G.; Infante, I.; Raab, J.; Gibson, J. K.; Gagliardi, L. *Phys. Chem. Chem. Phys.* **2008**, *10*, 7278.
(565) Archibong, E. F.; Ray, A. K. *THEOCHEM* **2000**, *530*, 165.
(566) (a) Ritter, D.; Weisshaar, J. C. *J. Phys. Chem.* **1990**, *94*, 4907. (b) Ritter, D.; Weisshaar, J. C. *J. Phys. Chem.* **1989**, *93*, 1576.
(567) (a) Campbell, M. L.; Hooper, K. L.; Kölsch, E. J. *Chem. Phys. Lett.* **1997**, *274*, 7. (b) Campbell, M. L. *Chem. Phys. Lett.* **1998**, *294*, 339. (c) Campbell, M. L.; McClean, R. E. *J. Phys. Chem.* **1993**, *97*, 7942. (d) Campbell, M. L. *J. Chem. Soc., Faraday Trans.* **1998**, *94*, 1687. (e) McClean, R. E.; Campbell, M. L.; Kölsch, E. J. *J. Phys. Chem. A* **1997**, *101*, 3348. (f) Campbell, M. L.; Hooper, K. L. *J. Chem. Soc., Faraday Trans.* **1997**, *93*, 2139. (g) Campbell, M. L.; McClean, R. E.; Harter, J. S. S. *Chem. Phys. Lett.* **1995**, *235*, 497. (h) Campbell, M. L.; McClean, R. E. *J. Chem. Soc., Faraday Trans.* **1995**, *91*, 3787.
(568) Higashiyama, T.; Ishida, M.; Matsumoto, Y.; Honma, K. *Phys. Chem. Chem. Phys.* **2005**, *7*, 2418.
(569) Sakurai, H.; Kato, S. *J. Phys. Chem. A* **2002**, *106*, 4350.
(570) Campbell, M. L. *J. Chem. Soc., Faraday Trans.* **1996**, *92*, 4377.
(571) Campbell, M. L. *J. Phys. Chem.* **1996**, *100*, 19430.
(572) Whetten, R. L.; Cox, D. M.; Trevor, D. J.; Kaldor, A. *J. Phys. Chem.* **1984**, *89*, 566.
(573) Mitchell, S. A.; Hackett, P. A. *J. Chem. Phys.* **1990**, *93*, 7822.
(574) Matsui, R.; Senba, K.; Honma, K. *J. Phys. Chem. A* **1997**, *101*, 179.
(575) Campbell, M. L. *J. Phys. Chem. A* **1998**, *102*, 892.
(576) Simons, J. *J. Phys. Chem. A* **2008**, *112*, 6401.
(577) (a) Knight, L. B., Jr. *Acc. Chem. Res.* **1996**, *19*, 313. (b) Knight, L. B., Jr.; Kerr, K.; Villanueva, M.; McKinley, A. J.; Feller, D. *J. Chem. Phys.* **1992**, *97*, 5363.
(578) *CRC Handbook of Chemistry and Physics*; CRC Press: Boca Raton, FL, 1985.
(579) Merritt, J. M.; Bondybey, V. E.; Heaven, M. C. *J. Chem. Phys.* **2009**, *130*, 144503.
(580) Goncharov, V.; Heaven, M. C. *J. Chem. Phys.* **2006**, *124*, 064312.
(581) Goncharov, V.; Kaledin, L. A.; Heaven, M. C. *J. Chem. Phys.* **2006**, *125*, 133202.
(582) (a) Aguirre, F.; Husband, J.; Thompson, C. J.; Stringer, K. L.; Metz, R. B. *J. Chem. Phys.* **2003**, *119*, 10194. (b) Husband, J.; Aguirre, F.; Ferguson, P.; Metz, R. B. *J. Chem. Phys.* **1999**, *111*, 1433.
(583) Thompson, C. J.; Stringer, K. L.; McWilliams, M.; Metz, R. B. *Chem. Phys. Lett.* **2003**, *376*, 588.
(584) Kamariotis, A.; Hayes, T.; Bellert, D.; Brucat, P. J. *Chem. Phys. Lett.* **2000**, *316*, 60.
(585) Linton, C.; Simard, B.; Loock, H. P.; Wallin, S.; Rothschopf, G. K.; Gunion, R. F.; Morse, M. D.; Armentrout, P. B. *J. Chem. Phys.* **1999**, *111*, 5017.
(586) Harrington, J.; Weisshaar, J. C. *J. Chem. Phys.* **1992**, *97*, 2809.
(587) Sappey, A. D.; Eiden, G.; Harrington, J. E.; Weisshaar, J. C. *J. Chem. Phys.* **1989**, *90*, 1415.
(588) Merer, A. J.; Cheung, A. S. C.; Taylor, A. W. *J. Mol. Spectrosc.* **1984**, *108*, 343.
(589) Dyke, J. M.; Gravenor, B. W. J.; Lewis, R. A.; Morris, A. *J. Chem. Soc., Faraday Trans. 2* **1983**, *79*, 1083.
(590) (a) Balfour, W. J.; Lindgren, B. *Phys. Scr.* **1980**, *22*, 36. (b) Phillips, J. G.; Davis, S. P. *Astrophys. J.* **1979**, *234*, 393.
(591) Stoll, H.; Peterson, K. A.; Merritt, J. M.; Heaven, M. C. *J. Phys. Chem. A* published online July 14, **2009**, doi: 10.1021/jp904936x.
(592) Nakao, Y.; Hirao, K.; Taketsugu, T. *J. Chem. Phys.* **2001**, *114*, 7935.
(593) Schröder, D.; Schwarz, H.; Shaik, S. *Struct. Bonding (Berlin)* **2000**, *97*, 91.
(594) Bauschlicher, C. W., Jr.; Gutsev, G. L. *Theor. Chem. Acc.* **2002**, *107*, 309.
(595) Carter, E. A.; Goddard, W. A., III. *J. Phys. Chem.* **1988**, *92*, 2109.
(596) Broclawik, E. *Int. J. Quantum Chem.* **1995**, *56*, 779.
(597) Schofield, K. *J. Phys. Chem. A* **2006**, *110*, 6938.
(598) (a) Zhao, Y. Y.; Wang, G. J.; Chen, M. H.; Zhou, M. F. *J. Phys. Chem. A* **2005**, *109*, 6621. (b) Zhao, Y. Y.; Gong, Y.; Chen, M. H.; Ding, C. F.; Zhou, M. F. *J. Phys. Chem. A* **2005**, *109*, 11765.
(599) Van Zee, R. J.; Li, S.; Weltner, W., Jr. *Chem. Phys. Lett.* **1994**, *217*, 381.
(600) Denning, R. G. *J. Phys. Chem. A* **2007**, *111*, 4125.
(601) Green, D. W.; Gabelnick, S. D.; Reedy, G. T. *J. Chem. Phys.* **1976**, *64*, 1697.
(602) Merritt, J. M.; Han, J.; Heaven, M. C. *J. Chem. Phys.* **2008**, *128*, 084304.
(603) Wang, X. F.; Andrews, L.; Li, J.; Bursten, B. E. *Angew. Chem., Int. Ed.* **2004**, *43*, 2554.
(604) Gagliardi, L.; Roos, B. O. *Chem. Phys. Lett.* **2000**, *331*, 229.
(605) Gál, M.; Groggin, P. L.; Mink, J. *Spectrochim. Acta A* **1992**, *48*, 121.
(606) Brümmer, M.; Kaposta, C.; Santambrogio, G.; Asmis, K. R. *J. Chem. Phys.* **2003**, *119*, 12700.
(607) Koyanagi, G. K.; Bohme, D. K.; Kretzschmar, I.; Schröder, D.; Schwarz, H. *J. Phys. Chem. A* **2001**, *105*, 4259.
(608) Zhou, M. F.; Wang, G. J.; Zhao, Y. Y.; Chen, M. H.; Ding, C. F. *J. Phys. Chem. A* **2005**, *109*, 5079.
(609) Dong, J.; Wang, Y.; Zhou, M. F. *Chem. Phys. Lett.* **2002**, *364*, 511.
(610) Li, Z. H.; Gong, Y.; Fan, K. N.; Zhou, M. F. Unpublished results.
(611) Gong, Y.; Zhou, M. F. *J. Phys. Chem. A* **2009**, *113*, 4990.
(612) Gong, Y.; Zhou, M. F., manuscript in preparation (ZnO_2^-, CdO_2^-).
(613) Palenik, G. J. *Inorg. Chem.* **1967**, *6*, 503.
(614) Weinstock, N.; Schulze, H.; Müller, A. *J. Chem. Phys.* **1973**, *59*, 5063.
(615) (a) Asmis, K. R.; Sauer, J. *Mass Spectrom. Rev.* **2007**, *26*, 542. (b) Asmis, K. R.; Fielicke, A.; von Helden, G.; Meijer, G. *Chem. Phys. Solid Surf.* **2007**, *12*, 327.
(616) Yang, S.; Knickelbein, M. B. *Z. Phys. D* **1994**, *31*, 199.
(617) Pramann, A.; Nakamura, Y.; Nakajima, A.; Kaya, K. *J. Phys. Chem. A* **2001**, *105*, 7534.
(618) (a) Wang, J.; Wang, Y.; Wu, G.; Zhang, X.; Zhao, X.; Yang, M. *Phys. Chem. Chem. Phys.* **2009**, *11*, 5980. (b) Yang, Z.; Xiong, S. J. *J. Chem. Phys.* **2008**, *129*, 124308.
(619) (a) Gu, G.; Dai, B.; Ding, X.; Yang, J. L. *Eur. Phys. J., D* **2004**, *29*, 27. (b) Dai, B.; Deng, K.; Yang, J. L. *Chem. Phys. Lett.* **2002**, *364*, 188.
(620) Gong, Y.; Zhang, Q. Q.; Zhou, M. F. *J. Phys. Chem. A* **2007**, *111*, 3534.
(621) Xiang, J.; Yan, X. H.; Xiao, Y.; Mao, Y. L.; Wei, S. H. *Chem. Phys. Lett.* **2004**, *387*, 66.
(622) Calatayud, M.; Maldonado, L.; Minot, C. *J. Phys. Chem. C* **2008**, *112*, 16087.
(623) Zhang, D.; Liu, P.; Liu, C. *J. Phys. Chem. C* **2008**, *112*, 16729.
(624) Hagfeldt, A.; Lunell, S.; Siegbahn, H. O. G. *Int. J. Quantum Chem.* **1994**, *49*, 97.
(625) Chen, S.; Yin, Y.; Wang, D.; Liu, Y.; Wang, X. *J. Cryst. Growth* **2005**, *282*, 498.

(626) von Helden, G.; Kirilyuk, A.; Heijnsbergen, D. van.; Sartakov, B.; Duncan, M. A.; Meijer, G. *Chem. Phys.* **2000**, *262*, 31.
(627) Qu, Z. W.; Kroes, G. J. *J. Phys. Chem. C* **2007**, *111*, 16808.
(628) Hamad, S.; Catlow, C. R. A.; Woodley, S. M.; Lago, S.; Mejías, J. A. *J. Phys. Chem. B* **2005**, *109*, 15741.
(629) Persson, P.; Gebhardt, J. C. M.; Lunell, S. *J. Phys. Chem. B* **2003**, *107*, 3336.
(630) Asmis, K. R.; Meijer, G.; Brümmer, M.; Kaposta, C.; Santambrogio, G.; Wöste, L.; Sauer, J. *J. Chem. Phys.* **2004**, *120*, 6461.
(631) Calatayud, M.; Andrés, J.; Beltran, A. *J. Phys. Chem. A* **2001**, *105*, 9760.
(632) Pykavy, M.; van Wullen, C.; Sauer, J. *J. Chem. Phys.* **2004**, *120*, 4207.
(633) Zhai, H. J.; Wang, L. S. *J. Chem. Phys.* **2002**, *117*, 7882.
(634) Beattie, I. R.; Ogden, J. S.; Price, D. D. *Inorg. Chem.* **1978**, *17*, 3296.
(635) Herwig, C.; Limberg, C. *Inorg. Chem.* **2008**, *47*, 2937.
(636) (a) Asmis, K. R.; Santambrogio, G.; Brümmer, M.; Sauer, J. *Angew. Chem., Int. Ed.* **2005**, *44*, 3122. (b) Santambrogio, G.; Brümmer, M.; Wöste, L.; Döbler, J.; Sierka, M.; Sauer, J.; Meijer, G.; Asmis, K. R. *Phys. Chem. Chem. Phys.* **2008**, *10*, 3992.
(637) Fielicke, A.; Meijer, G.; von Helden, G. *J. Am. Chem. Soc.* **2003**, *125*, 3659.
(638) Asmis, K. R.; Brümmer, M.; Kaposta, C.; Santambrogio, G.; von Helden, G.; Meijer, G.; Rademann, K.; Wöste, L. *Phys. Chem. Chem. Phys.* **2002**, *4*, 1101.
(639) Yang, D. S.; Zgierski, M. Z.; Rayner, D. M.; Hackett, P. A.; Martinez, A.; Salahub, D. R.; Roy, P. N.; Carrington, T., Jr. *J. Chem. Phys.* **1995**, *103*, 5335.
(640) (a) Martinez, A.; Calaminici, P.; Köster, A. M.; Salahub, D. R. *J. Chem. Phys.* **2001**, *114*, 819. (b) Calaminici, P.; Flores-Moreno, R.; Köster, A. M. *J. Chem. Phys.* **2004**, *121*, 3558.
(641) Green, S. M. E.; Alex, S.; Fleischer, N. L.; Millam, E. L.; Marcy, T. P.; Leopold, D. G. *J. Chem. Phys.* **2001**, *114*, 2653.
(642) Zhai, H. J.; Wang, B.; Huang, X.; Wang, L. S. *J. Phys. Chem. A* **2009**, *113*, 3866.
(643) Zhai, H. J.; Averkiev, B. B.; Zubarev, D. Y.; Wang, L. S.; Boldyrev, A. I. *Angew. Chem., Int. Ed.* **2007**, *46*, 4277.
(644) Pramann, A.; Koyasu, K.; Nakajima, A. *J. Chem. Phys.* **2002**, *116*, 6521.
(645) Zhai, H. J.; Döbler, J.; Sauer, J.; Wang, L. S. *J. Am. Chem. Soc.* **2007**, *129*, 13270.
(646) Vyboishchikov, S. F.; Sauer, J. *J. Phys. Chem. A* **2001**, *105*, 8588.
(647) (a) Reddy, B. V.; Khanna, S. N. *Phys. Rev. Lett.* **1999**, *83*, 3170. (b) Reddy, B. V.; Khanna, S. N.; Ashman, C. *Phys. Rev. B* **2000**, *61*, 5797.
(648) Xiang, K. H.; Pandey, R.; Recio, J. M.; Francisco, E.; Newsam, J. M. *J. Phys. Chem. A* **2000**, *104*, 990.
(649) (a) Tono, K.; Terasaki, A.; Ohta, T.; Kondow, T. *Phys. Rev. Lett.* **2003**, *90*, 133402. (b) Tono, K.; Terasaki, A.; Ohta, T.; Kondow, T. *J. Chem. Phys.* **2003**, *119*, 11221.
(650) Zhai, H. J.; Wang, L. S. *J. Chem. Phys.* **2006**, *125*, 164315.
(651) Paul, S.; Misra, A. *THEOCHEM* **2009**, *895*, 156.
(652) Zhang, Q. Q.; Zhao, Y. Y.; Gong, Y.; Zhou, M. F. *J. Phys. Chem. A* **2007**, *111*, 9775.
(653) Yoder, B. L.; Maze, J. T.; Raghavachari, K.; Jarrold, C. C. *J. Chem. Phys.* **2005**, *122*, 094313.
(654) Zhai, H. J.; Huang, X.; Cui, L. F.; Li, X.; Li, J.; Wang, L. S. *J. Phys. Chem. A* **2005**, *109*, 6019.
(655) Zhai, H. J.; Huang, X.; Waters, T.; Wang, X. B.; O'Hair, R. A. J.; Wedd, A. G.; Wang, L. S. *J. Phys. Chem. A* **2005**, *109*, 10512.
(656) Huang, X.; Zhai, H. J.; Waters, T.; Li, J.; Wang, L. S. *Angew. Chem., Int. Ed.* **2006**, *45*, 657.
(657) Huang, X.; Zhai, H. J.; Li, J.; Wang, L. S. *J. Phys. Chem. A* **2006**, *110*, 85.
(658) Huang, X; Zhai, H. J.; Kiran, B.; Wang, L. S. *Angew. Chem., Int. Ed.* **2005**, *44*, 7251.
(659) (a) Sun, Q.; Rao, B. K.; Jena, P.; Stolcic, D.; Ganteför, G.; Kawazoe, Y. *Chem. Phys. Lett.* **2004**, *387*, 29. (b) Bertram, N.; Kim, Y. D.; Ganteför, G.; Sun, Q.; Jena, P.; Tamuliene, J.; Seifert, G. *Chem. Phys. Lett.* **2004**, *396*, 341.
(660) (a) Janssens, E.; Hou, X. J.; Neukermans, S.; Wang, X.; Silverans, R. E.; Lievens, P.; Nguyen, M. T. *J. Phys. Chem. A* **2007**, *111*, 4150. (b) Wang, B.; Zhang, X. H.; Huang, X.; Zhang, Y. F. *Jiegou Huaxue* **2008**, *27*, 990. (c) Li, J. *J. Cluster Sci.* **2002**, *13*, 137.
(661) Tono, K.; Terasaki, A.; Ohta, T.; Kondow, T. *Chem. Phys. Lett.* **2004**, *388*, 374.
(662) Lombardi, J. R.; Davis, B. *Chem. Rev.* **2002**, *102*, 2431.
(663) Jones, N. O.; Khanna, S. N.; Baruah, T.; Pederson, M. R.; Zheng, W. J.; Nilles, J. M.; Bowen, K. H. *Phys. Rev. B* **2004**, *70*, 134422.
(664) Cao, Z.; Duran, M.; Solà, M. *J. Chem. Soc., Faraday Trans.* **1998**, *94*, 2877.
(665) Wang, L. S.; Wu, H. B.; Desai, S. R. *Phys. Rev. Lett.* **1996**, *76*, 4853.
(666) Gutsev, G. L.; Bauschlicher, C. W., Jr.; Zhai, H. J.; Wang, L. S. *J. Chem. Phys.* **2003**, *119*, 11135.
(667) Shiroishi, H.; Oda, T.; Hamada, I.; Fujima, N. *Mol. Simul.* **2004**, *30*, 911.
(668) Shiroishi, H.; Oda, T.; Hamada, I.; Fujima, N. *Polyhedron* **2005**, *24*, 2472.
(669) Jones, N. O.; Reddy, B. V.; Rasouli, F.; Khanna, S. N. *Phys. Rev. B* **2005**, *72*, 165411.
(670) Ding, X. L.; Xue, W.; Ma, Y. P.; Wang, Z. C.; He, S. G. *J. Chem. Phys.* **2009**, *130*, 014303.
(671) Sun, Q.; Wang, Q.; Parlinski, K.; Yu, J. Z.; Hashi, Y.; Gong, X. G.; Kawazoe, Y. *Phys. Rev. B* **2000**, *61*, 5781.
(672) Danset, D.; Manceron, L. *Phys. Chem. Chem. Phys.* **2005**, *7*, 583.
(673) Staemmler, V.; Reinhardt, P.; Allouti, F.; Alikhani, M. E. *Chem. Phys.* **2008**, *349*, 83.
(674) Pramann, A.; Koyasu, K.; Nakajima, A.; Kaya, K. *J. Phys. Chem. A* **2002**, *106*, 4891.
(675) Liu, L.; Zhao, R. N.; Han, J. G.; Liu, F. Y.; Pan, G. Q.; Sheng, L. S. *J. Phys. Chem. A* **2009**, *113*, 360.
(676) (a) Harding, D. J.; Mackenzie, S. R.; Walsh, T. R. *Chem. Phys. Lett.* **2009**, *469*, 31. (b) Harding, D. J.; Davies, R. D. L.; Mackenzie, S. R.; Walsh, T. R. *J. Chem. Phys.* **2008**, *129*, 124304.
(677) Allouti, F.; Manceron, L.; Alikhani, M. E. *Phys. Chem. Chem. Phys.* **2006**, *8*, 3715.
(678) Hübner, O.; Himmel, H.-J. *Phys. Chem. Chem. Phys.* **2009**, *11*, 2241.
(679) Wang, L. S.; Wu, H.; Desai, S. R.; Lou, L. *Phys. Rev. B* **1996**, *53*, 8028.
(680) Dai, B.; Tian, L.; Yang, J. L. *J. Chem. Phys.* **2004**, *120*, 2746.
(681) Jadraque, M.; Martín, M. *Chem. Phys. Lett.* **2008**, *456*, 51.
(682) Gong, Y. Su, J.; Li, J.; Zhou, M. F. manuscript in preparation.
(683) (a) von Gynz-Rekowski, F.; Bertram, N.; Ganteför, G.; Kim, Y. D. *J. Phys. Chem. B* **2004**, *108*, 18916. (b) von Gynz-Rekowski, F.; Bertram, N.; Ganteför, G.; Kim, Y. D. *Eur. Phys. J., D* **2005**, *36*, 187.
(684) (a) Stolcic, D.; Fischer, M.; Ganteför, G.; Kim, Y. D.; Sun, Q.; Jena, P. *J. Am. Chem. Soc.* **2003**, *125*, 2848. (b) Sun, Q.; Jena, P.; Kim, Y. D.; Fischer, M.; Ganteför, G. *J. Chem. Phys.* **2004**, *120*, 6510.
(685) Koyasu, K.; Niemietz, M.; Götz, M.; Ganteför, G. *Chem. Phys. Lett.* **2007**, *450*, 96.
(686) Kim, Y. D. *Int. J. Mass Spectrom.* **2004**, *238*, 17.
(687) (a) Kim, Y. D.; Ganteför, G. *Chem. Phys. Lett.* **2004**, *383*, 80. (b) Kim, Y. D.; Ganteför, G. *J. Mol. Struct.* **2004**, *692*, 139.
(688) Ding, X.; Dai, B.; Yang, J. L.; Hou, J. G.; Zhu, Q. S. *J. Chem. Phys.* **2004**, *121*, 621.
(689) (a) Mills, G.; Gordon, M. S.; Metiu, H. *J. Chem. Phys.* **2003**, *118*, 4198. (b) Mills, G.; Gordon, M. S.; Metiu, H. *Chem. Phys. Lett.* **2002**, *359*, 493.
(690) Wells, D. H., Jr.; Delgass, W. N.; Thomson, K. T. *J. Chem. Phys.* **2002**, *117*, 10597.
(691) Kim, Y. D.; Ganteför, G.; Sun, Q.; Jena, P. *Chem. Phys. Lett.* **2004**, *396*, 69.
(692) Franceschetti, A.; Pennycook, S. J.; Pantelides, S. T. *Chem. Phys. Lett.* **2003**, *374*, 471.
(693) Yoon, B.; Häkkinen, H.; Landman, U. *J. Phys. Chem. A* **2003**, *107*, 4066.
(694) Luo, C.; Fa, W.; Dong, J. *J. Chem. Phys.* **2006**, *125*, 084707.
(695) Wang, Y.; Gong, X. G. *J. Chem. Phys.* **2006**, *125*, 124703.

CR900185X